TECHNISCHE UNIVERSITÄT MÜNCHEN

FAKULTÄT FÜR MEDIZIN

The role of cGAS-STING signaling in graft-versus-host disease and intestinal epithelial regeneration

Gabriel Winfried Franz Eisenkolb

Vollständiger Abdruck der von der Fakultät für Medizin der Technischen Universität München zur Erlangung eines

Doktors der Medizinischen Wissenschaft (Dr. med. sci.)

genehmigten Dissertation.

Vorsitz:	Prof. Dr. Jürgen Ruland
Prüfer der Dissertation:	Prof. Dr. Hendrik Poeck
	Prof. Dr. Dirk H. Busch
	Prof. Dr. Percy A. Knolle

Die Dissertation wurde am 19.09.2022 bei der Technischen Universität München eingereicht und durch die Fakultät für Medizin am 17.05.2023 angenommen.

1 INTRODUCTION 6

1.1 Principles of innate immunity 6

1.1.1 Pattern recognition 6

1.1.2 The cGAS-STING pathway 7

1.1.3 Type I Interferons 10

1.2 Allogeneic hematopoietic stem cell transplantation and graft-versus-host disease 12

1.2.1 Clinical relevance of allogeneic hematopoietic stem cell transplantation 12

1.2.2 Epidemiology and clinical appearance of GVHD 13

1.2.3 Pathophysiology 14

1.3 The intestinal barrier and GVHD 16

1.4 Objectives 18

2 MATERIALS AND METHODS 19

2.1 Materials 19

2.1.1 Instruments and devices 19

2.1.2 Reagents 20

2.1.3 Cell culture media and reagents 20

2.1.4 Stimuli 22

2.1.5 Kits 22

2.1.6 Antibodies 22

2.1.7 Primers 23

2.1.8 Software 23

2.2 Methods 24

2.2.1 Mice 24

2.2.2 Murine allogeneic bone marrow transplantation 24

2.2.2.1 Recipient irradiation 24

2.2.2.2 Preparation of allo-graft 24

2.2.2.3 Reconstitution of recipient mice after total body irradiation 25

2.2.2.4 Clinical GVHD intensity and survival experiments 25

2.2.3 Treatment of mice with nucleic acids 26

2.2.4 Isolation and culture of small intestinal organoids 26

2.2.4.1 ENR-Media preparation 26

2.2.4.2 R-spondin-1-conditioned media 26
2.2.4.3 Small intestinal crypt isolation 27
2.2.4.4 Organoid culture 27
2.2.4.5 Organoid counts 28
2.2.4.6 Determination of organoid size 28
2.2.5 MTT assay 28
2.2.6 RNA extraction of organoid cultures 29
2.2.7 Quantitative Real-time PCR 29
2.2.7.1 Cell lysis 29
2.2.7.2 RNA isolation 29
2.2.7.3 cDNA synthesis 30
2.2.7.4 Quantitative real-time PCR 30
2.2.7.5 qPCR analysis 31
2.2.8 16S rRNA sequencing 31
2.2.8.1 Principle of 16S rRNA sequencing 31
2.2.8.2 DNA extraction 32
2.2.8.3 DNA sequencing and analysis 32
2.2.9 Measurement of plasma DNA levels 32
2.2.10 FITC Dextran translocation assay 33
2.2.11 Flow cytometry of small intestinal crypts and organoids 33
2.2.12 Histopathologic analysis 33
2.2.13 Statistics 34
3 RESULTS 35
3.1 STING signaling protects allo-BMT recipient mice from GVHD 35
3.1.1 Endogenous STING signaling protects from GVHD related mortality and morbidity 35
3.1.2 Differences in GVHD intensity are not associated with changes in the microbiota of *Sting*$^{gt/gt}$ mice 37
3.1.3 Total body irradiation and allo-BMT lead to a systemic release of DNA 38
3.1.4 cGAS-STING ligand ISD can be used therapeutically to prevent GVHD 40

3.2 STING activation limits small intestinal GVHD and protects the small intestinal barrier 42
3.2.1 Prophylactic STING activation reduces damage to the small intestine 42
3.2.2 Treatment of allo-BMT recipients with STING ligand ISD reduces intestinal permeability 45
3.3 STING signaling enhances small intestinal organoid growth in an IFN-I dependent manner 46
3.3.1 STING signaling promotes organoid formation and proliferation 47
3.3.2 ISD induces IFN-β expression in organoids which promotes organoid growth 50
3.3.3 cGAS-STING mediated effects on organoid growth are IFN-I dependent 51
3.4 STING activation promotes organoid regeneration ex vivo after murine allo-BMT 53
3.5 STING activation enforces mechanisms supporting intestinal barrier function and might increase stem cell frequencies in small intestinal crypts 54
3.5.1 cGAS-STING activation induces gene expression of RegIIIγ, Claudin 4 and cGAS 55
3.5.2 cGAS-STING activation mediates stem cell expansion in vitro 56
4 DISCUSSION 59
4.1 GVHD and the role of cGAS-STING and IFN-I inducing pathways 59
4.1.1 Experimental models of GVHD – MHC matched or mismatched? 59
4.1.2 IFN-I signaling affects the intestinal microbiota 60
4.1.3 Determining tissue specific effects of cGAS-STING in GVHD 61
4.1.4 Translational aspects of cGAS-STING and GVHD 63
4.2 cGAS-STING and the intestinal epithelial barrier 65
4.2.1 Organoid cultures to study intestinal epithelial regeneration 65
4.2.2 The interplay of the intestinal stem cell with its niche 67
4.2.3 Implications of the innate and adaptive immune system on the intestinal stem cell niche 71

5 SUMMARY 73

6 ZUSAMMENFASSUNG 74

7 REFERENCES 75

8 ABBREVIATIONS 88

9 ACKNOWLEDGEMENTS 91

1 Introduction

1.1 Principles of innate immunity

The immune system is a complex arrangement of different cellular and non-cellular components that react to various kinds of danger situation to the host's organism and is most commonly divided into two branches. The innate immune system consists of specialized sensor and effector cells that are able to establish a fast response to infectious and non-infectious threats. The adaptive immune system complements the innate immune system with its ability to generate a highly specific reaction to pathogens and establishes an immunological memory which can prevent severe re-infections (Murphy and Weaver 2016).

In innate immunity, specialized cells like dendritic cells, macrophages and neutrophil granulocytes have the ability to detect infections. These sensor cells make use of pattern recognition receptors (PRRs) that are able to discriminate between self and non-self. Subsequently, innate immune cells start fighting the pathogen and produce cytokines and chemokines to generate a state of inflammation. The purpose of inflammatory reactions is to create an environment that attracts immune cells and allows them to enter the site of infection or tissue damage (e.g., via increased blood perfusion and facilitated extravasation) (Murphy and Weaver 2016). Ultimately, inflammatory processes also promote regeneration to restore tissue integrity (Murphy and Weaver 2016, Eming, Wynn et al. 2017).

1.1.1 Pattern recognition

Pattern recognition receptors are the key sensors of innate immunity. They detect bacterial, viral or fungal components, referred to as pathogen associated molecular patterns (PAMPs) to initiate an immune response (Murphy and Weaver 2016). Additionally, some receptors bind to so called damage associated molecular patterns (DAMPs) to identify situations of non-infectious threats.

The group of Toll-like receptors (TLRs) was the first family of PRRs to be described and consists of nine different receptors in humans. They sense specific bacterial or viral particles: cell wall components like lipopolysaccharide (LPS), flagellin or lipoproteins, and nucleic acids like DNA containing unmethylated CpG

motifs or virus specific single-stranded RNA (Murphy and Weaver 2016). Upon activation, they recruit adaptor proteins, namely MyD88 and/or TRIF which then induce the expression of proinflammatory cytokines via the NFκB-pathway or the transcription of type I interferon genes via IRF3/7 (Brubaker, Bonham et al. 2015, Murphy and Weaver 2016).

Apart from the TLR family, there are multiple other groups of PRRs which are classified following their protein domains: e.g., nucleotide binding oligomerization domain receptors (NOD-like receptors) which recognize components of peptidoglycan in the cell wall of bacteria or the large family of C-type lectin receptors (CLRs) detecting a variety of viral, fungal or bacterial PAMPs.

The RIG-I/MAVS pathway senses cytosolic viral RNA which is characterized by its 5' triphosphate group (5'-3pRNA) (Hornung, Ellegast et al. 2006).

In general, different strategies enable innate immune receptors to distinguish between self and non-self: either, they sense specific microbial structures (e.g. LPS or 3pRNA), or they survey specific cellular compartments for molecules that are absent in this compartment under physiologic circumstances (e.g. nucleic acids in the endosome) (Brubaker, Bonham et al. 2015).

1.1.2 The cGAS-STING pathway

The discovery of TLR-3, -7, -8 and -9 as well as the RIG-I/MAVS pathway were a big step towards the understanding of how nucleic acids are recognized as a PAMP/DAMP and activate signaling pathways to induce potent immune responses. In this context, it has been proposed that cytosolic double-stranded DNA (dsDNA) activates innate immunity and Type-I IFN signaling in a TLR-independent way (Ishii, Coban et al. 2006). In 2008, the STimulator of INterferon Genes (STING) was identified as an adaptor protein located at the endoplasmatic reticulum that is activated by DNA-viruses and non-CpG containing DNA (interferon stimulatory DNA = ISD) which promotes a Type-I IFN response (Ishikawa and Barber 2008, Ishikawa, Ma et al. 2009).

Cyclic GMP-AMP synthase (cGAS) is an enzyme that binds dsDNA in the cytosol and catalyzes the formation of the second messenger cyclic GMP-AMP (cGAMP) from GTP and ATP (Sun, Wu et al. 2013, Wu, Sun et al. 2013). cGAS binds the DNA at its sugar-phosphate backbone which allows DNA recognition independent of its sequence (Civril, Deimling et al. 2013). Its product cGAMP is

then recognized by STING dimers on the ER membrane which traffics to the Golgi apparatus and in turn recruits TBK1 and IKK in order to activate IRF3 and NFκB, respectively (Ishikawa, Ma et al. 2009, Chen, Sun et al. 2016). IRF3 and NFκB enter the nucleus to induce the transcription of IFN-I and proinflammatory cytokines like TNF, IL-1β and IL-6 (Chen, Sun et al. 2016) (see **Fig. 1** for a schematic overview).

In order to end the immune response, cGAS-STING activation is negatively regulated at several stages of the pathway: cGAMP degradation, post-translational modifications of STING like polyubiquitination or ultimately degradation of STING after its translocation to the Golgi apparatus (Chen, Sun et al. 2016).

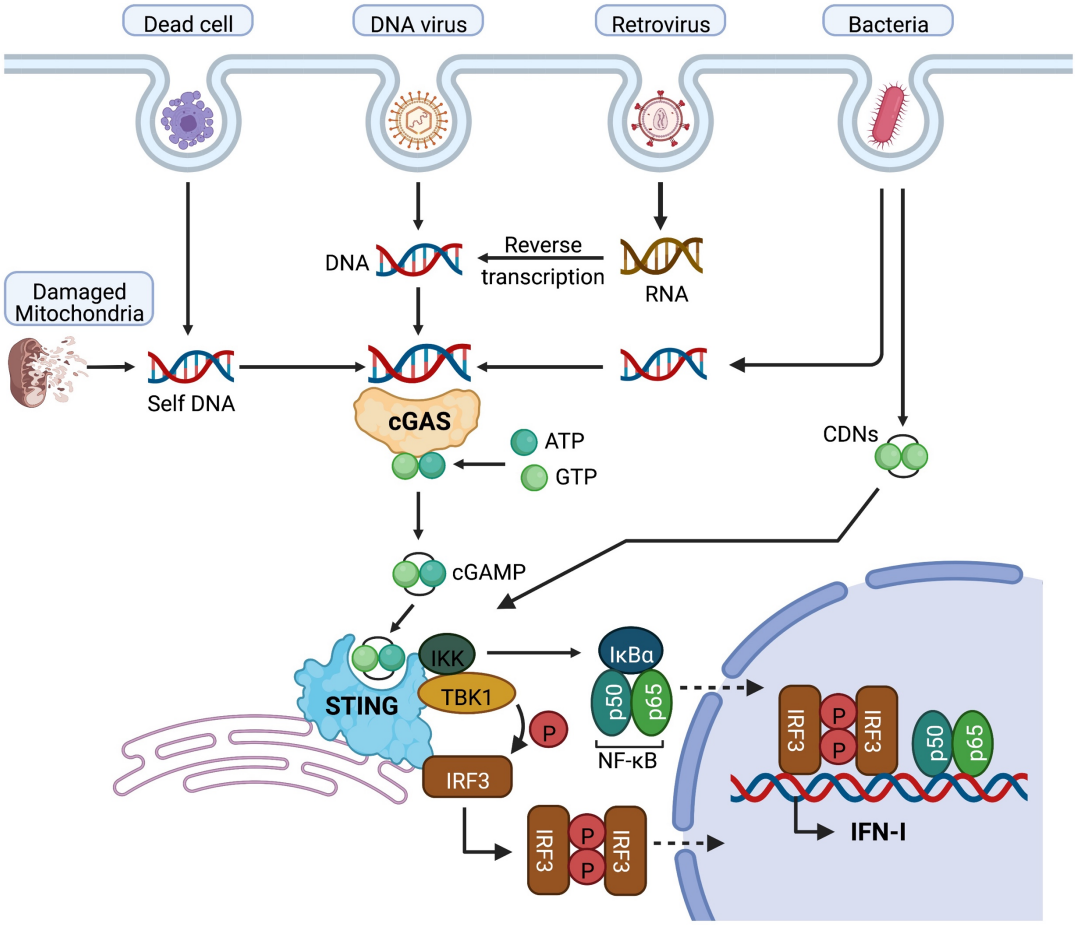

Fig. 1. Schematic overview of the cGAS-STING pathway of cytosolic DNA sensing. Adapted from (Chen, Sun et al. 2016). Created with *biorender.com*

The main function of cGAS-STING as an innate immune receptor is to recognize pathogens and initiate immune responses. cGAS recognizes a variety of DNA viruses like herpes simplex virus, cytomegalovirus, vaccinia virus, adenovirus and Kaposi's sarcoma-associated herpesvirus (KSHV) (Chen, Sun et al. 2016). In addition, cGAS also senses complementary DNA (cDNA) from retroviruses such as HIV-1 and HIV-2, which under normal circumstances is prevented by the viral capsid (Lahaye, Satoh et al. 2013). A variety of bacterial infections also result in cGAS-STING dependent IFN-I responses, including mainly intracellular bacteria like *Mycobacteria*, *Legionella*, *Listeria*, *Shigella*, *Chlamydia*, *Neisseria* and group B streptococcus (Hansen, Prabakaran et al. 2014, Zhang, Li et al. 2014, Watson, Bell et al. 2015, Andrade, Agarwal et al. 2016, Andrade, Firon et al. 2016, Chen, Sun et al. 2016). However, it is not only the bacterial DNA that causes cGAS-STING activation. Some bacteria produce cyclic dinucleotides like c-di-AMP or c-di-GMP that can directly activate STING, which has been shown to protect mice from M. tuberculosis infection (Burdette, Monroe et al. 2011, Dey, Dey et al. 2015).

Besides the field of infectious diseases, DNA sensing is critical in the area of cancer immunobiology. DNA damage is a central motif in both cancer development and cancer treatment. On the one hand, genomic instability and mutations can result in malignant transformation of cells and defective DNA repair mechanisms are causal for specific forms of colorectal cancer (hereditary non-polyposis colorectal cancer) or breast cancer (mutations of BRCA-1 and BRCA-2). On the other hand, a variety of cancer therapies aim to induce cytotoxic amounts of DNA damage in cancer cells, such as certain chemotherapies and irradiation. Multiple studies revealed that cGAS or STING deficiency rendered mice more susceptible to tumor growth and diminished efficacy of irradiation or immune checkpoint blockade (Li and Chen 2018). Consistently, treatment with cGAMP or other STING agonists boosted anticancer treatment in murine cancer models (Deng, Liang et al. 2014, Li, Cheng et al. 2016). These effects are partly attributable to increased APC activation upon cGAS-STING activation leading to improved immune responses (Li and Chen 2018). At the same time, tumor-intrinsic cGAS-STING signaling can lead to tumor regression and some cancer types lose cGAS or STING expression during malignant transformation and thus evade immunosurveillance (Flood, Higgs et al. 2019).

1.1.3 Type I Interferons

The Type I Interferon (IFN-I) family consists of IFNα and IFNβ which are produced after activation of different PRRs. Not only RIG-I/MAVS and cGAS-STING lead to IFN I production but also some TLRs (TLR3, 4, 7 and 8) and thus create an immunological response to different sites and types of infection (McNab, Mayer-Barber et al. 2015). IFNs carry their name, because they interfere with viral replication, one of their first described functions. Today, besides their broad role in infection control they have been linked to autoimmunity and antitumor activity (Lazear, Schoggins et al. 2019).

Upon secretion, IFNα and IFNβ bind to a common receptor expressed ubiquitously, named IFNα receptor (IFNAR) which then recruits receptor-associated protein tyrosine kinases Janus kinase 1 (JAK1) and tyrosine kinase 2 (TYK2). They phosphorylate signal transducer and activator of transcription 1 (STAT1) and STAT2 which form a complex with IFN-regulatory factor 9 (IRF9) to activate the transcription of so called IFN-stimulated genes (ISGs) (Ivashkiv and Donlin 2014). Their protein products interfere with viral life cycles at multiple stages and thus create an antiviral state of the cell. Besides this canonical IFN-I signaling, IFNAR activation can also lead to the formation of STAT1 homodimers, which then bind to gamma-activated sequences (GAS) and induce effector pathways associated with IFNγ-signaling like macrophage-activation and production of reactive oxygen species (MacMicking 2012, Lee and Ashkar 2018).

IFN-I effector functions are not limited to cell-intrinsic defense but also modulate innate and adaptive immune responses. For instance, IFN-I activate NK cells which recognize infected cells and initiate their killing (Murphy and Weaver 2016). IFNAR activation on APCs leads to upregulation of MHC I and MHC II receptors and costimulatory molecules CD80 and CD86 and thus potentiates T cell responses (Crouse, Kalinke et al. 2015). Additionally, IFN-I also influence T cell activation, proliferation and differentiation directly, depending on the time of secretion and costimulatory factors and can either induce or suppress T cell responses (Crouse, Kalinke et al. 2015).

The immunomodulatory functions of IFN-I are of great importance clinically. Overexpression of IFN-I is associated with a variety of autoimmune diseases. In systemic lupus erythematosus (SLE) patients, increased IFN-I activity could already be observed in the year prior to disease onset (Munroe, Lu et al. 2016)

and blood IFN-α levels correlated with disease activity (Baechler, Batliwalla et al. 2003). Similar observations of increased IFN-I activity were made for Sjögren's syndrome, myositis and to a lower degree for rheumatoid arthritis (Muskardin and Niewold 2018). In some rare diseases, grouped by the term "interferonopathies", single gene defects lead to increased IFN-I levels. Aicardi Goutières Syndrome (AGS) is an autoimmune disease leading to severe encephalitis in infancy which is associated with high IFN-I levels in cerebrospinal fluid. The cause is a mutation of Trex1 which leads to intracellular accumulation of DNA and high interferon responses (Stetson, Ko et al. 2008). Another interferonopathy named STING associated vasculopathy with onset in infancy (SAVI) manifests itself by cutaneous vasculopathy and pulmonary inflammation caused by a mutation in the STING gene (Liu, Jesus et al. 2014).

Apparently, overactivated IFN responses are associated with autoimmune diseases. At the same time, IFN-α and IFN-β signaling can influence inflammatory reactions in various contexts. In wounds, IFN-I produced by plasmacytoid dendritic cells (pDCs) promote an inflammatory response which is necessary for epithelization and healing (Gregorio, Meller et al. 2010). Recently, it was found that the skin microbiota attracts neutrophils that promote the recruitment of pDCs (Di Domizio, Belkhodja et al. 2020). These are a major source of IFN-I which accelerate wound repair. In the context of experimental inflammatory bowel disease, induction of IFN-I reduced the production of pro-inflammatory cytokines and the intensity of ulcerative colitis (Katakura, Lee et al. 2005, Yang, Kim et al. 2016).

Interestingly, these immunomodulatory effects of IFN-I are not limited to states of infection but are also attributed protective functions in anticancer immunity. In mouse models, IFN-I signaling protected from intestinal tumor formation (Tschurtschenthaler, Wang et al. 2014). In humans and mice, IRF7 mediated IFN-I production was associated with a reduction of bone metastases in certain breast cancer types (Bidwell, Slaney et al. 2012). Also, tumor infiltrating pDCs in aggressive breast cancer were shown to produce less IFN-I than circulating pDCs which was associated with higher tumor cell proliferation (Sisirak, Faget et al. 2012).

In the clinical setting, IFN-I have been exploited therapeutically in the treatment of specific malignancies (e.g., metastatic melanoma, hairy cell leukemia)

(Zitvogel, Galluzzi et al. 2015). Although treatment strategies for hepatitis B and C virus infections are currently changing towards interferon-free regimes, interferons still belong to the toolbox of standard drugs (Hu, Protzer et al. 2019, Mayberry and Lee 2019). In patients suffering from multiple sclerosis, interferon-β compounds are broadly used first-line therapeutics (Reich, Lucchinetti et al. 2018).

1.2 Allogeneic hematopoietic stem cell transplantation and graft-versus-host disease

1.2.1 Clinical relevance of allogeneic hematopoietic stem cell transplantation

Hematopoietic stem cell transplantation (HSCT) is a potentially curative treatment strategy for a variety of mainly malignant hematologic diseases. Two types of HSCT can be distinguished depending on the relationship between donor and recipient: autologous and allogeneic HSCT (Copelan 2006).

In autologous HSCT, hematopoietic stem cells are acquired from the patient himself before starting a high-dose chemotherapy. The most frequent indications for auto-HSCT are plasma cell disorders like multiple myeloma and Non-Hodgkin lymphoma (Passweg, Baldomero et al. 2021) which are treated by high-dose myeloablative chemotherapy. The following HSCT then serves as rescue therapy to reconstitute the patient with his or her own hematopoietic stem cells to prevent prolonged and otherwise life-threatening pancytopenia.

Patients undergoing allo-HSCT are most often diagnosed with acute myeloid leukemia, acute lymphocytic leukemia or myelodysplastic syndrome (Passweg, Baldomero et al. 2021). Allo-HSCT is performed after conditioning therapy using chemotherapy with or without additional total body irradiation (TBI). Increasing intensities of conditioning regimen can reduce relapse rates but are associated with higher toxicity and treatment related mortality (Bacigalupo, Ballen et al. 2009). As in auto-HSCT, the conditioning therapy serves as a cancer treatment but in this case myeloablation is also required to ensure engraftment (Copelan 2006). The aim of allo-HSCT is to treat the malignancy using the graft-versus-tumor/-leukemia (GVT/GVL) effect, where donor T cells recognize and destroy remaining tumor cells (Copelan 2006). This desired immune reaction comes at the cost of graft-versus-host disease (GVHD), where activated donor T cells start

attacking the host's organism. To reduce this serious side-effect, the donor's major histocompatibility antigens (HLAs) should match the recipients'. If available, HLA-matched siblings are the preferential source of stem cells, otherwise the search is extended to unrelated donors matching at least 9 of 10 HLA traits or haploidentical donors (e.g. the patient's child) (Muller and Muller-Tidow 2015).
In 2019, the European Society for Blood and Marrow Transplantation (EBMT) reported over 48.512 HSCTs in Europe and collaborating countries, among them 19.798 allo-HSCTs (41%).

1.2.2 Epidemiology and clinical appearance of GVHD

Graft-versus-host disease is commonly divided into an acute form (aGVHD) and the chronic form (cGVHD) depending on whether it appears within the first 100 days after allo-HSCT or later (Ferrara, Levine et al. 2009). aGVHD is one of the major limitations of HSCT and affects as many as 40-60% of transplant recipients, depending on the graft type (Jagasia, Arora et al. 2012). Together with relapse of the malignant disease and infections, GVHD is one of the leading causes of death among patients after transplantation (D'Souza A. 2016). Given that numbers of allo-HSCT are rising (Passweg, Baldomero et al. 2021) the incidence of GVHD is likely to increase in the coming years.
aGVHD affects the skin, gastro-intestinal tract and liver and can be divided into grade I-IV depending on the extent of typical GVHD symptoms. The major skin manifestation is a maculopapular rash causing pruritus and skin ulcerations in severe cases. Liver affection is quantified by increasing serum bilirubin levels and the typical symptom of GI affection is diarrhea which can cause stool volumes of >2000ml per day and hematochezia which is associated with a poor outcome (Jacobsohn and Vogelsang 2007, Harris, Young et al. 2016). The risk for development of grade II-IV aGVHD depends on the HLA disparity between donor and recipient and ranges between 20% for HLA-identical siblings and over 40% for one or two HLA-mismatches (Jacobsohn and Vogelsang 2007). Other risk factors include the choice and intensity of conditioning regimen and the use of a GVHD prophylaxis e.g., tacrolimus and methotrexate (Jagasia, Arora et al. 2012).

1.2.3 Pathophysiology

GVHD pathophysiology is commonly described as a process of three sequential phases: (I) priming of host APCs, (II) activation of donor T cells and (III) organ destruction (Ferrara, Levine et al. 2009). This concept is mainly based on murine experimental models of GVHD and helps to understand the most critical stages and relevant cell populations that impact on disease development. (See **Fig. 2** for a schematic overview)

(I) Priming of host APCs

Conditioning regimen prior to allo-HSCT leads to massive tissue damage. Subsequently, DAMPs like ATP, uric acid or dsDNA from host tissue as well as PAMPs like LPS or peptidoglycans from intestinal microbiota are released (Heidegger, van den Brink et al. 2014). The intestinal mucosa is a highly proliferative tissue and thus particularly sensitive to irradiation and chemotherapy. Upon damage, DAMPs are released from dying epithelial cells and the protective barrier function is impaired allowing translocation of PAMPs from the intestinal lumen (Heidegger, van den Brink et al. 2014), which is otherwise strictly separated from the rest of the organism. The resulting activation of PRRs leads to a systemic release of proinflammatory cytokines, a phenomenon called “cytokine storm” (Hill, Crawford et al. 1997). As a consequence, host APCs react by upregulating adhesion molecules and MHC antigens and by increased presentation of costimulatory molecules (Ferrara, Levine et al. 2009).

(II) Donor T cell activation

Depending on the presence and degree of HLA mismatch between donor and recipient, transplanted $CD4^+$ T cells will recognize MHC II differences whereas $CD8^+$ T cells are going to identify MHC I inconsistencies and induce aGVHD. In case of major HLA matching, minor HLA variations between donor and host can also cause GVHD. Donor-derived T cells encounter primed APCs in an environment dominated by proinflammatory cytokines. Primarily, those T cells mature towards a Th1 phenotype as the milieu is dominated by Th1 cytokines like TNF-α and IFN-γ (Henden and Hill 2015) and massively expand in response to the “cytokine storm”. Higher doses of TBI have been attributed with higher

TNF-α serum levels and worse GVHD pathology and survival in a preclinical model (Hill, Crawford et al. 1997). A special role is also attributed to IFN-γ in driving Th1-maturation during aGVHD and in being responsible for specific end organ damage (Yi, Chen et al. 2009). While Th1 cells are mainly associated with aGVHD, Th17 cells particularly play a role in inducing early stages of aGVHD (Kappel, Goldberg et al. 2009) and chronic GVHD is attributed to both Th1 and Th17 subsets (Chen, Vodanovic-Jankovic et al. 2007).

(III) Organ destruction

Upon activation, donor effector T cells migrate to GVHD target organs liver, intestine, skin and lungs and start destroying the tissue. Different Th cell subsets are responsible for damage in the respective organs. Whereas Th1 cells are mainly driving intestinal and liver pathology, Th2 and Th17 cells are causing substantial harm to the lung and skin in murine allo-HSCT models (Yi, Chen et al. 2009). The “cytokine storm” mentioned above is not only responsible for T cell maturation and expansion but also results in the expression of chemokines and their receptors facilitating the infiltration of cytotoxic T cells (CTLs) in GVHD target organs (Wysocki, Panoskaltsis-Mortari et al. 2005). The inflammatory environment of allo-HSCT recipients defined by the cytokine milieu is indispensable for T cell migration to target tissues (Chakraverty, Cote et al. 2006). Organ damage is mediated by interactions between CTLs and MHC antigens inducing apoptosis via the Fas/FasL pathway or the granzyme/perforin pathways (van den Brink and Burakoff 2002, Sun, Tawara et al. 2007). Inflammatory signals like TNF-α drive GVHD at various levels: activating DCs, recruiting T cells and direct induction of apoptosis in target organs (Sun, Tawara et al. 2007).

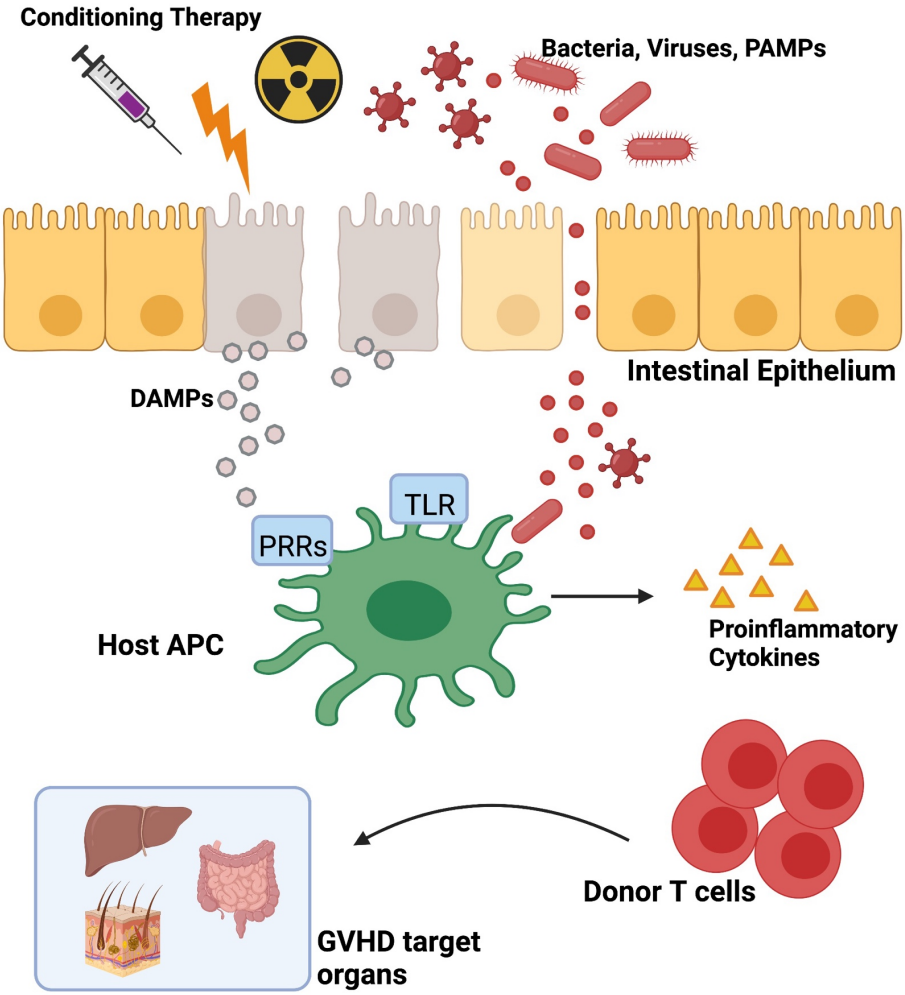

Fig. 2. Schematic overview of GVHD pathogenesis. Adapted from (Heidegger, van den Brink et al. 2014). Created with *biorender.com*

1.3 The intestinal barrier and GVHD

The anatomic and physiological properties of the intestinal tract are designed to cover two principal functions: nutrient uptake and separation from luminal bacteria, viruses or fungi.

The GI tract wall is formed by four layers: the mucosa, submucosa, muscularis and adventitia/serosa. Its innermost layer, the mucosa, can again be divided into the muscularis mucosae, the lamina propria and the epithelium. This single-layered epithelium covers approximately 400m^2 and is a highly specialized cellular compartment that consists of villi and crypts to increase the absorptive surface (the colon consists of crypts only) (Peterson and Artis 2014). The underlying lamina propria is rich in blood vessels, leukocytes and lymphoid tissue, the Peyer's patches (Murphy and Weaver 2016).

The intestinal stem cell compartment is located at the bottom of the crypts of Lieberkühn and harbors the intestinal stem cells (ISCs) which give rise to the different lineages of the intestinal epithelium: Paneth cells, goblet cells, enteroendocrine cells, tuft cells and intestinal epithelial cells (IECs).

Stem cells are characterized by surface marker Lgr5 and Olfm4 (Barker, van Es et al. 2007, van der Flier, Haegebarth et al. 2009) and reside at the crypt bottom where they divide into rapidly cycling transit amplifying cells which ultimately become IECs that move upwards the villi and are shed into the lumen after 3-5 days (Gehart and Clevers 2019). Paneth cells produce antimicrobial peptides (AMPs) to protect the host from commensal and pathogenic bacteria and provide niche factors for the adjacent ISCs (Sato, van Es et al. 2011). Mucus producing goblet cells hold up a physical barrier covering the epithelial cell layer to avoid contact with commensal or pathogenic bacteria (Johansson, Phillipson et al. 2008). IECs are the absorptive cell population responsible for nutrient supply and build a cellular barrier using cell-cell and cell-matrix interactions (Peterson and Artis 2014).

In the context of GVHD, the intestinal tract plays a critical role. Conditioning therapy like TBI and/or chemotherapy leads to massive intestinal damage which is one of the starting points of GVHD pathogenesis. Several studies showed that the extent of the initial intestinal damage correlates with disease intensity of GVHD in mice and humans (Hill and Ferrara 2000, Johansson and Ekman 2007). Translocation of PAMPs and DAMPs upon intestinal damage initiate the release of pro-inflammatory cytokines. Moreover, conditioning therapy induces changes to the intestinal microbiota and loss of diversity which was associated with poor outcome after allo-HSCT (Peled, Hanash et al. 2016, Peled, Gomes et al. 2020). During phases II and III of GVHD development, the intestine is also central: allogeneic T cells can be detected in Peyer's patches as early as 3 days after transplantation and spread throughout the intestines starting on day 4 (Beilhack, Schulz et al. 2005) where they contribute to further tissue damage. This results in even more immune activation and can be interpreted as "vicious circle" of immune activation and immune mediated tissue damage.

1.4 Objectives

The broad use of allo-HSCT as a curative therapy for hematologic malignancies is limited by GVHD which causes significant morbidity and mortality. The intestinal tract is a central site for disease development and at the same time target organ of GVHD.

Type I Interferons have been shown to limit intestinal inflammation (Katakura, Lee et al. 2005, Yang, Kim et al. 2016) and promote regeneration in epithelial surfaces like skin wounds (Gregorio, Meller et al. 2010). A major IFN-I inducer is the cGAS-STING pathway sensing dsDNA, which can potentially be released from bacteria or viruses, but also from host tissue like the damaged intestine.

For the development of new therapeutic approaches, a better understanding of inflammatory and regenerative processes in the intestines during GVHD is essential. At the same time, (murine) GVHD is a suitable model to investigate intestinal barrier loss and immune mediated tissue damage in general.

Using murine GVHD models and intestinal organoid cultures, this work aims to answer the following questions:

- Does cGAS-STING-signaling influence GVHD-associated morbidity and mortality?
- Is allo-HSCT-related – e.g. by radiation therapy as part of conditioning and immune mediated as part of allogeneic bone marrow transplantation – intestinal damage affected by cGAS-STING activation?
- If so, does cGAS-STING-signaling modulate intestinal epithelial regeneration and can we observe an impact on the intestinal stem cell niche?

2 Materials and methods

2.1 Materials

2.1.1 Instruments and devices

Accu jet pro	Brand	Wertheim, Germany
Analytical balance, Denver Instrument SI-64	Denver Instruments	Denver, USA
Analytical balance, Kern 440-35N	Kern & Sohn GmbH	Balingen-Frommern, Germany
Cell culture laminar flow HERASafe KS	Thermo Fisher Scientific	Waltham, USA
Cell-culture CO2 Incubator	Binder	Tuttlingen, Germany
Eppendorf Centrifuge 5810R	Eppendorf	Hamburg, Germany
Eppendorf Centrifuge 5417R	Eppendorf	Hamburg, Germany
FACS BD LSR II	BD Biosciences	Heidelberg, Germany
Illumina MiSeq platform	Illumina	San Diego, USA
Light Cycler® 480 II	Roche Molecular Systems	Pleasanton, USA
MACS MultiStand	Miltenyi Biotec	Bergisch Gladbach, Germany
MidiMACS Seperator	Miltenyi Biotec	Bergisch Gladbach, Germany
Mithras LB 940 Multimode Microplate Reader	Berthold Technologies	Bad Wildbad, Germany
Mouse Irradiation Unit	Gulmay Medical	Byfleet, United Kingdom
Nanodrop ND-1000 Spectrophotometer	Thermo Fisher Scientific	Waltham, USA
QuadroMACS Seperator	Miltenyi Biotec	Bergisch Gladbach, Germany
Qubit® 2.0 Fluorometer	Thermo Fisher Scientific	Waltham, USA
Shaker	Thermo Fisher Scientific	Waltham, USA
Thermocycler - PCR machine	Bio-Rad	Berkeley, USA
TissueLyser II	Qiagen	Hilden, Germany
Vortex-Genie 2	Scientific Industries	Bohemia, USA
Waterbath	Memmert GmbH	Schwabach, Germany
Zeiss Axio Observer Z1	Carl Zeiss AG	Oberkochen, Germany

Zeiss Axiovert 40C	Carl Zeiss AG	Oberkochen, Germany

2.1.2 Reagents

Aqua ad injectabilia	B. Braun Melsungen	Melsungen, Germany
Bovine Serum Albumin (BSA)	PAN-Biotech	Aidenbach, Germany
Chloroform	Sigma Aldrich	St. Louis, USA
Dimethyl sulfoxide (DMSO)	Sigma Aldrich	St. Louis, USA
Dulbecco's PBS	Sigma Aldrich	St. Louis, USA
Ethanol	Sigma Aldrich	St. Louis, USA
Ethylenediaminetetraacetic acid (EDTA), 0.5M	Invitrogen	Carlsbad, USA
Fluorescein Isothiocyanate-Dextran FD4	Sigma Aldrich	St. Louis, USA
In vivo-jetPEI®	Polyplus transfection	Illkirch-Graffenstaden, France
Lipofectamine 2000	Invitrogen	Carlsbad, USA
Low-TOX-M rabbit complement	Cedarlane Laboratories	Burlington, Canada
Methylthiazolyldiphenyl-tetrazolium bromide (MTT)	Sigma Aldrich	St. Louis, USA
PBS	Sigma Aldrich	St. Louis, USA
RBC lysis buffer, GDEXTM II	Intron Biotechnology	Seongnam, South Korea
TRIzol	Thermo Fisher Scientific	Waltham, USA
Trypan blue (0.4%) (gibco)	Thermo Fisher Scientific	Waltham, USA
TrypLE (gibco)	Thermo Fisher Scientific	Waltham, USA
Trypsin (0,05%) (gibco)	Thermo Fisher Scientific	Waltham, USA

2.1.3 Cell culture media and reagents

Advanced Dulbecco's Modified Eagle Medium/Ham's F-12 (DMEM/F-12) (gibco)	Thermo Fisher Scientific	Waltham, USA
B-27 supplement 50X (gibco)	Thermo Fisher Scientific	Waltham, USA
Corning® Matrigel® Growth Factor Reduced (GFR)	Corning	New York, USA

Basement Membrane Matrix, Phenol Red-Free, LDEV-Free		
Dulbecco's Modified Eagle Medium (DMEM) (gibco)	Thermo Fisher Scientific	Waltham, USA
Fetal Bovine Serum (FBS)	PAN Biotech	Aidenbach, Germany
GlutaMAX™ Supplement 100X (gibco)	Thermo Fisher Scientific	Waltham, USA
N-2 supplement 100X (gibco)	Thermo Fisher Scientific	Waltham, USA
N-2-hydroxyethylpiperazine-N-2-ethane sulfonic acid (HEPES) 1M (gibco)	Thermo Fisher Scientific	Waltham, USA
N-Acetyl-L-cysteine	Sigma Aldrich	St. Louis, USA
Opti-MEM® I Reduced-Serum Medium (gibco)	Thermo Fisher Scientific	Waltham, USA
Pencillin 10000U/ml + Streptomycin 10000µg/ml	Thermo Fisher Scientific (gibco)	Waltham, USA
Recombinant Murine EGF	PeproTech	Rocky Hill, USA
Recombinant Murine Noggin	PeproTech	Rocky Hill, USA
Roswell Park Memorial Institute (RPMI) 1640 Medium (gibco)	Thermo Fisher Scientific	Waltham, USA
Sodium pyruvate 100mM (gibco)	Thermo Fisher Scientific	Waltham, USA
Zeocin™ Selection Reagent	Thermo Fisher Scientific	Waltham, USA
β-Mercaptoethanol 50mM (gibco)	Thermo Fisher Scientific	Waltham, USA

Disposable plastic materials for in vivo experiments and cell culture were purchased from:

Becton Dickinson (Heidelberg, Germany), Braun (Melsungen, Germany), Eppendorf (Hamburg, Germany), Falcon (Heidelberg, Germany), Nunc (Rochester, USA), Sarstedt (Nümbrecht, Germany), Thermo Scientific (Walham, USA), VWR (Ismaning, Germany).

2.1.4 Stimuli

Interferon Stimulatory DNA (ISD)	Invivogen	San Diego, USA
Recombinant mouse Interferon Beta	PBL	Piscataway, USA

2.1.5 Kits

Invitrogen™ SuperScript™ II Reverse Transcriptase Kit	Thermo Fisher Scientific	Waltham, USA
QIAamp Circulating Nucleic Acid Kit	Qiagen	Hilden, Germany
Qubit™ dsDNA HS Assay Kit	Thermo Fisher Scientific	Waltham, USA
Rneasy Mini Kit	Qiagen	Hilden, Germany

2.1.6 Antibodies

FACS		
Alexa Fluor® 647 anti-mouse CD24 Antibody (clone M1/69)	Biolegend	San Diego, USA
PE/Cyanine7 anti-mouse CD326 (Ep-CAM) Antibody (clone G8.8)	Biolegend	San Diego, USA
T-cell depleted Bone Marrow		
InVivoMAb anti-mouse Thy1.2 (CD90.2) (clone 30H12)	BioXCell	Lebanon, USA
Blocking		
InVivoMAb anti m IFNalphaR1 (clone-MAR1-5A3)	BioXCell	Lebanon, USA
InVivoMAb Mouse IgG1 (clone MOPC-21)	BioXCell	Lebanon, USA
Microbeads		
Monoclonal anti-mouse CD4 antibodies (L3T4; isotype: rat IgG2b)	Miltenyi Biotec	Bergisch Gladbach, Germany
Monoclonal anti-mouse CD8a (Ly-2) antibodies (isotype: rat IgG2a)	Miltenyi Biotec	Bergisch Gladbach, Germany

2.1.7 Primers

mActin	fwd CACACCCGCCACCAGTTCG rev CACCATCACACCCTGGTGC
mcGAS	fwd: GTCGGAGTTCAAAGGTGTGGA rev: GACTCAGCGGATTTCCTCGTG
mCldn4	fwd: CGCTACTCTTGCCATTACG rev: ACTCAGCACACCATGACTTG
mIFNß	fwd ATAAGCAGCTCCAGCTCCAA rev GCAACCACCACTCATTCTGA
mRegIIIγ	fwd TTCCTGTCCTCCATGATCAAAA rev CATCCACCTCTGTTGGGTTCA

2.1.8 Software

Endnote X8.2 for Mac	Clarivate	London, United Kingdom
FlowJo Version V10	BD Bioscience	Heidelberg, Germany
Graphpad Prism 6	Graphpad Software	San Diego, USA
ImageJ 10.2	Public domain	National Institutes of Health, USA
Microsoft Office for Mac	Microsoft	Redmond, USA

2.2 Methods

2.2.1 Mice

Wild-type C57BL/6, B10.BR or BALB/c mice were purchased from Jackson Laboratory (USA) or Janvier (France). *Sting*$^{gt/gt}$ and Lgr5-EGFP-IRES-creERT2 (LGR5^{GFP}) mice were purchased from Jackson Laboratory (USA). *Ifnar*$^{-/-}$ mice were provided by J. Sun (MSKCC). Mice were kept in specific pathogen-free facilities at MSKCC in New York, USA or at ZPF at Klinikum rechts der Isar in Munich, Germany. If not indicated otherwise, mice were between 6 and 8 weeks of age when experiments were started. Co-housing of wild-type and knock-out was performed for at least 7 days before experiments were started.

2.2.2 Murine allogeneic bone marrow transplantation

2.2.2.1 Recipient irradiation

Recipient mice underwent total body irradiation (TBI) at the following doses: BALB/c mice received 9Gy in 2x4.5Gy split doses, C57BL/6 mice received 11Gy in 2x5.5Gy split doses. Time between irradiation steps was 4 hours minimum. Initial weight was measured at the time point of the first irradiation dose.

2.2.2.2 Preparation of allo-graft

All following cell preparation and washing steps were performed using cRPMI media unless stated otherwise. All centrifugation steps were performed at 400g, 5min, 4°C.

T cell depleted bone marrow cells

Femora and tibiae were collected from donor mice after euthanization and all surrounding tissue removed. To obtain bone marrow cells, one end of the bones was cut and flushed from the opposite side with a 27G needle and a 5ml syringe filled with cRPMI. The marrow was collected in a 100μm strainer and mashed with a syringe plunger. After centrifugation, the cell pellet was resuspended with 1ml of RBC lysis buffer and incubated for 5 min at room temperature to eliminate red blood cells. Cells were washed with 10ml of cRPMI. T cells were depleted

by incubation with anti–Thy-1.2 for 30 minutes at 4°C, followed by incubation with Low-TOX-M rabbit complement for 40 minutes at 37°C.

CD4$^+$/CD8$^+$ T cells

Donor mice were euthanized, and spleens harvested. Splenocytes were collected by mashing the organ with a syringe plunger through a 100μm strainer. After centrifugation, the cell pellet was resuspended with 1ml of RBC lysis buffer and incubated for 5 min at room temperature to eliminate red blood cells. Cells were washed with 10ml of cRPMI followed by an additional washing step with 10 ml of MACS buffer. All following steps were performed following the manufacturer's protocol. Cells were resuspended with MACS buffer and MicroBeads. For one spleen (corresponding to approximately 10^7 cells), 450 μl of MACS buffer, 25μl of CD4 (L3T4) MicroBeads and 25μl of CD8a (Ly-2) MicroBeads were used and the suspension incubated for 15min at 4°C. After washing with 10ml of MACS buffer, splenocytes were resuspended in 500μl and separated in a LS magnetic column. To ensure sufficient purity and yield, one column was used to separate cells from a maximum of 2 spleens. CD4$^+$/CD8$^+$ cells were counted using trypan blue in a counting chamber.

2.2.2.3 Reconstitution of recipient mice after total body irradiation

After the second irradiation, mice were injected with either T cell depleted bone marrow cells (BM) only or bone marrow cells and CD4$^+$/CD8$^+$ T cells via tail vein injection. Mice generally received 5x10^6 BM cells. T cells doses depended on the transplantation model and the objective of the individual experiment and are indicated in the figure legends. After injection, mice were transferred to clean cages.

2.2.2.4 Clinical GVHD intensity and survival experiments

Mice that underwent allo-BMT were monitored for weight loss daily during the first week and every second day for the rest of the experiment. Additionally, mice were examined for GVHD intensity following a score consisting of weight, posture, fur, skin and activity. Each category was given a score of 0, 0.5, 1, 1.5 or 2 which were subsequently summed up to a clinical GVHD score. Mice that lost more than

30% of their initial weight or reached a GVHD score of 5 or higher were euthanized.

2.2.3 Treatment of mice with nucleic acids

The ratio for complexation with in vivo JetPEI was 1μg of nucleic acid on 0.16μl of in vivo JetPEI in 5% Glucose. This scheme was adapted to the number of treated mice. For one mouse receiving 25μg of ISD, the protocol was as follows: in one Eppendorf tube, 25μg of ISD were dissolved in 100μl of 5% Glucose solution. In a second tube, 4μl of in vivo JetPEI were diluted in 96μl of 5% Glucose solution. Both tubes were combined, gently vortexed and incubated for 15min at room temperature. Each mouse received a volume of 200μl via tail vein injection.

2.2.4 Isolation and culture of small intestinal organoids

2.2.4.1 ENR-Media preparation

Organoid culture media is referred to as ENR-Media (EGF-Noggin-Rspondin-Media) and was prepared as follows: advanced DMEM/F-12 containing 10mM HEPES, 100U/ml Penicillin, 100μg/ml Streptomycin, 1x GlutaMAX, 1x N2 supplement, 1x B27 supplement, 50ng/ml recombinant mEGF, 100ng/ml recombinant mNoggin, 1.25mM N-Acetyl-L-cysteine, 10% human R-spondin-1-conditioned media from R-spondin -1-transfected HEK 293T cells.

2.2.4.2 R-spondin-1-conditioned media

R-spondin-1-transfected HEK 293T cells were thawed from liquid nitrogen storage and cultured in growing medium consisting of DMEM media supplemented with 10% FBS, 100U/ml Penicillin, 100μg/ml Streptomycin and 300μg/ml Zeocin for selection of R-spondin-1 expressing cells in a 175cm^2 cell culture flask. When cells reached confluency, the flask was split into 5x 175cm^2 cell culture flasks with growing media and 1x 175cm^2 cell culture flask with growing media without Zeocin.

When the cells in the 5 flasks were confluent, growing media was replaced with conditioning media: Advanced DMEM/F-12 media containing 10mM HEPES, 100U/ml Penicillin, 100μg/ml Streptomycin, 1x GlutaMAX. After 7 days, the media

was collected, centrifuged (400g, 5min, 4°C), filtered through a 0.22μm filter and aliquots were stored at -20°C until use.
The remaining flask containing Zeocin was used to repeat the procedure or to expand cells for storage.

2.2.4.3 Small intestinal crypt isolation

All steps were performed on ice or at 4°C and the reagents used were ice cold to obtain optimal crypt viability. Small intestines were harvested, adipose tissue removed from the surface and then opened longitudinally. The luminal side was gently scraped with a glass cover slip to remove villi and feces and intestines were cut into 2mm pieces and placed into 15ml ice cold PBS in a 50ml conical tube. To wash the tissue, the tubes were vortexed for 5 seconds and PBS removed using a Pasteur pipette. 15ml of fresh PBS was added and this step was repeated once. After addition of 15ml of fresh PBS, the tubes were incubated on a rocker at 4°C for 5 min at 80/min for further washing. After removal of the supernatant, 15ml of 10mM EDTA in PBS (PBS-EDTA) were added and the tubes were incubated on a rocker at 4°C for 5 min. The supernatant was replaced with new PBS-EDTA and intestines incubated on a rocker at 4°C for another 25 min.
After PBS-EDTA incubation, the supernatant was removed and replaced with 20ml of PBS. To release crypts from the intestinal tissue, tubes were shaken vigorously 10 times and the fluid passed through a 100μm strainer in a new 50ml conical tube. All following steps were performed under sterile circumstances. Subsequently, the tubes were centrifuged (800rpm, 5min, 4°C) and the supernatant removed. 15ml of Advanced DMEM-F12 Media supplemented with 10mM HEPES, 100U/ml Penicillin, 100μg/ml Streptomycin, 1x GlutaMAX were added and the pellet resuspended by gentle shaking. Crypt concentration was determined by counting the number of intact crypts in 10μl under the microscope.

2.2.4.4 Organoid culture

After counting, the required volume of crypt suspension was transferred to a 15ml conical tube, centrifuged (1000rpm, 5min, 4°C) and the supernatant replaced with ENR-Media. Pipetting was kept to a minimum to avoid disrupting crypts to single cells. Liquid Matrigel was added at a 2:1 ratio (Matrigel : crypts in ENR-Media)

and 30µl drops plated on a 24-well non-tissue-culture-treated plate. After Matrigel polymerization in the incubator (20min, 37°C), 500µl of ENR-Media were added to each well. Media was changed at day 3 and 5 after plating. For culture of organoids isolated from mice on d8 after allo-BMT, an additional media change was performed on day 1 of the culture.

2.2.4.5 Organoid counts

Organoids were manually counted at indicated timepoints. Viable organoids were identified by their typical morphology. All viable structures per well were counted.

2.2.4.6 Determination of organoid size

Bright field images of each well were taken using a Zeiss Axio Observer Z1 microscope at indicated timepoints. All organoids of 4 representative regions per well were analyzed using the freehand selection tool of ImageJ software. Organoid size was assessed by measurement of the area and perimeter covered by the organoids.

2.2.5 MTT assay

Organoid viability was quantified by colorimetric analysis of metabolically active cells using Methylthiazolyldiphenyl-tetrazolium bromide (MTT). Mitochondrial dehydrogenases of viable cells reduce yellow MTT solution to a dark-blue MTT formazan which accumulates inside the cell. After lysis of the cells and solubilizing with acidified isopropanol, the concentration of the MTT formazan can be measured at 590nm.

ENR-Media from organoid cultures was removed and replaced with the MTT-solution (0.5mg/ml MTT in advanced DMEM-F12). Plates were incubated for 3-4h at 37°C until dark blue crystals form in the organoids. MTT-solution was removed, and organoids were lyzed in 150µl of acidified isopropanol (0.1M HCl) on ice. Absorbance was measured on a plate reader at 590nm with a reference wavelength of 630nm.

2.2.6 RNA extraction of organoid cultures

After removal of ENR-Media, organoids and matrigel were lyzed by repeated pipetting with 500µl of TRIzol reagent. At least two wells were combined to obtain sufficient RNA concentrations. Lysates were stored at -20°C for short term storage or -80°C for long term storage.

2.2.7 Quantitative Real-time PCR

2.2.7.1 Cell lysis

Cells were lysed with TRIzol reagent by repeated pipetting and stored at -20°C for short term storage or -80°C for long term storage.

2.2.7.2 RNA isolation

Samples in TRIzol were thawed on ice. 100µl of Chloroform were added, mixed by vortexing and incubated for 2min at room temperature. To separate the phases, tubes were centrifuged at 12000g for 15min at 4°C. The clear upper phase containing the RNA was transferred to a new Eppendorf tube and 300µl of 70% ethanol were added followed by vortexing. The next steps follow the manufacturer's protocol (Qiagen RNeasy Mini Kit): The solution was transferred to a RNeasy Mini spin column, centrifuged at 8000g for 15sec and the flow-through discarded. The following washing steps consist of the addition of a buffer solution followed by centrifugation at 8000g for 15sec and discarding the flow-through. The first washing step was performed using 700µl of Buffer RW1, washing step two and three using 500µl of Buffer RPE. The column was then placed in a new collection tube and centrifuged for 2 min at maximum speed (20000g) to dry the column. For RNA elution, the column was transferred to a 1.5ml Eppendorf tube. 30µl of RNase-free water were carefully administered to the column membrane and incubated for 1min at room temperature. RNA was collected in the Eppendorf tube after centrifugation at 20000g for 1min. RNA yield and purity were assessed with a Nanodrop 1000 spectrophotometer.

2.2.7.3 cDNA synthesis

RNA was reversely transcribed using Superscript II Reverse Transcriptase: 11µl of eluted RNA were combined with 0.03µl of Random Primers (stock 3µg/µl), 1µl of dNTP mix (stock 10mM) and incubated at 65°C for 5min to denature the RNA's secondary structure. After addition of 4µl of first strand buffer and 0,2µl of DTT (stock 0.1M), a first annealing step took place at 25°C for 2min. 0.8µl of Superscript II Reverse Transcriptase were added and reverse transcription started in a thermal cycler: 25°C for 10min (annealing), 42°C for 50min (cDNA synthesis), 70°C for 15min (denaturation). cDNA was stored at -20°C.

2.2.7.4 Quantitative real-time PCR

Quantitative real-time PCR (often referred to as qRT-PCR or qPCR) measures fluorescence emission over time to allow quantification of a target gene sequence. We used the SYBR Green fluorescent dye, which intercalates with double-stranded DNA. During repeated amplification steps, only the target sequence flanked by specific primers is amplified and fluorescence emission correlates with the amount of inserted DNA. Normalization to a reference gene, which is not affected by experimental interventions, allows to quantify gene expression levels.

All qPCR assays were performed using a qPCR Core Kit for SYBR Green and primers were designed with the help of the Universal ProbeLibrary Assay Design Center (Roche). qPCR was performed in white 96 well plates and the experimental assay prepared as follows:

Component	Volume	Final concentration
10x reaction buffer	5 µl	1x
$MgCl_2$	3.5 µl	3.5 mM
dNTP mix	2 µl	200 µM
Forward primer	5 µl	100 nM
Reverse primer	5 µl	100 nM
HotGoldStart	0.25 µl	0.025 U/µl
Diluted SYBR	1.5 µl	
Water, PCR-grade	22.75 µl	
cDNA	5 µl	

Amplification was performed on a LightCycler 480 II system using LightCycler 480 II Software 1.5.0 SP4. The thermocycler programming was as follows:

Cycles	Description	Target temperature	Hold time
1	Pre-Incubation	95 °C	10 min
40	Denaturation	95 °C	15 s
	Annealing	60 °C	20 s
	Elongation	72 °C	40 s
1	Cooling	40 °C	30 s

2.2.7.5 qPCR analysis

Housekeeping gene β-actin was used for normalization and relative expression levels were calculated using the $2^{-\Delta\Delta CT}$-method:

$\Delta C_T = C_T$ (target) - C_T (β-actin)

$\Delta\Delta C_T = \Delta C_T$ (intervention) - ΔC_T (control)

relative expression = $2^{-\Delta\Delta CT}$

2.2.8 16S rRNA sequencing

2.2.8.1 Principle of 16S rRNA sequencing

16S rRNA sequencing is used to profile the intestinal microbial composition, also called microbiota. Prokaryotic cells differ from eukaryotic cells in their ribosomal structure which is defined by the size and composition of their subunits. The process of mRNA translation takes place between the two ribosomal subunits that are built of proteins and ribosomal RNA (rRNA). The so called 70S ribosome of prokaryotes is composed of a large 50S subunit and a small 30S subunit, whereas the 80S eukaryotic ribosome is characterized by a 60S and a 40S subunit. The gene sequences (i.e. DNA sequence) of the 16S rRNA within the 30S subunit are highly conserved within bacterial species. This allows identification of phylogenetic trees, meaning characterization of bacterial phyla, classes, families, genus and species and quantification of the different subsets. 16S rRNA sequencing gives insights in the diversity and proportions of the intestinal bacterial microbiota.

2.2.8.2 DNA extraction

DNA was isolated from mouse fecal samples using phenol-chloroform extraction. Stool pellets were collected and stored at -20°C in cryovials. After thawing the samples, 400µl of zirconia/silica beads, 500µl of SDS DNA extraction buffer and 400µl of phenol/chloroform were added. Tubes were transferred to a bead beater and homogenized for 2min at maximum speed. Tubes were then centrifuged at maximum speed for 2min at 4°C, 300µl of the top phase transferred to tubes filled with 300µl of phenol/chloroform and carefully mixed. After 2min centrifugation at maximum speed for 2min, 200µl of the top phase were transferred to new tubes filled with 20µl of sodium acetate (3M) and 440µl of 95% ethanol. The content was carefully mixed and the tubes placed at -80°C for 60min. To precipitate the DNA, the samples were centrifuged at maximum speed at 4°C for 5min, the supernatant thoroughly decanted and the tubes dried in a SpeedVac concentrator. The DNA was eventually dissolved in 200µl TE buffer.

2.2.8.3 DNA sequencing and analysis

Sequencing of the 16S rRNA gene, data processing and classification were performed by Melissa Docampo and Robert R. Jenq in collaboration with the Molecular Microbiology core facility at Memorial Sloan Kettering Cancer Center (MSKCC) in New York, USA.

In short, specimen were analyzed on a Illumina MiSeq platform for sequencing of the V4-V5 region of the 16S rRNA gene. Sequence data were compiled and processed using mothur version 1.34 (Schloss, Westcott et al. 2009), screened and filtered for quality (Gilbert, Schloss et al. 2011), then classified to the species level (Wang, Garrity et al. 2007) using a modified form of the Greengenes reference database (DeSantis, Hugenholtz et al. 2006).

2.2.9 Measurement of plasma DNA levels

24h after TBI (9Gy) or 8 days after allo-BMT (BM + T cells), blood was collected from the facial vein of BALB/c mice into EDTA coated tubes. The blood was then transferred to Eppendorf tubes, centrifuged to separate plasma from cells and the plasma frozen at -20°C. For DNA extraction, the QIAamp Circulating Nucleic Acid kit was used following the manufacturer's protocol. As DNA concentrations

were too low for quantification with a Nanodrop device, a Qubit fluorometer and Qubit dsDNA HS Assay for high-sensitivity detection of double-stranded DNA was used instead following the manufacturer's protocol.

2.2.10 FITC Dextran translocation assay

After food and water withdrawal for 8h, mice were administered FITC-Dextran by oral gavage. The amount of FITC Dextran in water (concentration 50mg/ml) given to each mouse was dependent on the body weight (750mg/kg body weight). Blood was collected 4.5h later, the plasma separated via centrifugation (10min, 8800rcf) and diluted at a 1:1 ratio with PBS before analysis in a fluorescence microplate reader at an excitation wavelength of 485 nm and an emission wavelength of 535 nm. Plasma concentrations were determined using a standard dilution series of known concentrations.

2.2.11 Flow cytometry of small intestinal crypts and organoids

Crypt cells or organoids were harvested and incubated in 1ml of TrypLE at 37 °C for 10 minutes. Repeated pipetting was performed to obtain a single cell suspension which was then passed through a 40μm strainer. Cells were washed with FACS-Buffer (1x PBS, 3% FCS) and counted.
Staining was started with a Fixable Viability Dye eFluor 506 (eBioscience) at a concentration of 1:1000 and Fc-block (1:200) in 1xPBS for 20 min at 4 °C in the dark. Subsequently, fluorescent antibodies against surface markers EPCAM for epithelial cells (anti-mouse EPCAM – PE-Cy7) and CD24 for Paneth cells (anti-mouse CD24 – Alexa Fluor 647) at a dilution of 1:400 in 1xPBS were added and incubated at 4 °C in the dark. After washing 2x with FACS-Buffer, cells were resuspended in 100μl of FACS-Buffer and analyzed in a FACS BD LSR II (BD Bioscience). The gating strategy was as follows: single, viable, EPCAM+. Gating on Lgr5+ and CD24+SSChigh cells is shown in the figure.

2.2.12 Histopathologic analysis

8 days after allo-BMT, animals were euthanized and small and large intestines, liver and skin harvested. Samples were fixed in formalin. Embedding in paraffin,

sectioning and hematoxylin and eosin (HE) staining were performed by the Pathology core facility at MSKCC, New York, USA.
Slides were analyzed by an experienced pathologist in the field of human and murine GVHD, Chen Liu, MD, PhD at Rutgers University, New Jersey, USA in a blinded manner. Parameters of scoring are depicted in **Table 1**.

2.2.13 Statistics

Animal numbers are shown in the figures. Survival was analyzed using the Log-rank test. Differences between two experimental groups were analyzed using two-tailed, unpaired t-test. Comparison of 3 or more groups was performed using ordinary one-way Anova with Dunett's multiple comparisons test. Data are presented as mean ± SEM. Significance was set at * $p < 0,05$, ** $p < 0,01$, *** $p < 0,001$. Statistical calculations were made using Prism 6 for Mac OS X (GraphPad Software, Inc.)

3 Results

3.1 STING signaling protects allo-BMT recipient mice from GVHD

3.1.1 Endogenous STING signaling protects from GVHD related mortality and morbidity

In a first experiment, we aimed to determine whether STING signaling has an impact on the outcome after allo-HSCT. We therefore used STING deficient mice for murine allogeneic bone marrow transplantation (allo-BMT) experiments. These so-called STING-goldenticket (*Sting*$^{gt/gt}$) mice are bred on a C57BL/6 background and carry a single nucleotide variant of STING leading to a missense mutation and thus fail to produce the STING protein (Sauer, Sotelo-Troha et al. 2011). To study the relevance of STING in GVHD development we used a major-mismatch mouse model of GVHD with B10.BR donor mice ($H2^k$) and C57BL/6 WT or *Sting*$^{gt/gt}$ mice (both $H2^b$) as recipients (Schroeder and DiPersio 2011).
All *Sting*$^{gt/gt}$ mice that were transplanted with TCD BM and T cells died from GVHD until day 50, whereas 40% of WT mice survived over the 90-day time course (**Fig. 3**). Although it seems that in the BM control groups STING deficiency could represent a survival benefit, this difference was not statistically significant. Apparently, endogenous STING signaling protects from GVHD associated mortality in mice.

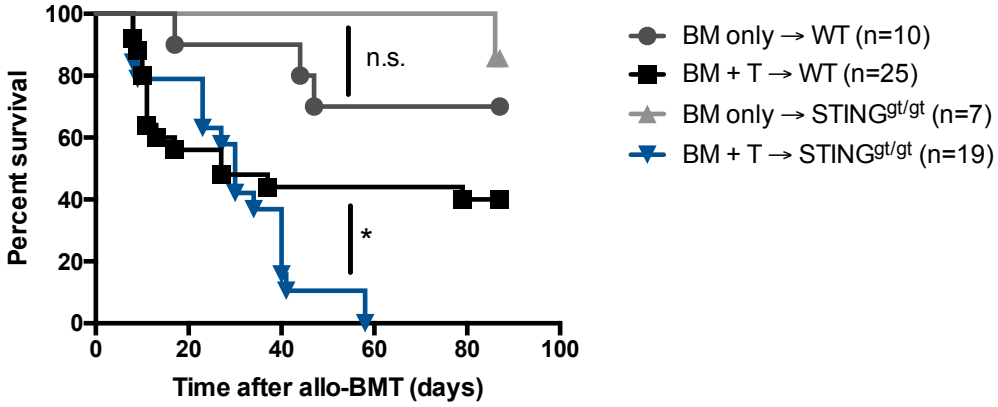

Fig. 3. STING signaling protects mice from GVHD related mortality Co-housed C57BL/6 WT or *Sting*$^{gt/gt}$ mice underwent 11Gy TBI and were transplanted with either $5x10^6$ TCD BM cells alone or with $1x10^6$ T cells from donor B10.Br mice. Recipient mice were monitored 90 days for survival. Pooled data from 2 independent experiments. Animal numbers per group are depicted in the figure. Comparison of survival curves was analyzed using Log-rank test, significance was set at * $p < 0,05$, ** $p < 0,01$, *** $p < 0,001$

In murine GVHD models, morbidity can be quantified by monitoring weight loss and other clinical symptoms of GVHD such as appearance of the fur and skin, and the mice' activity and behavior. We observed that *Sting*$^{gt/gt}$ allo-HSCT recipients exhibited greater weight loss over time than did their WT controls (**Fig. 4A**). On d8 after transplantation, when the first nadir of weight loss is reached, *Sting*$^{gt/gt}$ mice had lost 17.6% of their initial weight vs. 15.7% in the WT control group (**Fig 4B**). Clinical scoring of GVHD associated symptoms revealed that *Sting*$^{gt/gt}$ recipients developed worse GVHD within the first 4 weeks (**Fig. 4C**) and on d8 after allo-HSCT (**Fig. 4D**). Interestingly, also the *Sting*$^{gt/gt}$ mice receiving BM only also lost more weight on d8 and showed a higher clinical GVHD intensity than did WT mice (**Fig. 4B, D**). Although being not statistically significant, maybe due to low numbers in the BM control groups, this could be a hint towards a protective role of STING signaling and IFN-I in the phase of early damage after TBI.

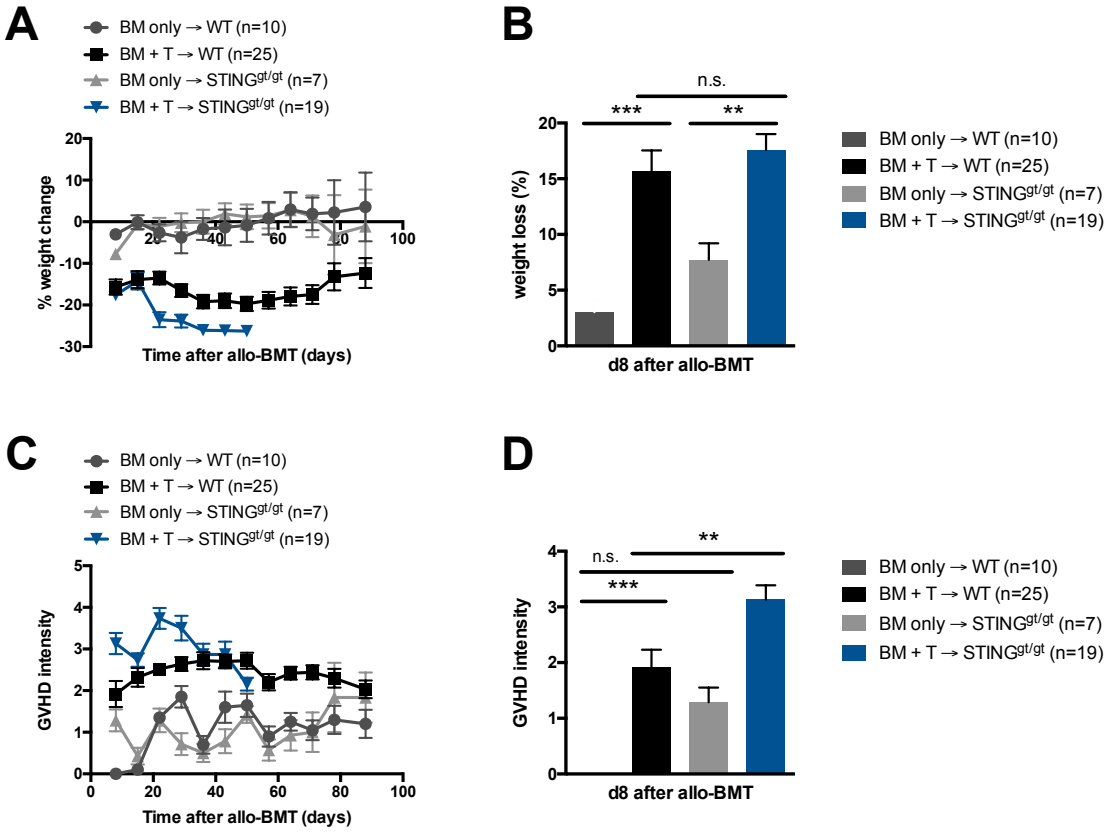

Fig. 4. STING signaling protects mice from GVHD related morbidity

Co-housed C57BL/6 WT or *Sting*$^{gt/gt}$ mice underwent 11Gy TBI and were transplanted with either 5x10^6 TCD BM cells alone or with 1x10^6 T cells from donor B10.Br mice. **A** Relative weight change of recipient mice compared to the weight on d0 over time. **B** Percent weight loss on d8 after allo-BMT. **C** Clinical GVHD intensity

of recipient mice over time. **D** Clinical GVHD intensity on d8 after allo-BMT. Pooled data of 2 independent experiments. Animal numbers per group are depicted in the figure. Experiments were analyzed using one-way ANOVA, significance was set at * p < 0,05, ** p < 0,01, *** p < 0,001

3.1.2 Differences in GVHD intensity are not associated with changes in the microbiota of *Sting*$^{gt/gt}$ mice

The intestinal microbiota has attracted growing attention in the last years. Increasing evidence highlights that the intensity and profile of immune responses is dependent on the intestinal microbial composition (Honda and Littman 2016). Genetically modified mouse strains have been shown to differ in their microbiota compared to WT mice, which has been associated with increased susceptibility for inflammatory bowel disease (Elinav, Strowig et al. 2011, Lamas, Richard et al. 2016). For GVHD, it was shown that microbial derived short-chain fatty acids like butyrate dampened GVHD mortality (Mathewson, Jenq et al. 2016) and that the use of broad-spectrum antibiotics worsened GVHD-associated mortality in humans and mice (Shono, Docampo et al. 2016).

Using littermates as controls for mouse experiments can be seen as gold-standard when aiming to reduce effects of the microbiota on the observed phenotype (McCoy, Geuking et al. 2017). Murine allo-BMT experiments, especially for survival analyses, often require larger group sizes to observe distinct phenotypes between groups and obtain reproducible results. We hence decided to use co-housed mice when the exclusive use of littermates was not possible to limit possible effects of altered microbiota. Mice were co-housed for a minimum of 7 days before starting the experiments.

In the understanding of GVHD pathogenesis, the release of DAMPs and PAMPs during pre-transplant conditioning results in immune activation. Differences in the intestinal microbiota could potentially lead to changes in the amount and types of PAMPs and DAMPs released after TBI. Given the role of STING as nucleic acid sensor and the potential important release of DNA after TBI, we wanted to test whether *Sting*$^{gt/gt}$ mice had an altered intestinal microbiota that could be responsible for our phenotype in GVHD. We collected stool samples from C57BL/6 WT and co-housed *Sting*$^{gt/gt}$ mice for 16S-rRNA sequencing which allows quantitative assessment and subsequent comparison of the intestinal

bacterial composition. In the resulting plot each bar represents one mouse and displays the most frequent bacterial genus as a differently colored proportion. Our analysis revealed that *Sting*$^{gt/gt}$ mice didn't differ from WT controls in their intestinal microbial composition (**Fig. 5**) and that our co-housing strategy ensured similarity of microbiota at the starting points of our experiments. Nonetheless, this does not exclude a role of a genotype-specific microbiota regulation during the course of an allo-BMT, but this requires further studies.

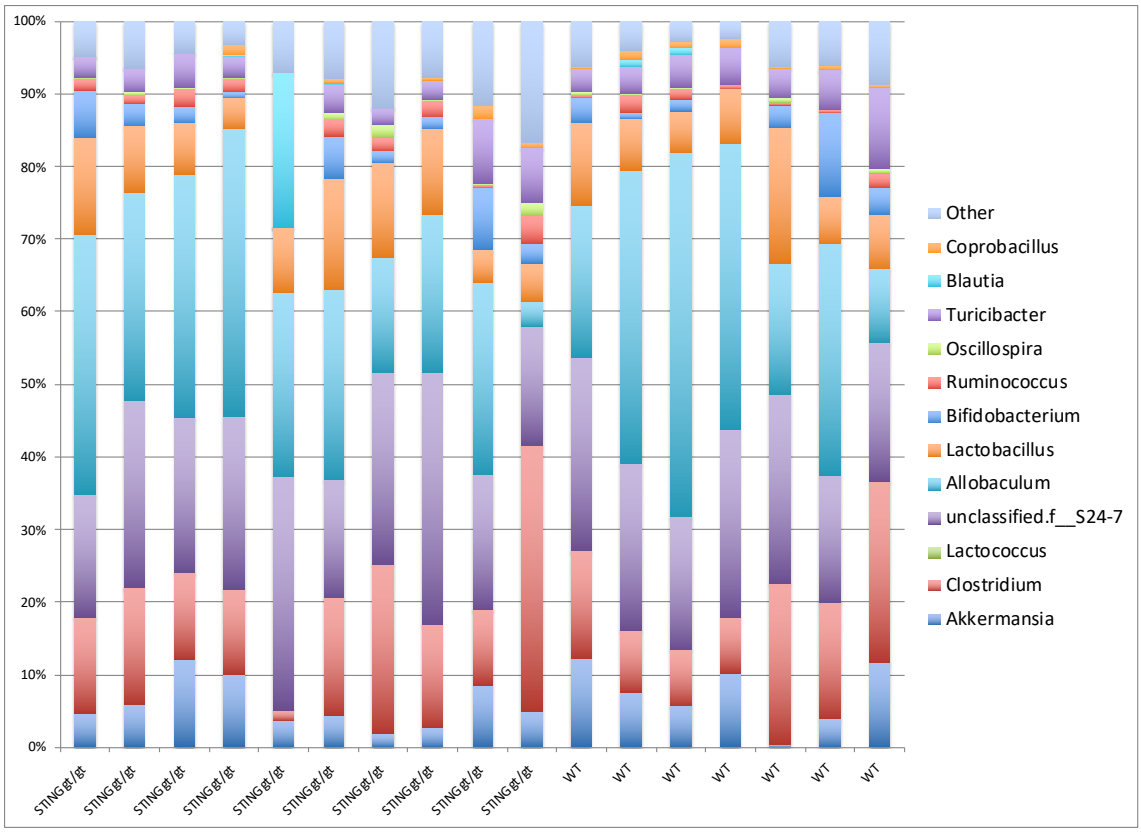

Fig. 5. 16S-rRNA sequencing reveals similar intestinal microbiota of WT and *Sting*$^{gt/gt}$ mice

Relative abundance of bacterial genus in fecal samples of co-housed C57BL/6 WT and *Sting*$^{gt/gt}$ mice. One representative of two independent experiments is shown.

3.1.3 Total body irradiation and allo-BMT lead to a systemic release of DNA

As described in the introduction, the cGAS-STING pathway has been identified as IFN-I producer in response to cytosolic DNA or cyclic dinucleotides. Some sources of these intracellular ligands have been identified, such as *Herpes simplex virus 1* (HSV-1) or *L. monocytogenes* (Ishikawa and Barber 2008, Sauer, Sotelo-Troha et al. 2011). But still in many cases such as immune disorders or

cancer autoimmunity, the exact ligands of cGAS-STING and the mechanism of cell entry remain unknown.

TBI leads to systemic damage to the organism and cell destruction, especially to tissues with high cellular turn-over like the intestines (Gu, Chen et al. 2020). We hypothesized that this damage would lead to a release of DNA from dying cells and wondered whether we could detect increased levels of circulating cell-free DNA.

Extracting cell-free DNA from solid tissue is highly complicated as processing of tissue or cells will lead to cellular damage and release of DNA. At the same time, DNases are ubiquitous enzymes that digest cell-free DNA. We decided to use blood samples from mice that underwent TBI or allo-BMT and measure DNA levels in the plasma. Making use of a highly sensitive quantification kit we were indeed able to quantify DNA in the serum of untreated WT mice at a concentration of 17.3 ng/μl. TBI increased these levels of DNA approximately 2.3-fold to 39.1 ng/μl 24h after irradiation (**Fig. 6**). In a third group, we analyzed serum of allo-BMT recipients 8 days after transplantation and also found a trend towards increased levels of DNA in the serum. These results prove that pre-transplant conditioning leads to a systemic release of cell-free DNA which could act as cGAS-STING ligand and induce IFN-I production.

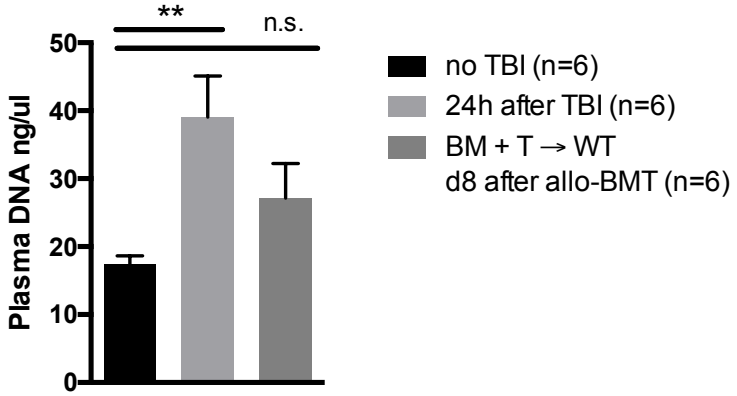

Fig. 6. Plasma levels of circulating DNA increase after TBI and allo-BMT BALB/c mice were either left untreated, underwent 9 Gy TBI alone or followed by transplantation of $5x10^6$ BM cells with $0,5x10^6$ T cells. At indicated time points blood samples were taken and plasma DNA levels quantified. Pooled data from 3 independent experiments. Animal numbers per group are depicted in the figure. Results were analyzed using one-way ANOVA and significance was set at * $p < 0,05$, ** $p < 0,01$, *** $p < 0,001$

3.1.4 cGAS-STING ligand ISD can be used therapeutically to prevent GVHD

The cGAS-STING pathway can be selectively activated by its specific ligand ISD when delivered to the cytosol. We have shown that conditioning therapy leads to a systemic release of DNA and that STING signaling plays a beneficial role in the development of GVHD. Hence, we wanted to test whether this effect could be exploited therapeutically. From previous experiments investigating RIG-I/MAVS and its activator 3pRNA we knew that it is crucial to administer the nucleic acid ligand prior to allo-BMT to obtain therapeutic effects (Fischer, Bscheider et al. 2017). In our murine GVHD model, we treated mice with ISD and monitored them for survival and GVHD severity. We chose to inject a single dose of ISD intravenously on d-1 before transplantation and complexed it with a cationic polymer-based transfection reagent (in vivo-jetPEI®) to ensure cytosolic delivery. Delivery to the cytosol is essential because of the cytosolic localization of cGAS and injection of nucleic acids without prior complexation would lead to recognition via endosomal TLRs and not cGAS-STING (Murphy and Weaver 2016).
Survival experiments showed that allo-BMT recipients treated with TCD BM + T cells and ISD on d-1 exhibited significantly improved survival compared to untreated controls (**Fig. 7)**.

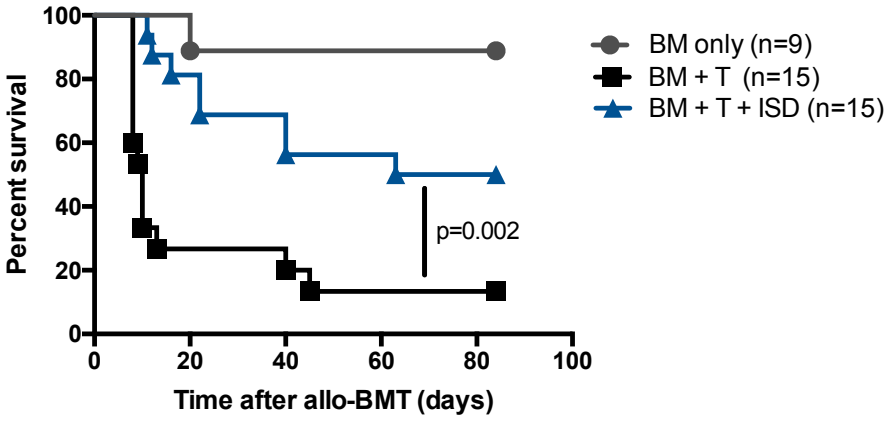

Fig. 7. cGAS-STING activation protects mice from GVHD related mortality

Co-housed C57BL/6 WT mice underwent 11Gy TBI and were transplanted with either $5x10^6$ TCD BM cells alone or with $1x10^6$ T cells from donor B10.Br mice. On the day before allo-BMT, recipients were treated with 25µg of ISD in indicated groups. Mice were monitored 90 days for survival. Pooled data from 2 independent experiments. Animal numbers per group are depicted in the figure. Comparison of survival curves was analyzed using Log-rank test, significance was set at * $p < 0,05$, ** $p < 0,01$, *** $p < 0,001$

Additionally, ISD treated mice lost significantly less weight on d8 after allo-BMT (**Fig. 8B**) and displayed lower clinical intensity of GVHD (**Fig. 8D**) than did their co-housed untreated controls. Importantly, these differences of weight loss and of GVHD associated morbidity were constant over the 90-days period of the experiment (**Fig. 8A, C**). Apparently, cGAS-STING signaling can be exploited therapeutically when administered prior to allo-BMT and subsequently reduces GVHD associated morbidity and mortality.

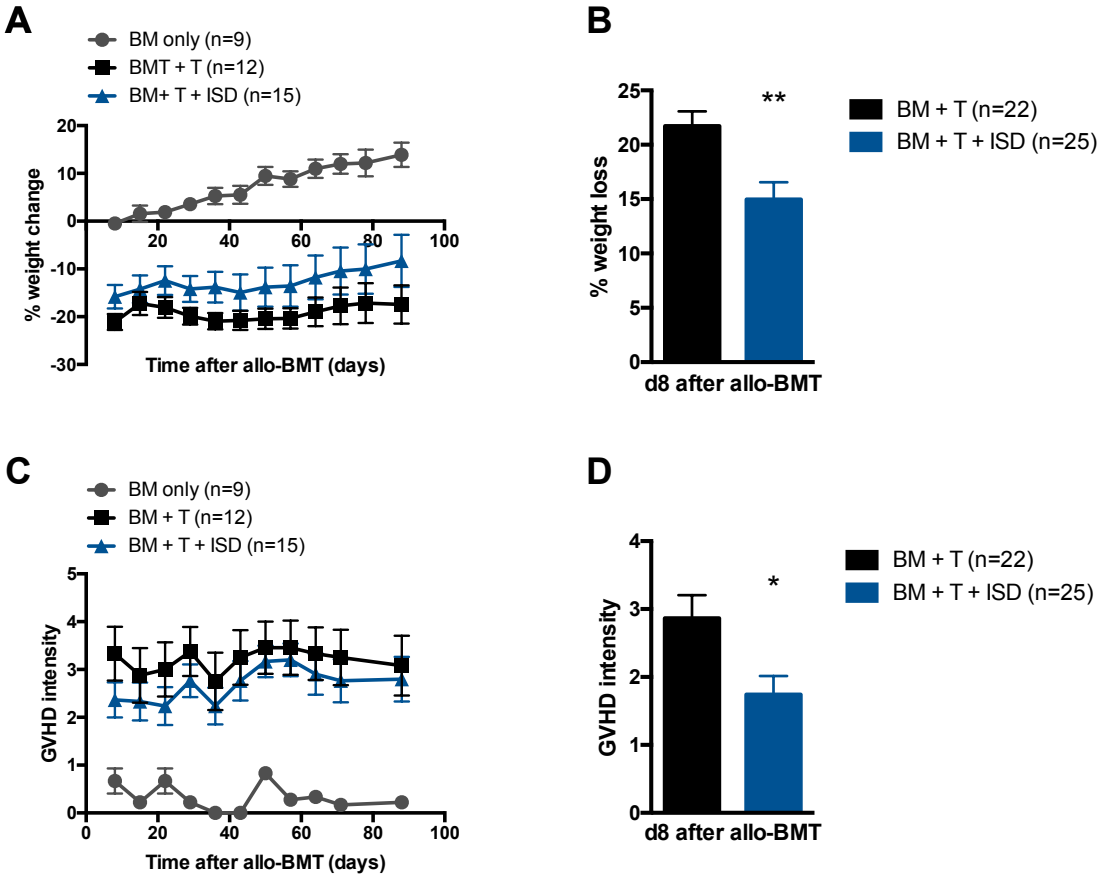

Fig. 8. cGAS-STING activation protects mice from GVHD related morbidity

Co-housed C57BL/6 WT mice underwent 11Gy TBI and were transplanted with either $5x10^6$ TCD BM cells alone or with $1x10^6$ T cells from donor B10.Br mice. On the day before allo-BMT, recipients were treated with 25µg of ISD in indicated groups. **A** Relative weight change of recipient mice over time. Data of 2 independent experiments. **B** Percent weight loss on d8 after allo-BMT. Data of 3 independent experiments. **C** Clinical GVHD intensity of recipient mice over time. Data of 2 independent experiments. **D** Clinical GVHD intensity on d8 after allo-BMT. Data of 3 independent experiments. Animal numbers per group are depicted in the figure. Experiments were analyzed using two-tailed unpaired t-test, significance was set at * $p < 0,05$, ** $p < 0,01$, *** $p < 0,001$

3.2 STING activation limits small intestinal GVHD and protects the small intestinal barrier

The cGAS-STING pathway's ability to sense DNA and induce IFN-I responses has been shown to modulate a broad range of inflammatory and neoplastic diseases (Motwani, Pesiridis et al. 2019). Still, a potential role in modulating intestinal inflammation remains unclear.

Recent work has shown that chronic viral infections and elevated systemic IFN-I levels in mice resulted in increased cellular turnover in low- and high-turnover epithelial organs like kidney, liver, salivary glands and small intestine (Sun, Miyoshi et al. 2015). These effects of IFN-I were associated with improved healing of small intestinal ulcers in mice after diclofenac induced gut damage (Sun, Miyoshi et al. 2015). Another study linking IFN-I and intestinal damage has shown that the presence of commensal enteric viruses dampens DSS-induced colitis in mice (Yang, Kim et al. 2016). This reduction of intestinal inflammation was mediated by TLR-3 and TLR-7-dependent production of IFN-β by gut-resident plasmacytoid dendritic cells (pDCs) (Yang, Kim et al. 2016).

We could show that endogenous STING signaling, and prophylactic activation of cGAS-STING have beneficial effects on allo-BMT recipients. Given the anti-inflammatory effect of IFN-I in the intestines and the intestines' central role in GVHD development, we were motivated to investigate potential effects of STING signaling on the intestinal barrier.

3.2.1 Prophylactic STING activation reduces damage to the small intestine

GVHD target organs include the small and large intestine, the liver and the skin. In a first step, we analyzed early GVHD-related organ damage in murine allo-BMT recipients. On day 8 after allo-BMT, we isolated tissue from recipient mice and used hematoxylin and eosin-stained slides for examination. Analyses were performed by an experienced pathologist in the field of GVHD, Chen Liu, MD, PhD (Kim, Terwey et al. 2008, Kappel, Goldberg et al. 2009, Ghosh, Holland et al. 2013, Lindemans, Calafiore et al. 2015, Shono, Docampo et al. 2016). Histologic criteria for quantification of GVHD intensity were specific for each target organ (**Tab. 1**) and add up to a score.

Small Bowel		**Large Bowel**		**Liver**	
Architecture	Villus blunting	**Architecture**	Crypt regeneration	**Portal Triads**	Portal tract expansion
	Crypt regeneration		Surface erosion		Neutrophil infiltrate
	Surface erosion		Ulceration		Mononuclear infiltrate
	Ulceration		Lamina propria inflammation	**Bile Ducts/Ductules**	Mononuclear infiltrate of epithelium
	Lamina propria inflammation		Atrophy (chronic)		Nuclear pleomorphism
	Atrophy (chronic)		Crypt branching (chronic)		Cytoplasmic eosinophilia
	Endocrine cell excess (chronic)		Endocrine cell excess (chronic)		Nuclear multilayering
	Paneth cell excess (chronic)		Paneth cell excess (chronic)		Pyknotic duct cells
Epithelial Cytology	Vacuolization	**Epithelial Cytology**	Vacuolization		Intraluminal epithelial cells
	Loss of microvillus brush order		Attenuation (from columnar)		Other intraluminal cells
	Attenuation (from columnar)		Apoptosis	**Vascular**	Endothelialitis
	Apoptosis		Sloughing into lumen		Mononuclear cells around CV
	Sloughing into lumen		Lymphocytic infiltrate	**Hepatocellular damage**	Confluent necrosis
	Lymphocytic infiltrate		Neutrophilic infiltrate		Acidophilic bodies
	Neutrophilic infiltrate				Mitotic figures
Skin					Foamy change
Number of apoptotic cells per millimeter					Ballooning degeneration
					Neutrophil accumulations
					Macrophage aggregates
					Macrocytosis (regeneration)

Table 1. List of histopathologic criteria defining GVHD intensity in target organs small bowel, large bowel and liver. Each of the listed criteria obtains a score between "0" if not present and "4" if most distinct. The values for each parameter are added to obtain a histopathological "GVHD score" for the specific organ.

We observed that mice that had been pre-treated with ISD on the day before allo-BMT showed a significantly lower intensity of small intestinal GVHD compared to co-housed untreated control mice (**Fig. 9A**).

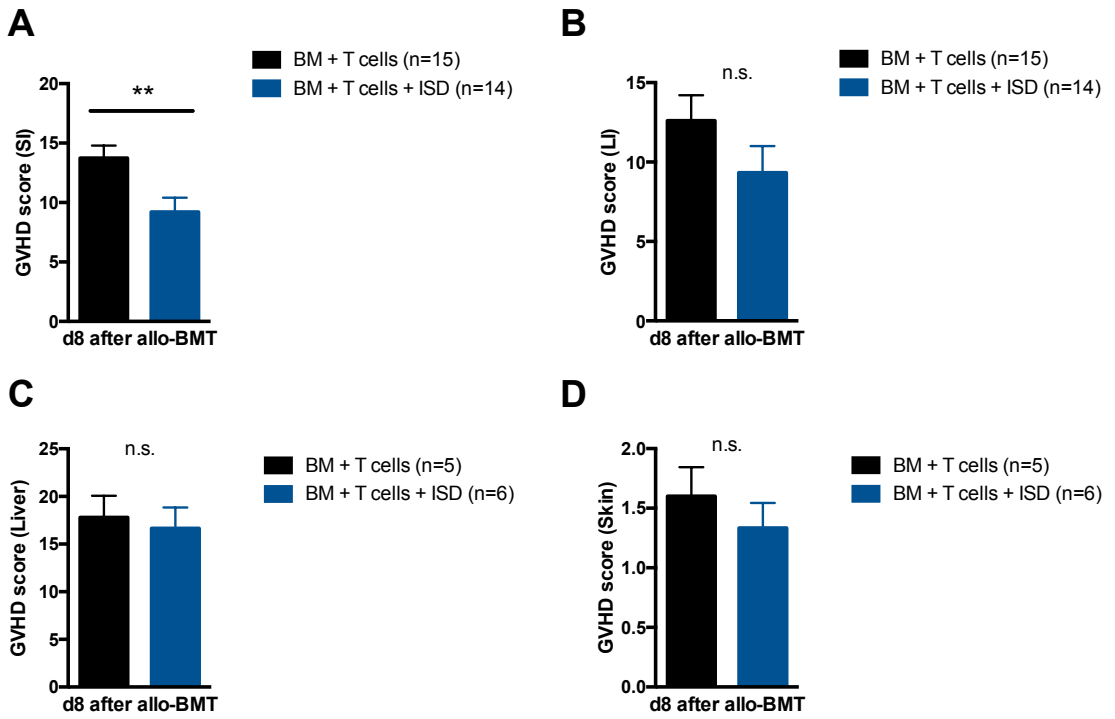

Fig. 9. cGAS-STING activation reduces GVHD severity in mouse small intestines (SI) but not in the large intestine, liver or skin

Co-housed C57BL/6 WT mice underwent 11Gy TBI and were transplanted with $5x10^6$ TCD BM cells and $1x10^6$ T cells from donor B10.Br mice. On the day before allo-BMT, recipients were treated with 25µg of ISD in indicated groups. **A** Small intestines, **B** Large intestines, **C** Liver samples and **D** Skin samples were isolated 8 days after allo-BMT and used or histopathological examination. **A, B** Pooled data from 3 independent experiments. **C, D** One representative out of 3 independent experiments is shown. Animal numbers per group are depicted in the figure. Experiments were analyzed using two-tailed unpaired t-test and significance was set at * $p < 0,05$, ** $p < 0,01$, *** $p < 0,001$

Large intestinal tissue samples of ISD treated mice showed a trend towards reduced GVHD severity (**Fig. 9B**), which was statistically insignificant. We didn't detect differences in skin or liver GVHD among ISD treated or control mice on d8 after allo-BMT (**Fig. 9C, D**). Typically, skin manifestations of murine GVHD occur later in the time course of disease development, which is reflected in the low scores detected in our skin samples (**Fig. 9D**). Although high GVHD scores were noted in liver samples of both groups, ISD treatment showed no effect. The better responsiveness of intestines to ISD treatment might be due to the radiation sensitivity of the intestinal epithelium and its higher exposure to gut commensals. Analysis of cGAS or STING expression levels in GVHD target organs would help

to further understand the different responsiveness of small and large intestines, skin and liver to ISD treatment in GVHD.

3.2.2 Treatment of allo-BMT recipients with STING ligand ISD reduces intestinal permeability

We observed reduced small intestinal GVHD intensity early after allo-BMT and ISD treatment (**Fig. 9A**) which was associated with reduced weight loss (**Fig. 8B**) and clinical GVHD related morbidity (**Fig. 8D**).

Histopathology allows to determine morphologic signs of damage or inflammation, but lacks functional information about the investigated tissue.

To obtain more insights in the functional state of the intestinal barrier in the setting of GVHD, we performed FITC-dextran translocation assay in allo-BMT recipient mice. Dextrans are high-molecular polysaccharides consisting of glucose chains that are mainly connected by α-1,6-links (Jeanes, Haynes et al. 1954). The assay's principle is to measure blood concentrations of this orally administered, indigestible molecule which is too large to pass the intestinal epithelial barrier when intact (Wang, Llorente et al. 2015). When coupled to fluorescein isothiocynate (FITC), fluorescence can be quantified in the serum and is proportional to the amount of FITC-dextran that has passed the intestinal barrier. Thus, the assay allows investigation of intestinal barrier function in vivo.

We used our well-established murine model of allo-BMT and performed the FITC-dextran translocation assay in recipients with or without pretreatment with ISD. Application of the cGAS-STING ligand reduced FITC translocation significantly, reflecting a protection of intestinal barrier function properties (**Fig. 10**). Our data indicates that systemic STING activation reduces GVHD intensity in the small intestine resulting in maintenance of barrier function.

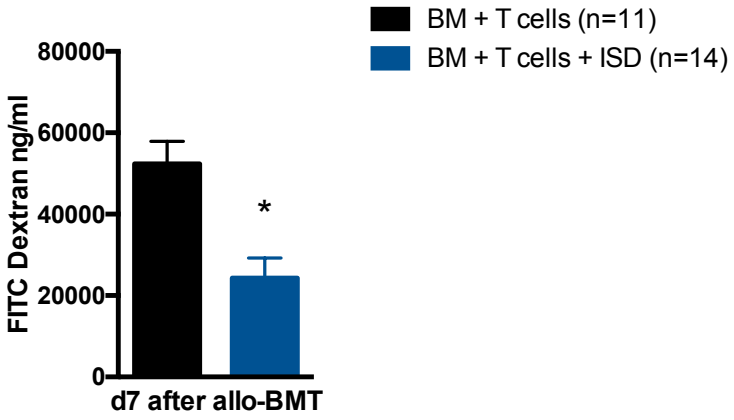

Fig. 10. cGAS-STING activation reduces FITC-dextran translocation in allo-BMT recipient mice FITC-dextran concentrations in blood serum of mice on d7 after allo-BMT. Co-housed BALB/c WT mice underwent 9Gy TBI and were transplanted with $5x10^6$ TCD BM cells and $0,5x10^6$ T cells from donor C57BL/6 mice. On the day before allo-BMT, recipients were treated with 50µg of ISD in indicated groups. Data of 2 independent experiments. Animal numbers per group are depicted in the figure. Experiments were analyzed using two-tailed unpaired t-test, significance was set at * $p < 0,05$, ** $p < 0,01$, *** $p < 0,001$

3.3 STING signaling enhances small intestinal organoid growth in an IFN-I dependent manner

An organoid can be defined as “a 3D structure grown from stem cells and consisting of organ-specific cell types that self-organizes through cell sorting and spatially restricted lineage commitment” (Clevers 2016). Today, organoid cultures are used to study a variety of organs like the intestines, pancreas, kidneys, brain or mammary gland for a better understanding of organ development, regeneration or inflammatory and neoplastic diseases.

In the intestinal tract, organoid cultures helped to identify the $Lgr5^+$ stem cell population (Sato, Vries et al. 2009) and how it interacts with its so called “stem cell niche” (Gehart and Clevers 2019). After isolation, intestinal stem cells or intestinal crypts containing stem cells build three-dimensional structures in vitro which follow physiologic properties of the intestinal epithelium. These organoids grow buds reflecting the crypt domains of the epithelium and give rise to all different lineages of the intestinal epithelium like Paneth cells, goblet cells and enterocytes (van der Flier and Clevers 2009).

Before the establishment of these three-dimensional cell cultures, in vitro studies were mainly limited to immortalized cell lines, which lack many physiological properties as they consist of only one cell population. Importantly, as a primary tissue culture, organoids can be grown from almost any genetically modified mouse strain which facilitates investigation of specific pathways in the intestinal epithelium. Additionally, the culture of long-lasting human organoids offers new possibilities to study human stem cells in health and disease and to translate findings from murine studies to the human organism.

3.3.1 STING signaling promotes organoid formation and proliferation

So far, our data indicate that the protective role of cGAS-STING signaling in GVHD is associated with a reduction of small intestinal GVHD intensity and protection of the intestinal barrier. To further dissect this phenotype, we aimed to study whether cGAS-STING signaling had a direct impact on the intestinal epithelium and the stem cell niche. To study the role of endogenous STING signaling in the small bowel we used untreated co-housed WT and *Sting*$^{gt/gt}$ mice and isolated small intestinal crypts for organoid cultures. Starting concentrations of crypts were set equal between groups. Additionally, we performed in vitro treatment with ISD, complexed with lipofectamine for cytosolic delivery, to examine the influence of exogenous cGAS-STING activation on the organoid culture.

The numbers of evolving organoids were counted after 5 days of culture. Counts revealed that fewer organoids could be derived from *Sting*$^{gt/gt}$ crypts than from WT control crypts (**Fig. 11A, C**). To confirm this, we carried out an MTT assay, which is used for quantification of viable, metabolically active cells. It relies on the reduction of the yellow colored MTT salt (3-(4,5-dimethylthiazol-2-yl)-2,5-diphenyltetrazolium bromide) to a blue formazan product which can then be quantified using an ELISA plate reader (Mosmann 1983). The reaction requires NAD(P)H-dependent oxidoreductases in viable cells (Berridge and Tan 1993). In our cultures, the MTT assay showed that the viable cell mass in *Sting*$^{gt/gt}$ organoid cultures was lower compared to WT controls (**Fig. 11B**) which mirrors the differences in organoid counts. Addition of ISD to the cultures did not change organoid counts or MTT absorbance in WT or *Sting*$^{gt/gt}$ cultures (**Fig. 11A, B**).

In a next step, we aimed to compare organoid growth by measurements of the area and perimeter covered by the organoids after 5 days of culture. As the crypts at the beginning of the culture period are all approximately similar in size, the increase after several days of culture can be seen as a parameter of proliferation. After taking digital high-resolution images (**Fig. 11C, F**) of the gel drop containing the organoids, their size can be assessed on the computer using an image processing software.

We found that addition of ISD to the culture increased organoid growth in terms of area and perimeter (**Fig. 11D, E**). ISD treatment of *Sting*$^{gt/gt}$ crypts did not increase organoid size which confirmed the STING specificity of the ligand (**Fig. 11D, E**). Also, this STING dependency of the observed phenotype proved that the transfection method for cytosolic delivery was suitable in the setting of three-dimensional cell cultures in Matrigel.

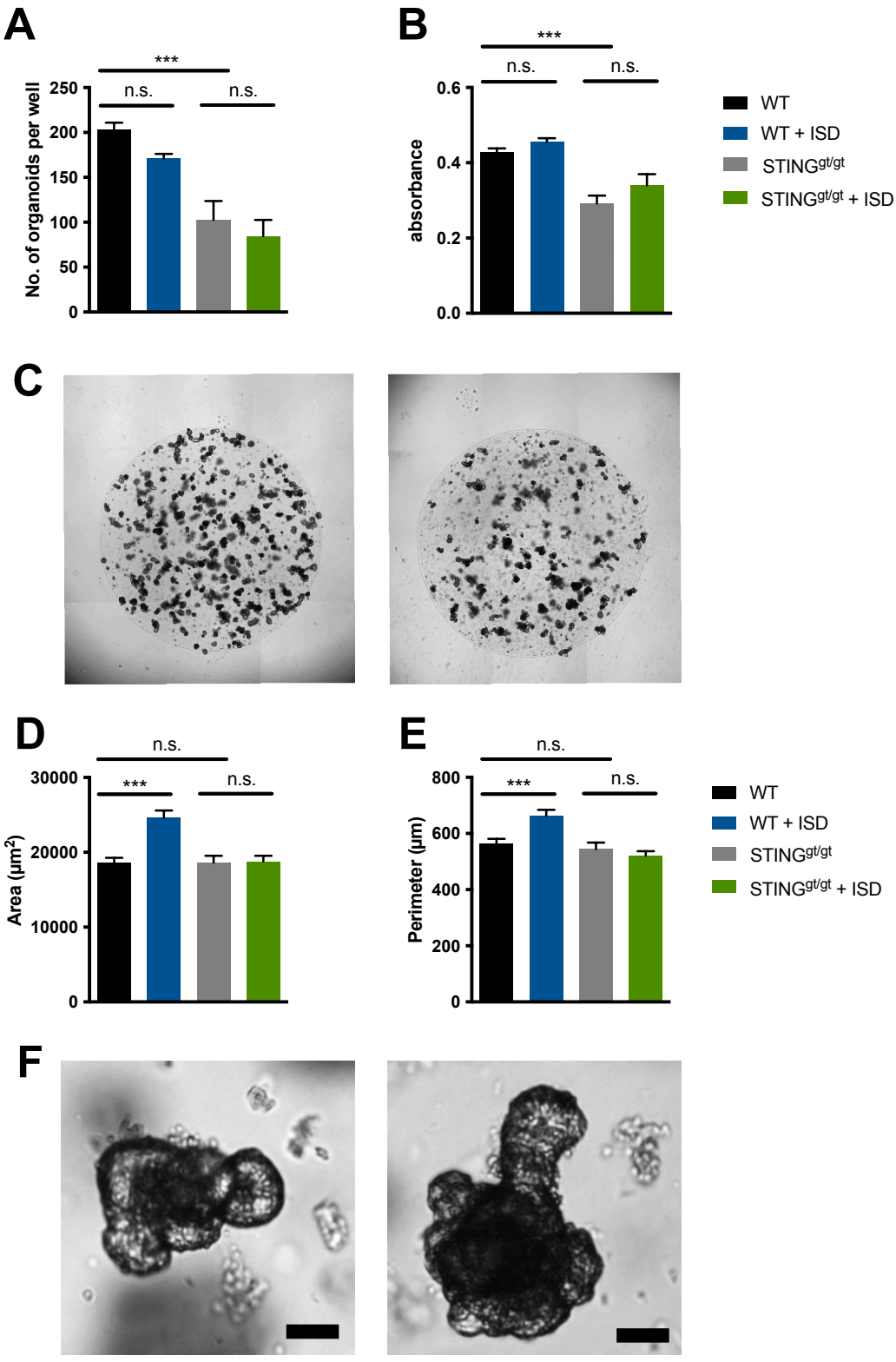

Fig. 11. cGAS-STING signaling promotes small intestinal organoid growth

Small intestinal crypts of C57BL/6 WT and STING$^{gt/gt}$ mice were isolated and organoid cultures were started with equal concentrations of 400 crypts/well. Where indicated, ISD was added to the cultures at a concentration of 2µg/ml complexed with Lipofectamine. **A** Number of organoids per well after 5 days of culture. **B** Absorbance of MTT reagent after 7 days of culture. **C** representative pictures of the

Matrigel drop with organoids after 5 days of culture. Left picture: WT, right picture: *Sting*$^{gt/gt}$. **D** Area and **E** Perimeter of organoids after 5 days of culture. **F** representative picture of an untreated WT organoid (left) and an ISD treated WT organoid (right) reflecting the average size displayed in **D** (scale bar = 50μm). Pooled data of 3 independent experiments (**A**, **D**, **E**) and one representitve experiment of 2 independent experiments (**B**) are shown. Experiments were analyzed using one-way ANOVA and significance was set at * $p < 0,05$, ** $p < 0,01$, *** $p < 0,001$

3.3.2 ISD induces IFN-β expression in organoids which promotes organoid growth

The cGAS-STING pathway is expressed ubiquitously throughout different tissues, among them the small intestine (Ishikawa and Barber 2008). For a better understanding of the responsiveness of intestinal epithelial cells to ISD stimulation, we were interested whether organoids were producing IFN-I upon cGAS-STING activation. Direct quantification of the IFN-α/β protein in the organoid culture media by ELISA was not feasible due to concentrations below the detection threshold. A possible reason could be the limited number of cells in culture and their cultivation in Matrigel-drops which might reduce diffusion into the media. We decided to analyze gene-expression levels of IFN-β mRNA by qPCR in organoids 24h after stimulation with ISD and observed a 4-fold increase in IFN-β expression (**Fig. 12A**).

In a separate experiment, we next sought to explore the effect of IFN-I on small intestinal crypts. Cultivation of crypts with recombinant IFN-β protein led to augmented organoid growth (**Fig. 12B**) while leaving organoid numbers unchanged (**Fig. 12C**).

Apparently, cGAS-STING activation with ISD initiates an IFN-I response in intestinal epithelial cells and exposure to IFN-β represents a proliferative stimulus which is comparable to cGAS-STING activation.

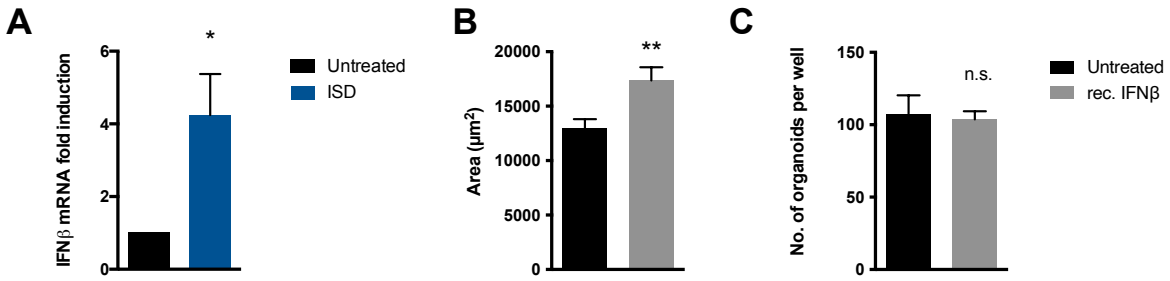

Fig. 12. Small intestinal organoids are responsive to IFN-I

Small intestinal crypts of C57BL/6 WT mice were isolated, and organoid cultures were started with equal concentrations of 400 crypts/well. Where indicated, 2µg/ml of ISD complexed with Lipofectamine or 10µg/ml of recombinant IFNβ were added to the culture **A** Quantitative polymerase chain reaction (qPCR) of IFNβ expression 24h after stimulation with ISD **B** Number of organoids per well after 7 days of culture. **C** Average area of organoids after 7 days of culture. Pooled data of 3 independent experiments. Experiments were analyzed using two-tailed unpaired t-test and significance was set at * $p < 0,05$, ** $p < 0,01$, *** $p < 0,001$

3.3.3 cGAS-STING mediated effects on organoid growth are IFN-I dependent

The previous experiments implied that the effects of cGAS-STING activation might be mediated by IFN-I as stimulation with ISD or recombinant IFN-β resulted in similar changes of organoid growth. We wondered whether these observations were indeed IFN-I dependent.

IFN-α and IFN-β bind to the same heterodimeric receptor named IFNAR on the cell surface which is composed of two subunits named IFNAR1 and IFNAR2 (Ivashkiv and Donlin 2014). Mice deficient of the IFNAR1 subunit (*Ifnar1*$^{-/-}$) fail to respond to IFN-I and are more susceptible to viral infections (Muller, Steinhoff et al. 1994). Targeting the IFNAR1 receptor subunit with a recombinant blocking antibody (αIFNAR1) leads to abrogation of downstream IFN-I signaling and can be used in vivo (Calame, Mueller-Ortiz et al. 2014).

We first used *Ifnar1*$^{-/-}$ mice for small intestinal crypt isolation and treated them with ISD as in previous experiments. The organoid formation capacity of *Ifnar1*$^{-/-}$ crypts was strongly impaired compared to WT control crypts (**Fig. 13A**).

In order to test whether the proliferative stimulus of STING activation on organoid growth was IFN-I dependent, we chose to use αIFNAR1-blocking antibodies in our organoid culture system. The rationale of in vitro blockade of downstream

IFN-I signaling was to exclude pre-existing defects of IFNAR1-deficiency in the organism, which could have led to the reduction of counts in *Ifnar1*$^{-/-}$ organoid cultures (**Fig. 13A**). αIFNAR1-blockade in organoid cultures did not change organoid counts as expected (**Fig. 13B**) but abrogated the increase of organoid growth of in vitro ISD stimulation (**Fig. 13C**).

These findings suggest a crucial role for IFN-I signaling in small intestinal organoid development and imply that ISD mediated effects on organoid growth are dependent on IFN-I production upon STING activation.

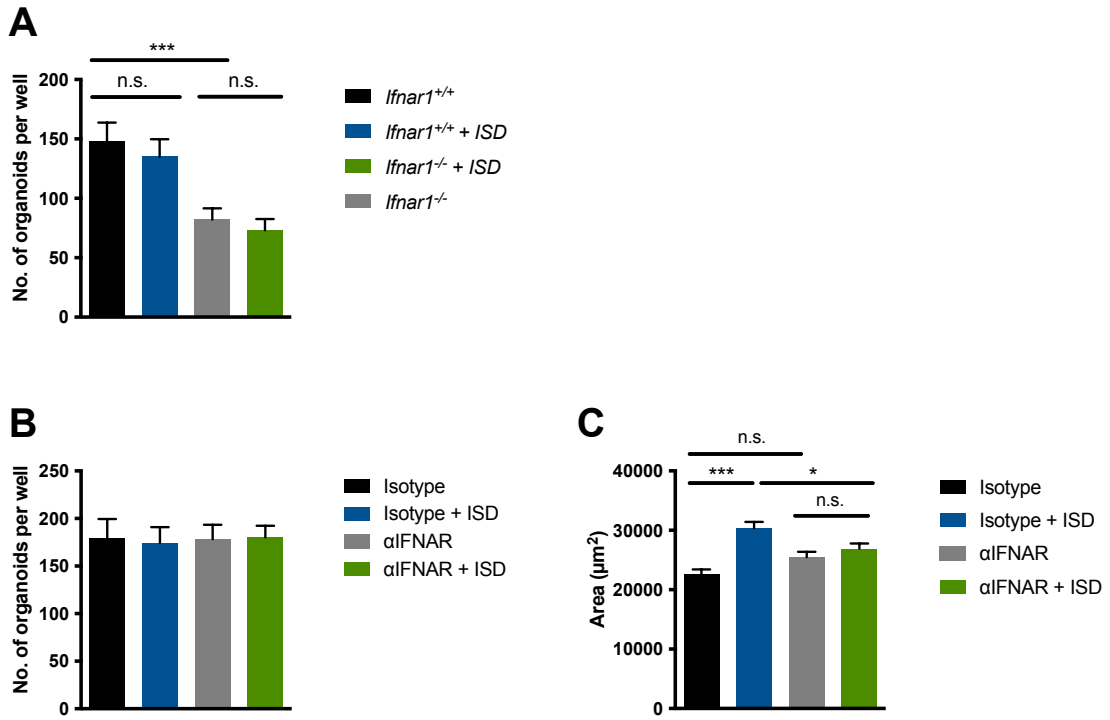

Fig. 13. IFN-I signaling enhances organoid formation

A Small intestinal crypts of C57BL/6 WT and co-housed *Ifnar*$^{-/-}$ mice were isolated, and organoid cultures were started with equal concentrations of 400 crypts/well. Number of organoids per well after 5 days of culture. **B** Small intestinal crypts of C57BL/6 WT mice were isolated, and organoid cultures were started with equal concentrations of 400 crypts/well. αIFNAR-blocking antibody or IgG1 isotype control antibody (Isotype) were added at a concentration of 10µg/ml at indicated groups. Number of organoids per well after 5 days of culture. **C** Average area of organoids of B after 5 days of culture. Where indicated, ISD was added to the cultures at a concentration of 2µg/ml complexed with Lipofectamine. Pooled data of 2 (A) and 3 (B, C) independent experiments. Experiments were analyzed using one-way ANOVA and significance was set at * $p < 0,05$, ** $p < 0,01$, *** $p < 0,001$

3.4 STING activation promotes organoid regeneration ex vivo after murine allo-BMT

So far, we could show that STING and IFNAR signaling are required for organoid formation in vitro. Furthermore, exogenous activation of cGAS-STING by its specific ligand ISD promotes organoid growth in an IFN-I-dependent manner.

We have observed a protective role of STING signaling in murine GVHD experiments and a protection of barrier function properties. Hence, we pursued to link our in vitro findings to the setting of irradiation- and immune-mediated tissue damage occurring during allo-BMT.

Preliminary experiments showed that isolation of murine small intestinal crypts within the first two days after administering a lethal dose of TBI yielded no organoid growth (data not shown). 4 days after TBI, isolated crypts started to form organoids again in a very reduced proportion. Apparently, the stem cell and/or its niche are too fragile in the early phase after irradiation to survive the isolation process or the in vitro culture conditions.

Our in vivo studies in murine GVHD experiments showed a protective effect of cGAS-STING signaling on the intestinal barrier in the early phase of damage 8 days after allo-BMT. This is why we chose to isolate small intestinal crypts from allo-BMT recipients for organoid cultures at this timepoint. These experiments revealed that ISD treatment of allo-BMT recipients *in vivo* prior to allo-BMT led to a considerable increase of organoid formation capacity *ex vivo* (**Fig. 14**). *Sting*$^{gt/gt}$ allo-BMT recipients did not benefit from pre-transplant ISD treatment. Our finding indicates that cGAS-STING activation *in vivo* leads to a protection of the intestinal stem cell niche which can be visualized using organoid cultures.

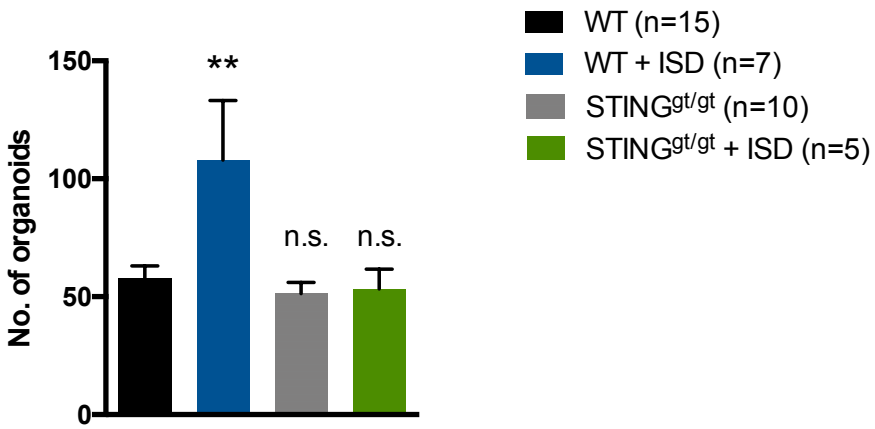

Fig. 14. cGAS-STING activation in vivo prior to allo-BMT increases ex vivo organoid formation

Co-housed C57BL/6 WT or *Sting$^{gt/gt}$* mice underwent 11Gy TBI and were transplanted with 5x10^6 TCD BM cells and 0,5x10^6 T cells from donor BALB/c mice. On the day before allo-BMT recipients were treated with 50µg of ISD in indicated groups. Small intestinal crypts were isolated on d8 after allo-BMT, and organoid cultures were started with equal concentrations of 250 crypts/well. **A** Number of organoids per well after 3 days of culture. Pooled data from 3 independent experiments. Animal numbers per group are depicted in the figure. Results were analyzed using one-way ANOVA and significance was set at * $p < 0,05$, ** $p < 0,01$, *** $p < 0,001$

3.5 STING activation enforces mechanisms supporting intestinal barrier function and might increase stem cell frequencies in small intestinal crypts

So far, our studies using organoid cultures revealed growth inducing effects in vitro and protection of the stem cell niche in vivo which resulted in elevated numbers of organoids.

The intestinal epithelium has to fulfill different requirements for optimal function in health and disease. Besides resorption of nutrients, its barrier function protects the epithelium and the tissue underneath from penetrating microorganisms and the digestive tract content. Barrier malfunction can lead to inflammatory reactions and is a potential threat to the intestinal stem cell.

Also, short-lived enterocytes and their specialized neighbors like Paneth and Goblet cells need constant replenishment from the crypt bottom. A possible explanation for the increase in organoid numbers and growth could be a cGAS-

STING mediated raise in stem cell frequencies in the crypt bottom. We next wanted to investigate potential mediators of enhanced barrier function and gain functional insights in the intestinal stem cell compartment.

3.5.1 cGAS-STING activation induces gene expression of RegIIIγ, Claudin 4 and cGAS

Under physiological conditions, commensal bacteria are segregated from the intestinal epithelium by a mucus layer which harbors a zone of approximately 50μm devoid of bacterial colonization (Johansson, Phillipson et al. 2008). Paneth cells "keep watch" of this critical zone and secrete antimicrobial peptides, among them RegIIIγ, upon contact with commensal bacteria (Vaishnava, Behrendt et al. 2008). It was shown that RegIIIγ-secretion was fundamental to maintain this germ-free space above the epithelium and that RegIIIγ-deficiency in mice was associated with bacterial colonization at the epithelial cell surface leading to inflammatory reactions (Vaishnava, Yamamoto et al. 2011). We wanted to test whether cGAS-STING activation had an influence on RegIIIγ mediated barrier function and carried out qPCR-analyses of RegIIIγ-mRNA in small intestinal organoids. Stimulation of crypts with ISD led to an increase in RegIIIγ-expression in organoids (**Fig. 15A**). Addition of blocking antibodies of the IFNAR-receptor reversed this effect (**Fig. 15A**).

As mentioned in the introduction, tight junction (TJ) proteins ensure intercellular attachments on epithelial surfaces and contribute to cell-matrix interactions (Groschwitz and Hogan 2009). Claudins belong to the family of TJ proteins and are expressed in the intestinal tract among several other tissues (Turksen and Troy 2004). To further evaluate potential roles of STING signaling on intestinal barrier function, we tested gene expression levels of Claudin-4 in small intestinal organoids and found an upregulation of Claudin-4 24h after stimulation with ISD which was dependent on IFN-I signaling (**Fig. 15B**).

Further qPCR analysis revealed an upregulation of cGAS (**Fig. 15C**) upon ISD stimulation. cGAS belongs to the group of Interferon-stimulated genes (ISGs) (Rusinova, Forster et al. 2013) and is upregulated in response to IFN-I.

Our analyses revealed an ISD-induced and IFN-I-dependent upregulation of important mediators of intestinal barrier function like RegIIIγ and Claudin-4 which

could be responsible for STING-mediated protection of allo-BMT related barrier damage. As cGAS belongs to the family of ISGs its upregulation is not surprising. Still, an ISD-induced upregulation of cGAS prior to allo-BMT is notable: Higher cGAS expression at the time of TBI would lead to more IFN-I production when DNA is released from dying intestinal cells, bacteria or viruses. This could in part explain why the treatment prior to conditioning is important in our setting.

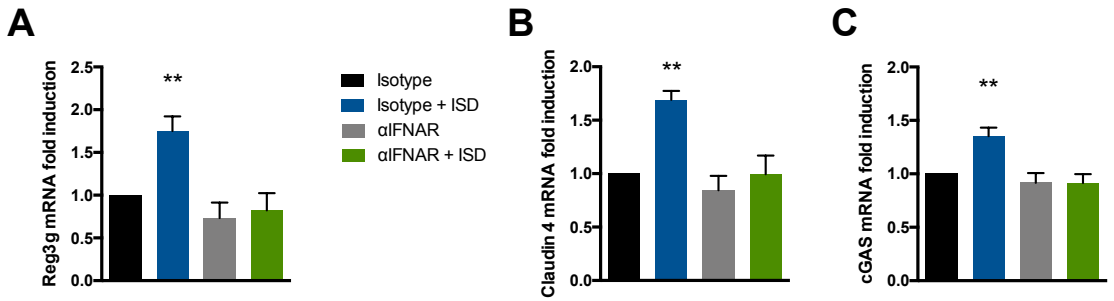

Fig. 15. cGAS-STING activation leads to upregulation of RegIIIγ, Claudin-4 and cGAS

Small intestinal crypts of C57BL/6 WT mice were isolated, and organoid cultures were started with equal concentrations of 400 crypts/well. Where indicated, ISD was added to the cultures at a concentration of 2μg/ml complexed with Lipofectamine. αIFNAR-blocking antibody or IgG1 isotype control antibody were added at a concentration of 10μg/ml to indicated groups. qPCR of **A** Reg3g, **B** Claudin4 and **C** cGAS mRNA 24h after stimulation with ISD + antibodies. Pooled data of 3 independent experiments. Experiments were analyzed using one-way ANOVA and significance was set at * $p < 0,05$, ** $p < 0,01$, *** $p < 0,001$

3.5.2 cGAS-STING activation mediates stem cell expansion in vitro

Intestinal stem cells (ISCs) play a central role in epithelial regeneration after damage. Organoids can be grown from a single $Lgr5^{+}$ stem cell without surrounding niche cells if the required growth factors are substituted (Sato, Vries et al. 2009). Our observations of enhanced organoid formation and growth raised the question whether cGAS-STING signaling had direct effects on the ISC. We used $Lgr5^{EGFP}$ mice in which $Lgr5^{+}$ ISCs express an enhanced green fluorescent protein (EGFP) and thus are useful to trace intestinal stem cells.

Initially, we isolated small intestinal crypts from $Lgr5^{EGFP}$ mice and performed organoid culture experiments under in vitro stimulation with ISD. After 3 days of

culture, organoids were collected, disrupted to obtain a single cell suspension and used for fluorescence activated cell sorting (FACS). After gating on live single cells, a distinct population of Lgr5^{+} stem cells can be identified (**Fig. 16A**). It has been shown that among this Lgr5^{+} population, further differentiation between cells highly positive for Lgr5 (Lgr5^{high}) and those with low to medium positivity (Lgr5$^{low/medium}$) can be useful: Lgr5^{high} cells are enriched for the stem cells located at the crypt bottom whereas the Lgr5$^{low/medium}$ cells represent mostly the distinct population at the +4 position (Wang, Scoville et al. 2013).

Paneth cells carry the surface marker CD24 and appear as a distinct population on the side scatter (SSC^{high}) due to their granular morphology (Sato, van Es et al. 2011) (**Fig. 16B**). The second CD24^{+} SSC^{low} population has been identified as enteroendocrine cell population (Sato, van Es et al. 2011).

FACS-analysis of organoid cells showed an increase in Lgr5^{total} cells after ISD stimulation compared to control organoids (**Fig. 16C**). However, the fraction of Lgr5^{high} cells was comparable between both conditions (**Fig. 16D**). Similarly, the proportion of Paneth cells was unaffected by in vitro ISD treatment (**Fig. 16E**).

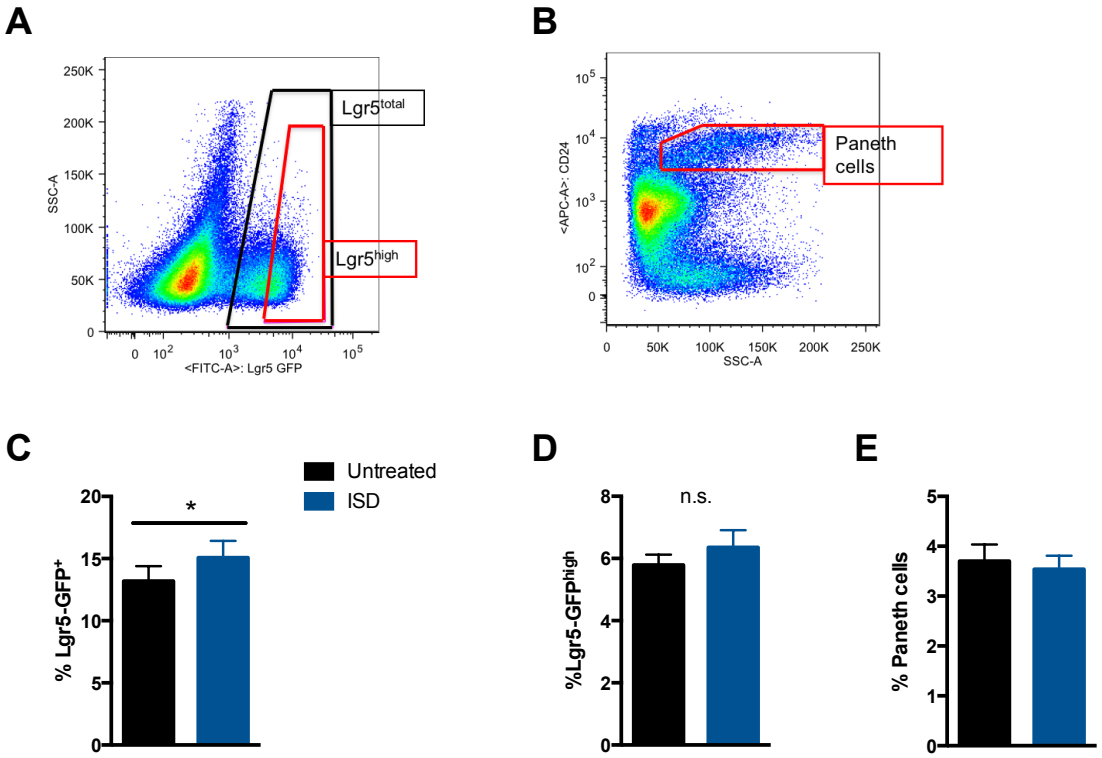

Fig. 16. cGAS-STING activation in vitro leads to an increase of Lgr5^{+} ISCs

Small intestinal crypts of LGR5^{EGFP} mice were isolated, and organoid cultures were started with equal concentrations of 400 crypts/well. Where indicated, ISD was

added to the cultures at a concentration of 2µg/ml complexed with Lipofectamine. After 3 days of culture, organoids were disrupted and used for flow cytometry. **A** Percent Lgr5-GFP^{total} cells, **B** Percent Lgr5-GFP^{high} cells, **C** Percent Paneth cells. **D, E** Representative images of gating on the cell populations mentioned above after pre-gating on live, single cells. Pooled data of 2 independent experiments. Results were analyzed using two-tailed unpaired t-test and significance was set at * p < 0,05, ** p < 0,01, *** p < 0,00

Next, we aimed to test whether in vivo treatment with ISD lead to changes in the crypt bottom's cell populations. Lgr5^{EGFP} mice were treated with ISD following the pre-transplant protocol of our GVHD experiments. 24h after the injections, the timepoint when mice usually undergo TBI, crypts were isolated and taken into culture. Three days later, organoids were collected and analyzed by flow cytometry. The resulting plots did not show differences in Lgr5^{+} ISCs or Paneth cells (**Fig. 17A-B**) 24h after ISD treatment.

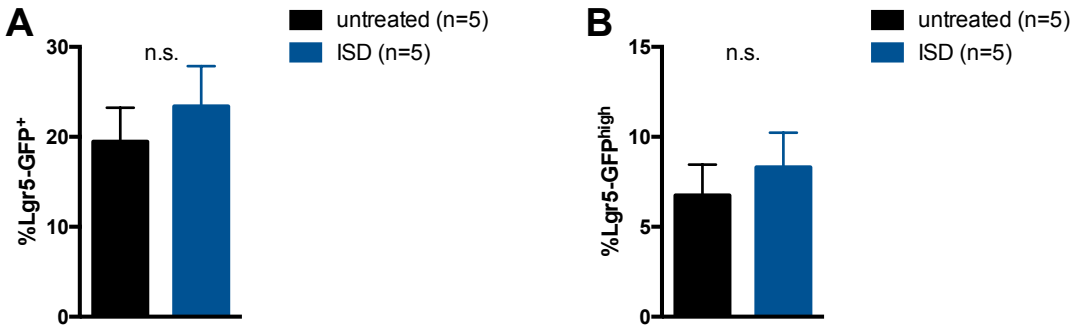

Fig. 17 cGAS-STING activation in vivo has no significant effect on Lgr5^{+} ISCs
Lgr5^{GFP} mice were treated with 50µg of ISD in indicated groups. 24h after treatment small intestinal crypts were isolated and organoid cultures were started with equal concentrations of 200 crypts/well. On d3 of culture organoids were disrupted and used for flow cytometry. **A** Percent Lgr5-GFP^{+} cells, **B** Percent Lgr5-GFP^{high} cells. Animal numbers are depicted in the figure. Pooled data of 2 independent experiments. Results were analyzed using two-tailed unpaired t-test and significance was set at * p < 0,05, ** p < 0,01, *** p < 0,001

In summary, it can be stated that in the experimental settings that were analyzed, we could not observe changes in Paneth cell frequencies but do note a discrete increase of Lgr5^{+} ISCs in small intestinal organoids after in vitro activation of the cGAS-STING pathway. Further in vivo experiments at different timepoints after ISD treatment with or without subsequent allo-BMT are required to exclude or confirm effects of cGAS-STING activation on stem cell frequencies.

4 Discussion

A protective role of IFN-I signaling in GVHD has formerly been described (Robb, Kreijveld et al. 2011) but sources of endogenous IFN-I and mechanisms explaining these beneficial properties are poorly understood.

This work proposes that the cGAS-STING pathway exerts a protective function in GVHD which could be shown for endogenous STING signaling as well as exogenous activation of cGAS-STING with its ligand ISD. Activation of cGAS-STING reduced GVHD-associated mortality and morbidity, limited damage to the small intestine and led to a protection of the intestinal barrier reducing FITC-dextran translocation. Using the intestinal organoid culture system, STING was identified as an important regulator of small intestinal regeneration which was reflected in reduced organoid formation of *Sting*$^{gt/gt}$ crypts. We identified that cGAS-STING derived IFN-I promotes intestinal epithelial proliferation as seen in enhanced organoid growth. This could be due to an increase in stem cell frequencies. cGAS-STING activation also promoted mechanisms that increase intestinal barrier function like the expression of RegIIIγ and Claudin-4. Still, the precise influence of cGAS-STING and IFN-I signaling on the intestinal stem cell niche requires further investigation.

4.1 GVHD and the role of cGAS-STING and IFN-I inducing pathways

4.1.1 Experimental models of GVHD – MHC matched or mismatched?

Studies involving murine models of allo-BMT have contributed to a deep understanding of the pathophysiology and therapy of GVHD. Like other murine disease models, they allow to equalize environmental influences, to use relatively large group sizes, to include genetically modified mouse strains as donors or recipients, to investigate experimental effects at various time points and to study therapeutic interventions (Markey, MacDonald et al. 2014).

This study includes major-mismatched allo-BMT experiments in the following settings: B10.Br → C57BL/6, BALB/c → C57BL/6 and C57BL/6 → BALB/c. The choice of donors and recipients was dependent on the background of genetically modified mice (e.g. *Sting*$^{gt/gt}$ on C57BL/6). At the same time, obtaining coherent results after using different backgrounds of donors and recipients shows that our observations are probably not strain specific. Our experiments evaluating

endogenous or exogenous STING signaling in allo-BMT recipients were performed in a B10.Br → C57BL/6 model and showed protective effects of STING in this setting.

MHC-mismatched mouse models are most frequently used in the field of GVHD-research and their advantage is the development of a robust and reproducible intensity of GVHD (Schroeder and DiPersio 2011) and the possibility to conduct survival studies. Bone marrow transplantation in humans is generally MHC-matched to limit GVHD occurrence.

A recent study investigated the role of STING in MHC-matched mouse models of GVHD (Bader, Barreras et al. 2020). It was shown that STING signaling was fueling GVHD after MHC-matched allo-BMT which is contrary to our findings after MHC-mismatched bone marrow transplantation. Yet, the authors reproduced our findings in MHC-mismatched BALB/c → C57BL/6 or *Sting*$^{-/-}$ allo-BMT experiments. They hypothesize that these opposing effects of STING in GVHD rely on the activation of different T cell subsets: CD4^{+} T cells in MHC mismatched allo-BMT vs. CD8^{+} T cells in MHC-matched transplants. Interestingly, their phenotype of reduced GVHD in *Sting*$^{-/-}$ mice was dependent on the timepoint of conditioning therapy and was only observed when conditioning was performed on the same day as the transplant (Bader, Barreras et al. 2020). These recent findings highlight that GVHD results from complex immune activation processes including different subsets of APCs and T cells as well as non-hematopoietic cells like IECs. Again, it was shown that slight differences in the timing of immune activation can abrogate experimental observations. Further studies will be needed to break down the role of STING signaling in different transplant settings and specially to elucidate how STING is involved in human GVHD development.

4.1.2 IFN-I signaling affects the intestinal microbiota

A different study on IFN-I reported that IFNAR1 deletion in the intestinal epithelial compartment (*Ifnar1*$^{-/-(IEC)}$) led to significant changes in Paneth cell frequencies, epithelial proliferation and tumor development in a DSS-colitis model (Tschurtschenthaler, Wang et al. 2014). Interestingly, these observations were associated with alterations of the caecal microbial composition and were completely revoked upon co-housing of *Ifnar1*$^{-/-(IEC)}$ and *Ifnar1*$^{+/+(IEC)}$ mice. This indicates that on the one hand IFN-I signaling affects the intestinal microbiota but

also, that on the other hand experimental phenotypes can be based on changes of the microbial ecosystem. We carried out 16S rRNA sequencing of WT and *Sting*$^{gt/gt}$ mice and did not find differences in the microbiota of co-housed mice (**Fig. 5**). All experiments were performed under co-housing conditions to rule out this potential confounder. Still, studying the effects of cGAS-STING and IFN-I signaling on the microbial flora of allo-BMT recipients is of interest. ISD stimulation led to an upregulation of antimicrobial peptide RegIIIγ (**Fig. 15A**) which we could also show for 3pRNA induced RIG-I/MAVS activation in vitro and in vivo (Fischer, Bscheider et al. 2017). AMPs like RegIIIγ protect the mucus layer from microbial invasion and are induced by commensal bacteria (Vaishnava, Behrendt et al. 2008, Vaishnava, Yamamoto et al. 2011). This way, they reduce inflammatory reactions of the intestinal epithelium (Loonen, Stolte et al. 2014). In pediatric IBD patients, changes of the intestinal microbiota were associated with changes of AMP expression (Jalanka, Cheng et al. 2020) pointing towards a reciprocal relationship of AMPs and commensal bacteria.

Our data shows comparable microbiota of co-housed WT and *Sting*$^{gt/gt}$ mice at steady state conditions. To test this in the context of disease, further experiments should include 16S rRNA sequencing of the intestinal microbiota of allo-BMT recipient mice deficient for cGAS-STING or other IFN-I inducing pathways.

Given that the degree of intestinal microbial diversity predicted survival of allo-HSCT patients (Taur, Jenq et al. 2014, Peled, Gomes et al. 2020) and the growing evidence highlighting the importance of the intestinal microbiota and antibiotic treatments on survival and relapse after BMT (Shono and van den Brink 2018), further investigation of the interplay of IFN-I inducing pathways and the intestinal microbiota could be promising.

4.1.3 Determining tissue specific effects of cGAS-STING in GVHD

The previously described protective role of IFN-I signaling in GVHD attributed this effect to a reduction of $CD4^+$ T cell proliferation and differentiation which was mediated by IFN-I signaling in the hematopoietic system (Robb, Kreijveld et al. 2011).

This dissertation highlights the impact of cGAS-STING derived IFN-I on the intestinal epithelium i.e., non-hematopoietic cells. Bone marrow chimeric mice are frequently used to determine whether a genetic defect influences

experimental GVHD in the hematopoietic and/or non-hematopoietic system (Calcaterra, Sfondrini et al. 2008, Penack, Smith et al. 2009, Hossain, Jaye et al. 2011). Generation of bone marrow chimera consists in syngeneic transplantation of wild-type bone marrow into knock-out recipient mice and vice versa to generate mice which carry a genetic defect in either one of the two compartments or both. These mice then serve as recipients for allo-BMT and further read-outs.

Our group's studies on the RIG-I/MAVS-pathway have shown that RIG-I/MAVS signaling protected from GVHD in allo-BMT recipient mice (Fischer, Bscheider et al. 2017). We could link this protective effect to RIG-I/MAVS signaling in the non-hematopoietic system using *Mavs*$^{-/-}$ bone marrow chimera for survival experiments and histopathological analyses after allo-BMT.

These observations could point to a similar phenotype for the cGAS-STING pathway. We have shown that cGAS-STING activation acts on intestinal epithelial cells i.e., non-hematopoietic cells in different ways using organoid cultures (**Fig. 11, 13**). Further experiments with *Sting*$^{gt/gt}$ bone marrow chimeras would help to confirm that these observations indeed play a role in regulating GVHD related morbidity and mortality.

A more precise differentiation of pathway-related effects on specific tissues can be achieved with conditional knock-out mice. Their generation is based on the principle of the Cre-*loxP* system (Bouabe and Okkenhaug 2013, Kim, Kim et al. 2018). In short, *loxP* sequences (34 bp), which are the target sequence for the Cre recombinase (Cre), are inserted on both ends of a target gene sequence (then called a "floxed" gene). Then, a second mouse strain is modified so that Cre is expressed under control of a tissue or cell type specific promoter. Crossing Cre expressing mice with mice carrying floxed gene sequences results in tissue specific deletion of the floxed gene in the offspring.

Villin^{Cre} mice with Cre expression in intestinal epithelial cells under the Villin-promoter (Madison, Dunbar et al. 2002) and Lgr5$^{EGFP\text{-}IRES\text{-}creERT2}$ mice with a tamoxifen inducible Cre recombinase in Lgr5^{+} ISCs (Barker, van Es et al. 2007) are already commercially available. The generation of *Sting*$^{fl/fl}$ (floxed) mice would open new perspectives in studying the functions of STING in IECs and ISCs in the context of GVHD and intestinal regeneration.

4.1.4 Translational aspects of cGAS-STING and GVHD

The terms of “translational medicine” or “translational research” are frequently used as a quality criterion for modern biomedical research. Often simplified as “bench to bedside”, one aspect of translational research is „the transfer of new understandings of disease mechanisms gained in the laboratory into the development of new methods for diagnosis, therapy, and prevention and their first testing in humans” (Sung, Crowley et al. 2003).

In this work, various effects of cGAS-STING activation with ISD in allo-BMT recipient mice are described. We could show that prophylactic treatment with a single i.v. dose of ISD reduces mortality after allo-BMT in mice (**Fig. 7**), improves clinical scores of disease activity (**Fig. 8**), decreases damage to the small intestine (**Fig. 9**) and enhances barrier function (**Fig. 10**).

The time-point of treatment on d-1 before allo-BMT was chosen after previous experiments using RIG-I ligand 3pRNA in allo-BMT experiments. These have shown that administration of 3pRNA on the day after allo-BMT did not protect mice from GVHD and that the treatment effect relied on activated IFN-I signaling at the timepoint of conditioning and transplantation (Fischer, Bscheider et al. 2017). Measurements of *Lysozyme P* and *Lgr5* gene expression revealed a decrease 24h after TBI. We postulated that the loss of potential target cell populations like Paneth cells or ISCs after conditioning therapy could explain why 3pRNA treatment was not effective at later timepoints. Gene expression analysis revealed that ISD treatment augments cGAS expression in IECs (**Fig. 15C**) which could “prepare” the intestine for the TBI-associated release of DNA. We have found reliable effects of ISD treatment on the day before transplantation, but possibly different treatment protocols could prove even more effective.

Although our therapeutic approaches using STING or RIG-I ligands to limit GVHD intensity are far from being tested in human patients, several aspects of our proposed therapeutic interventions meet the idea of translational research:

Firstly, the idea of prophylactic cGAS/STING or RIG-I/MAVS ligand administration harbors substantial benefits. The development of GVHD relies on conditioning therapy-induced tissue damage and intestinal barrier loss leading to a “cytokine storm” and systemic activation of the immune system. Limitation of barrier damage and these first events represents a causal approach to protect allo-HSCT recipients from GVHD. The widely used immunosuppression with

corticosteroids or calcineurin-inhibitors in allo-HSCT patients does not address the primary damage of conditioning therapy.

Secondly, IFN-I are already used in clinical routine. They are most established in therapy of multiple sclerosis, where IFN-ß belongs to the first line therapeutics (Reich, Lucchinetti et al. 2018). Unfortunately, the main limitation of the clinical use of IFN-I are their side-effects mainly flu-like symptoms which lower quality of life and lead to decreased adherence.

Moreover, our improvements in GVHD are achieved after a single-dose treatment with ISD which produced long-lasting effects in allo-BMT recipient mice: survival of ISD treated mice was higher 90 days after transplantation (**Fig. 7**) and mice lost less weight over the 90 days' time course (**Fig. 8**). Apparently, targeted immune activation at a specific timepoint can modulate the outcome of an entire cascade of events following the treatment.

Targeting STING therapeutically is already tested in a variety of oncological clinical trials, mainly for therapy of solid tumors (Le Naour, Zitvogel et al. 2020). The most frequently used STING agonist in these trials is 5,6-dimethylxanthenone-4-acetic acid (DMXAA) which has been known even before the discovery of the STING pathway itself (Prantner, Perkins et al. 2012). Using this established agent in murine allo-BMT experiments would be a potential next step for the translation of therapeutic STING activation in allo-BMT.

The recent findings about how IL-22 regulates GVHD highlights the relevance of preclinical GVHD research and shows how fast preclinical findings can be translated into clinical trials. IL-22 is a cytokine which has been associated with beneficial effects on the intestinal epithelium in multiple ways: it regulates epithelial proliferation, barrier function and defense against pathogens (Keir, Yi et al. 2020). After murine allo-BMT, IL-22 protects recipients from GVHD and has been shown to improve barrier function, increase ISC frequencies and epithelial regeneration (Lindemans, Calafiore et al. 2015) and also exerts protective effects on thymic epithelial cells (Dudakov, Mertelsmann et al. 2017). This has led to a phase I clinical trial on a recombinant human interleukin-22 dimer (F-652) (Tang, Lickliter et al. 2019) and momentarily a phase IIa clinical trial testing human IL-22 in patients with grade II-IV lower GI aGVHD is ongoing (NCT02406651).

For a better understanding of cGAS-STING induced IFN-I in GVHD, expression levels of STING in tissue samples collected from human GVHD patients would

be of high interest. It was shown that multiple human cancer cell lines, although expressing STING, showed a strongly reduced responsiveness to STING ligands in vitro which was proposed as a potential mechanism of cancer cells to escape immune surveillance (Xia, Konno et al. 2016). Evaluation of STING-activation in human GVHD patients would help defining if and in what way it could be targeted clinically.

4.2 cGAS-STING and the intestinal epithelial barrier

4.2.1 Organoid cultures to study intestinal epithelial regeneration

The term “tissue regeneration” is widely used but definitions are often vague. Broadly, regeneration describes “the regrowth or repair of cells, tissues and organs” (Sanchez Alvarado and Tsonis 2006). “Regenerative strategies include the rearrangement of pre-existing tissue, the use of adult somatic stem cells and the dedifferentiation and/or transdifferentiation of cells, and more than one mode can operate in different tissues of the same animal. All these strategies result in the re-establishment of appropriate tissue polarity, structure and form“ (Sanchez Alvarado and Tsonis 2006).

In the intestinal epithelium, regeneration or cell-renewal is constantly ongoing due to the short lifespan (3-5 days) of the differentiated enterocyte. At the same time, the word regeneration is often used to describe tissue renewal after damage e.g., after irradiation or inflammation.

In this work, several aspects of intestinal regeneration and the influence of cGAS-STING signaling on regenerative abilities of the intestinal epithelium were studied.

Histopathology was used to quantify damage of untreated vs. ISD-treated allo-BMT recipient mice following a standardized GVHD damage score (**Table 1**). We noticed that GVHD associated damage of the small intestine was lower, when mice had received ISD before transplantation (**Fig. 9**). Histopathology is a suitable tool to study morphologic aspects of damage, inflammation or cancer. Its advantage is that tissue samples remain intact, and that the investigator can observe cells in their specific arrangement, describe changes to the cell’s morphology, and determine infiltration of immune cells. At the same time, histopathologic analyses are only a snapshot of a dynamic process.

The organoid culture system has opened open new doors to study regeneration because we can now study a functional unit of cells, the intestinal crypt, in a dynamic situation.

Isolation of crypts from WT and *Sting*$^{gt/gt}$ mice revealed an important role for STING and IFN-I signaling on organoid development as the same number of *Sting*$^{gt/gt}$ or *Ifnar*$^{-/-}$ crypts grew into fewer organoids than did WT crypts (**Fig. 11A**). Even without a previous damaging intervention (e.g., TBI), this assay reflects intestinal regenerative capacities. Crypt extraction consists of multiple mechanical and chemical steps to separate crypts from the villi and underlying lamina propria. This deprives ISCs from important signals that regulate proliferation, differentiation and cell localization at the crypt bottom like Wnt or Bmp-signaling (Shyer, Huycke et al. 2015, Farin, Jordens et al. 2016). Organoid formation in vitro thus requires a strong potential of regeneration.

We also tested organoid regeneration after in vivo damage and isolated small intestinal crypts from allo-BMT recipient mice. In this setting, the intestines had suffered irradiation- and immune mediated damage by infiltrating T cells which are known to invade the intestines within the first days after transplantation and spread throughout the small and large bowel by day 6 (Beilhack, Schulz et al. 2005). Crypts isolated from allo-BMT recipient mice that had been treated with ISD formed a higher number of organoids than crypts derived from untreated mice (**Fig. 14**). This experiment shows that activation of the cGAS-STING pathway prior to transplantation exerted a protective effect on the intestinal crypt and promoted intestinal regeneration.

Additionally, microscopic images were used to determine the organoids' size after three or five days in culture. An MTT assay confirmed that a larger average area and perimeter covered by the organoids correlated with an increase in the viable cell mass (**Fig. 11B**). We concluded that an increase in organoid's size reflects enhanced cellular proliferation within the organoid. ISD stimulation in vitro resulted in enhanced organoid size which was dependent on downstream IFN-I signaling (**Fig. 13C**). Addition of recombinant IFN-β also boosted organoid growth (**Fig. 12B**), indicating that IFN-I signaling and cGAS-STING signaling provide a direct proliferative stimulus on the intestinal epithelium.

To correlate these findings with processes in vivo is difficult. Lineage tracing experiments could demonstrate faster cell-cycling and migration towards the

villus tip. We hypothesize that an increase of organoid proliferation in vitro represents higher turnover in vivo meaning faster regeneration from TBI, maintenance of barrier function, reduction of inflammation and ultimately reduced GVHD intensity.

4.2.2 The interplay of the intestinal stem cell with its niche

The stem cell and its niche have been subject of intensive research over the last fifty years with great advances in recent times. The identification of a potential stem cell population was substantiated in 1974, when Cheng and Leblond provided evidence that so called crypt-base columnar cells give rise to different lineages of the intestinal epithelium (Cheng and Leblond 1974). Different stem cell populations have now been identified and their interplay with epithelial and mesenchymal cells forming a stem cell niche is the cornerstone to understand epithelial homeostasis and regeneration.

Intestinal stem cells

The source of all different cell lineages of the intestinal epithelium are the stem cells located at the crypt bottom, often described as crypt-base columnar cells (CBCs) carrying the stem cell marker Lgr5 (Leucine-rich repeat-containing, G protein-coupled Receptor 5) (Barker, van Es et al. 2007). Lgr5 associates with Wnt receptors and binds soluble R-spondins to enhance Wnt signaling in stem cells (de Lau, Barker et al. 2011). $Lgr5^+$ ISCs represent a rapidly dividing cell population responsible for constant replenishment of epithelial cells and divide approximately once per day (Barker, van Es et al. 2007). A second and distinct population of stem cells is located four cells above the crypt base and are named +4 cells. These +4 cells can be identified by the marker Bmi1, cycle less rapidly than $Lgr5^+$ cells and can be considered as a quiescent stem cell population with minimal contribution to intestinal epithelial homeostasis (Sangiorgi and Capecchi 2008, Yan, Chia et al. 2012). When $Lgr5^+$ CBCs are experimentally ablated in mice, $Bmi1^+$ +4 cells are able to replenish the stem cell pool at the crypt bottom (Tian, Biehs et al. 2011). Interestingly, after irradiation induced damage to the small intestine by 12Gy TBI, $Lgr5^+$ ISCs are almost completely destroyed within 2 days whereas $Bmi1^+$ ISCs remain viable, transform to a proliferative state and

replenish cells up to the villus tip by day 7 (Yan, Chia et al. 2012). At this timepoint, Lgr5$^+$ ISCs were only slowly reappearing at the crypt bottom.

Intestinal stem cells are reduced in mice after allo-BMT (Hanash, Dudakov et al. 2012) and are directly attacked by allogeneic T cells in GVHD (Fu, Egorova et al. 2019). We found an increase of Lgr5$^+$ ISCs in organoids after in vitro stimulation with ISD in FACS analysis (**Fig. 16C**). Treatment of allo-BMT recipient mice with 3pRNA on the day before transplantation resulted in enhanced Lgr5 mRNA expression in the small intestine highlighting that activation of IFN-I signaling through cytosolic nucleic acid sensors acts on the stem cell niche (Fischer, Bscheider et al. 2017).

Still, more evidence is needed to elucidate the implications of IFN-I signaling on ISCs during homeostasis and damage. IFN-I have been associated with increased epithelial turnover (Sun, Miyoshi et al. 2015) but if and how they act on ISCs is unclear. A proteomic screen of Lgr5$^+$ ISCs by Munoz et al shows that ISCs express STING and IFN-α (Munoz, Stange et al. 2012) so they might be able to react directly to STING activation.

Further experiments are required to clarify whether STING and IFN-I signaling have an impact on ISCs directly. In the context of allo-BMT, histopathologic samples of STING-deficient or ISD treated mice could be analyzed for ISC frequencies. Unfortunately, the use of Lgr5^{GFP} mice for quantitative studies of ISC numbers is limited due to “variegated expression of the Lgr5-EGFP-IRES-CreERT2 transgene in the small intestine and colon” (https://www.jax.org/strain/008875). A variety of antibodies for Lgr5 staining are now commercially available and could be tested in our STING deficient mice or ISD treated allo-BMT recipient mice (Kim, Jung et al. 2018). We also performed fluorescence in situ hybridization with an Olfm4-specific RNA-probe but results are preliminary and require further validation (data not shown).

As mentioned before, Lgr5$^+$ stem cells are only one of at least two known stem cell populations. The role of Bmi1$^+$ stem cells in intestinal regeneration after allo-BMT and immune-mediated damage during GVHD is still unclear but requires further consideration given the radiation sensitivity of Lgr5$^+$ stem cells.

Paneth cells

Paneth cells belong to the secretory line of intestinal epithelial cells and cover two principal functions: They are essential for host defense against intestinal microbiota and constitute an important niche cell for $Lgr5^+$ stem cells. Residing at the crypt bottom of the small intestine, Paneth cells are pyramidal shaped cells containing numerous intracellular granules that store antimicrobial peptides (AMPs) (Bevins and Salzman 2011). The family of AMPs comprises among others α-defensins, Lysozyme and RegIII (RegIIIα in humans, RegIIIγ in mice) (Bevins and Salzman 2011). Defensins are bactericidal on gram-positive and gram-negative bacteria and beyond that, act as chemoattractant for dendritic cells (Yang, Chertov et al. 1999). Lysozyme is a glycosidase that hydrolyses peptidoglycans in bacterial cell walls and is constitutively expressed by Paneth cells, why it is often used as target for immunohistochemical staining for this cell population (Bevins and Salzman 2011, Farin, Van Es et al. 2012, Tschurtschenthaler, Wang et al. 2014). The C-type lectin RegIIIγ also interacts with peptidoglycans and is an inducible AMP that is expressed upon contact with microbes through TLR signaling adaptor MyD88 (Cash, Whitham et al. 2006, Vaishnava, Behrendt et al. 2008). The combination of AMPs helps to protect the host from intestinal pathogens by keeping the mucus barrier nearly free of bacteria (Bevins and Salzman 2011, Vaishnava, Yamamoto et al. 2011).

Additionally, Paneth cells function as important niche cell for the $Lgr5^+$ CBC cells, which are intermingled between Paneth cells (Sato, van Es et al. 2011). They provide proliferation and differentiation signals for stem cells like EGF, TGFα, Wnt3 and the Notch ligand Dll4 (Sato, van Es et al. 2011). In vivo, Wnt signals are provided by Paneth cells and mesenchymal cells, whereas organoid cultures depend on Paneth cells as singular source of Wnt (Farin, Van Es et al. 2012). Addition of Paneth cells to single Lgr5 cells in vitro dramatically increases organoid formation (Sato, van Es et al. 2011). Wnt signaling is essential to maintain a stable stem cell population at the crypt base but also induces Paneth cell differentiation in an autocrine manner (Yin, Farin et al. 2014). Moreover, the Wnt gradient from high levels at the crypt bottom towards lower concentrations at the villus tip is (partly) responsible for the differentiation processes of different epithelial lineages (Farin, Jordens et al. 2016).

In the context of GVHD, studies showed that Paneth cell numbers and levels of α-defensins are drastically reduced after allo-BMT in mice which worsens GVHD survival and correlated with changes in the microbiota of allo-BMT recipient mice (Eriguchi, Takashima et al. 2012). Furthermore, IFNAR1-deletion in the intestinal epithelium (*Ifnar1*$^{-/-(IEC)}$) lead to an increase in Paneth cell frequencies in the small intestine which was dependent on housing-conditions and the altered microbiota of *Ifnar1*$^{-/-(IEC)}$ and *Ifnar1*$^{+/+(IEC)}$ mice (Tschurtschenthaler, Wang et al. 2014).

As Paneth cells act as important niche cells for ISCs and provide growth factors, we were interested whether our observations of increased organoid size after cGAS-STING activation relied on elevated Paneth cell numbers. We found that ISD treatment in organoids had no effect on Paneth cell proportions in vitro after few days of culture (**Fig. 16E**). Still, prophylactic activation of RIG-I/MAVS by 3pRNA administration to allo-BMT recipient mice resulted in increased Paneth cell numbers and Lysozyme P expression on d8 after transplantation (Fischer, Bscheider et al. 2017). Although this hypothesis remains to be tested for STING pathway activation, the prophylactic activation of IFN-I signaling, and the resulting protection of the intestinal barrier could be – in part – mediated by a protection of the Paneth cell population. cGAS-STING activation led to increased expression of RegIIIγ in small intestinal organoids (**Fig. 15A**) which indicates that Paneth cells react to ISD stimulation.

It also remains to be tested whether cGAS-STING or other IFN-I inducing pathways induce Wnt or Notch-ligand expression which act as stimuli for the ISC population and could explain the increase in organoid proliferation. Paneth cells and the stem cell populations seem to be differently sensitive to irradiation. Time course experiments after conditioning therapy and allo-BMT would help to identify which cell population of the intestinal crypt is most damaged at what moment and how IFN-I and STING signaling are potentially protective for Paneth cells or ISCs.

4.2.3 Implications of the innate and adaptive immune system on the intestinal stem cell niche

This work has highlighted the beneficial role of cGAS-STING signaling in the context of murine allo-BMT and we have shown that STING activation protects the intestinal barrier and promotes organoid regeneration and proliferation. Isolation of small intestinal crypts from allo-BMT recipient mice allowed to study intestinal regeneration ex vivo after in vivo damaging by irradiation and activated immune cells. For a better understanding of GVHD and other inflammatory diseases, the mechanisms how the ISC niche reacts to T cell mediated injury is of great interest.

In a recent study, co-culture experiments of organoids with activated T cells showed that organoids are attacked by T cells which leads to a reduction of $Lgr5^+$ ISCs and Paneth cells (Eriguchi, Nakamura et al. 2018). Murine GVHD models and 3D microscopy demonstrated that activated donor T cells migrate preferentially to the lower crypt area which is mediated by MAdCAM-1 expression on surrounding blood vessels (Fu, Egorova et al. 2019). Conditioning therapy by TBI induces an early reduction of $Lgr5^+$ ISCs by day 4 which recover by day 10 when transplantation is performed using TCD BM only (Takashima, Martin et al. 2019). Importantly, co-transplantation of allogeneic T cells provoked a long-lasting suppression of $Lgr5^+$ ISCs (Takashima, Martin et al. 2019). This detrimental effect on the ISCs could be linked to T cell derived IFNγ which induces JAK/STAT mediated apoptosis (Eriguchi, Nakamura et al. 2018, Takashima, Martin et al. 2019).

A recent study investigated the effects of different Th cell subsets and Th cytokines on ISC proliferation and differentiation. They demonstrated that T_{reg} cells and IL-10 promoted ISC self-renewal and increased ISC numbers in organoids whereas Th1, Th2 and Th17 cells and their associated cytokines pushed ISCs towards differentiation and increased numbers of transit-amplifying cells (Biton, Haber et al. 2018).

Moreover, $Lgr5^+$ ISCs act as antigen presenting cells expressing MHC II on their cell surface which points out that direct T cell-ISC interactions are possible in the crypt region (Biton, Haber et al. 2018, Fu, Egorova et al. 2019).

These current findings highlight the various interactions of immune cells with cells with the intestinal epithelium. Immune cells are not only predators, but provide

signals which drive ISCs towards proliferation or differentiation and thus contribute to intestinal regeneration and homeostasis.

Further co-culture experiments of organoids and T cells will help to understand how T cells attack epithelial cells and how organoids and stem cells evade tissue damage. After passing a nadir of weight loss on d8 after allo-BMT, recipient mice recover before again losing weight and developing signs of acute GVHD (**Fig. 4A, 8A**). Isolation of intestinal crypts at different timepoints after allo-BMT or after different doses of transplanted T cells or TBI could elucidate kinetics of intestinal regeneration and differentially regulated pathways that drive regeneration after damage.

5 Summary

Allogeneic hematopoietic stem cell transplantation (allo-HSCT) is a potentially life-saving therapy for a variety of hematologic malignancies and the number of patients treated with allo-HSCT is constantly rising. Unfortunately, its broader use is limited by the highly toxic pre-transplant conditioning like high-dose chemotherapy and/or TBI and subsequent GVHD which affects 40-60% of transplant recipients.

This work demonstrates that innate immune sensing pathway cGAS-STING exerts a protective role in GVHD. In a first part, using murine models of allogeneic bone marrow transplantation (allo-BMT), it could be shown that STING signaling improved survival after allo-BMT and reduced signs of GVHD related morbidity. This effect could be exploited therapeutically in the setting of a prophylactic treatment with cGAS-STING agonist ISD prior to allo-BMT. ISD treatment resulted in increased survival which was associated with protection of the intestinal barrier and underlines the effectiveness of targeted and well-timed immune therapies.

In a second part, the role of cGAS-STING signaling in the intestinal epithelium was studied more closely. Using small intestinal organoid cultures, it was demonstrated that STING positively regulates intestinal regeneration which was dependent on downstream IFN-I signaling. Experiments with organoids derived from allo-BMT recipient mice showed that cGAS-STING activation in vivo protects the intestinal crypt and results in increased organoid numbers in vitro. The observed effects of cGAS-STING and IFN-I signaling in intestinal organoids point towards a potential role of STING signaling in the intestinal stem cell or its niche. Experiments using flow cytometry revealed an expansion of $Lgr5^+$ ISCs in organoids. Further studies using intestinal organoid cultures from GvHD patients as well as preclinical animal models will help to further understand how innate immune signaling influences intestinal stem cells and drives epithelial regeneration.

6 Zusammenfassung

Die allogene Stammzelltransplantation (allo-SZT) ist eine potenziell lebensrettende Therapie verschiedener hämatologischer Neoplasien, und die Zahl der durchgeführten allo-SZT steigt stetig. Leider wird ihr breiterer Einsatz durch die hochtoxische Konditionierungstherapie vor der Transplantation (Hochdosis-Chemotherapie und/oder Ganzkörperbestrahlung) und die daraus resultierende GVHD, von der 40-60 % der Empfänger betroffen sind, limitiert.

Diese Arbeit beschreibt eine protektive Funktion des cGAS-STING Signalwegs in der GVHD. Im ersten Teil wurde anhand von Mausmodellen für die allogene Knochenmarkstransplantation (allo-KMT) gezeigt, dass der STING Signalweg die Mortalität und Morbidität nach allo-KMT reduziert. Dieser Effekt ließ sich therapeutisch nutzen, indem vor der Stammzelltransplantation eine prophylaktische Behandlung mit dem cGAS-STING Agonisten ISD durchgeführt wurde. Die Behandlung mit ISD erhöhte die Überlebensrate und reduzierte den Darmbarriereschaden, was die Bedeutung von zielgerichteten und zeitlich abgestimmten Immuntherapien unterstreicht.

Im zweiten Teil wurde die Rolle des cGAS-STING-Signalwegs im Darmepithel näher untersucht. Anhand intestinaler Organoid-Kulturen konnte ein positiver Einfluss von STING, in Abhängigkeit der resultierenden Typ-I Interferon-Antwort, auf die Epithelregeneration des Darms gezeigt werden. Organoid-Kulturen aus Krypten von allo-KMT Empfängermäusen legen nahe, dass durch cGAS-STING Aktivierung eine Protektion der Darmkrypte erreicht werden kann, welche in gesteigerten Organoid-Zahlen resultierte. Weitere Ergebnisse aus Organoid-Experimenten deuten auf einen Einfluss des cGAS-STING Signalwegs auf intestinale Stammzellen, bzw. die Stammzellnische hin: Messungen mit Hilfe der Durchflusszytometrie ergaben eine erhöhte Zahl der $Lgr5^+$ Stammzellen in Organoiden in vitro. Weitere Studien an intestinalen Organoiden aus humanen Gewebeproben nach allo-SZT und mithilfe präklinischer Tiermodelle werden zu einem besseren Verständnis davon beitragen, wie Signalwege des angeborenen Immunsystems die intestinale Stammzelle und die epitheliale Regeneration beeinflussen.

7 References

Andrade, W. A., S. Agarwal, S. Mo, S. A. Shaffer, J. P. Dillard, T. Schmidt, V. Hornung, K. A. Fitzgerald, E. A. Kurt-Jones and D. T. Golenbock (2016). "Type I Interferon Induction by Neisseria gonorrhoeae: Dual Requirement of Cyclic GMP-AMP Synthase and Toll-like Receptor 4." Cell Rep **15**(11): 2438-2448.

Andrade, W. A., A. Firon, T. Schmidt, V. Hornung, K. A. Fitzgerald, E. A. Kurt-Jones, P. Trieu-Cuot, D. T. Golenbock and P. A. Kaminski (2016). "Group B Streptococcus Degrades Cyclic-di-AMP to Modulate STING-Dependent Type I Interferon Production." Cell Host Microbe **20**(1): 49-59.

Bacigalupo, A., K. Ballen, D. Rizzo, S. Giralt, H. Lazarus, V. Ho, J. Apperley, S. Slavin, M. Pasquini, B. M. Sandmaier, J. Barrett, D. Blaise, R. Lowski and M. Horowitz (2009). "Defining the intensity of conditioning regimens: working definitions." Biol Blood Marrow Transplant **15**(12): 1628-1633.

Bader, C. S., H. Barreras, C. O. Lightbourn, S. N. Copsel, D. Wolf, J. Meng, J. Ahn, K. V. Komanduri, B. R. Blazar, L. Jin, G. N. Barber, S. Roy and R. B. Levy (2020). "STING differentially regulates experimental GVHD mediated by CD8 versus CD4 T cell subsets." Sci Transl Med **12**(552).

Baechler, E. C., F. M. Batliwalla, G. Karypis, P. M. Gaffney, W. A. Ortmann, K. J. Espe, K. B. Shark, W. J. Grande, K. M. Hughes, V. Kapur, P. K. Gregersen and T. W. Behrens (2003). "Interferon-inducible gene expression signature in peripheral blood cells of patients with severe lupus." Proc Natl Acad Sci U S A **100**(5): 2610-2615.

Barker, N., J. H. van Es, J. Kuipers, P. Kujala, M. van den Born, M. Cozijnsen, A. Haegebarth, J. Korving, H. Begthel, P. J. Peters and H. Clevers (2007). "Identification of stem cells in small intestine and colon by marker gene Lgr5." Nature **449**(7165): 1003-1007.

Beilhack, A., S. Schulz, J. Baker, G. F. Beilhack, C. B. Wieland, E. I. Herman, E. M. Baker, Y. A. Cao, C. H. Contag and R. S. Negrin (2005). "In vivo analyses of early events in acute graft-versus-host disease reveal sequential infiltration of T-cell subsets." Blood **106**(3): 1113-1122.

Berridge, M. V. and A. S. Tan (1993). "Characterization of the cellular reduction of 3-(4,5-dimethylthiazol-2-yl)-2,5-diphenyltetrazolium bromide (MTT): subcellular localization, substrate dependence, and involvement of mitochondrial electron transport in MTT reduction." Arch Biochem Biophys **303**(2): 474-482.

Bevins, C. L. and N. H. Salzman (2011). "Paneth cells, antimicrobial peptides and maintenance of intestinal homeostasis." Nat Rev Microbiol **9**(5): 356-368.

Bidwell, B. N., C. Y. Slaney, N. P. Withana, S. Forster, Y. Cao, S. Loi, D. Andrews, T. Mikeska, N. E. Mangan, S. A. Samarajiwa, N. A. de Weerd, J. Gould, P. Argani, A. Moller, M. J. Smyth, R. L. Anderson, P. J. Hertzog and B. S. Parker (2012). "Silencing of Irf7 pathways in breast cancer cells promotes bone metastasis through immune escape." Nat Med **18**(8): 1224-1231.

Biton, M., A. L. Haber, N. Rogel, G. Burgin, S. Beyaz, A. Schnell, O. Ashenberg, C. W. Su, C. Smillie, K. Shekhar, Z. Chen, C. Wu, J. Ordovas-Montanes, D. Alvarez, R. H. Herbst, M. Zhang, I. Tirosh, D. Dionne, L. T. Nguyen, M. E. Xifaras, A. K. Shalek, U. H. von Andrian, D. B. Graham, O. Rozenblatt-Rosen, H. N. Shi, V. Kuchroo, O. H. Yilmaz, A. Regev and R. J. Xavier (2018). "T Helper Cell

Cytokines Modulate Intestinal Stem Cell Renewal and Differentiation." Cell **175**(5): 1307-1320 e1322.

Bouabe, H. and K. Okkenhaug (2013). "Gene targeting in mice: a review." Methods Mol Biol **1064**: 315-336.

Brubaker, S. W., K. S. Bonham, I. Zanoni and J. C. Kagan (2015). "Innate immune pattern recognition: a cell biological perspective." Annu Rev Immunol **33**: 257-290.

Burdette, D. L., K. M. Monroe, K. Sotelo-Troha, J. S. Iwig, B. Eckert, M. Hyodo, Y. Hayakawa and R. E. Vance (2011). "STING is a direct innate immune sensor of cyclic di-GMP." Nature **478**(7370): 515-518.

Calame, D. G., S. L. Mueller-Ortiz, J. E. Morales and R. A. Wetsel (2014). "The C5a anaphylatoxin receptor (C5aR1) protects against Listeria monocytogenes infection by inhibiting type 1 IFN expression." J Immunol **193**(10): 5099-5107.

Calcaterra, C., L. Sfondrini, A. Rossini, M. Sommariva, C. Rumio, S. Menard and A. Balsari (2008). "Critical role of TLR9 in acute graft-versus-host disease." J Immunol **181**(9): 6132-6139.

Cash, H. L., C. V. Whitham, C. L. Behrendt and L. V. Hooper (2006). "Symbiotic bacteria direct expression of an intestinal bactericidal lectin." Science **313**(5790): 1126-1130.

Chakraverty, R., D. Cote, J. Buchli, P. Cotter, R. Hsu, G. Zhao, T. Sachs, C. M. Pitsillides, R. Bronson, T. Means, C. Lin and M. Sykes (2006). "An inflammatory checkpoint regulates recruitment of graft-versus-host reactive T cells to peripheral tissues." J Exp Med **203**(8): 2021-2031.

Chen, Q., L. Sun and Z. J. Chen (2016). "Regulation and function of the cGAS-STING pathway of cytosolic DNA sensing." Nat Immunol **17**(10): 1142-1149.

Chen, X., S. Vodanovic-Jankovic, B. Johnson, M. Keller, R. Komorowski and W. R. Drobyski (2007). "Absence of regulatory T-cell control of TH1 and TH17 cells is responsible for the autoimmune-mediated pathology in chronic graft-versus-host disease." Blood **110**(10): 3804-3813.

Cheng, H. and C. P. Leblond (1974). "Origin, differentiation and renewal of the four main epithelial cell types in the mouse small intestine. V. Unitarian Theory of the origin of the four epithelial cell types." Am J Anat **141**(4): 537-561.

Civril, F., T. Deimling, C. C. de Oliveira Mann, A. Ablasser, M. Moldt, G. Witte, V. Hornung and K. P. Hopfner (2013). "Structural mechanism of cytosolic DNA sensing by cGAS." Nature **498**(7454): 332-337.

Clevers, H. (2016). "Modeling Development and Disease with Organoids." Cell **165**(7): 1586-1597.

Copelan, E. A. (2006). "Hematopoietic stem-cell transplantation." N Engl J Med **354**(17): 1813-1826.

Crouse, J., U. Kalinke and A. Oxenius (2015). "Regulation of antiviral T cell responses by type I interferons." Nat Rev Immunol **15**(4): 231-242.

D'Souza A., Z. X. (2016). "Current Uses and Outcomes of Hematopoietic Cell Transplantation (HCT): CIBMTR Summary Slides, 2016." **Available at: http://www.cibmtr.org**.

de Lau, W., N. Barker, T. Y. Low, B. K. Koo, V. S. Li, H. Teunissen, P. Kujala, A. Haegebarth, P. J. Peters, M. van de Wetering, D. E. Stange, J. E. van Es, D. Guardavaccaro, R. B. Schasfoort, Y. Mohri, K. Nishimori, S. Mohammed, A. J. Heck and H. Clevers (2011). "Lgr5 homologues associate with Wnt receptors and mediate R-spondin signalling." Nature **476**(7360): 293-297.

Deng, L., H. Liang, M. Xu, X. Yang, B. Burnette, A. Arina, X. D. Li, H. Mauceri, M. Beckett, T. Darga, X. Huang, T. F. Gajewski, Z. J. Chen, Y. X. Fu and R. R. Weichselbaum (2014). "STING-Dependent Cytosolic DNA Sensing Promotes Radiation-Induced Type I Interferon-Dependent Antitumor Immunity in Immunogenic Tumors." Immunity **41**(5): 843-852.

DeSantis, T. Z., P. Hugenholtz, N. Larsen, M. Rojas, E. L. Brodie, K. Keller, T. Huber, D. Dalevi, P. Hu and G. L. Andersen (2006). "Greengenes, a Chimera-Checked 16S rRNA Gene Database and Workbench Compatible with ARB." Applied and Environmental Microbiology **72**(7): 5069-5072.

Dey, B., R. J. Dey, L. S. Cheung, S. Pokkali, H. Guo, J. H. Lee and W. R. Bishai (2015). "A bacterial cyclic dinucleotide activates the cytosolic surveillance pathway and mediates innate resistance to tuberculosis." Nat Med **21**(4): 401-406.

Di Domizio, J., C. Belkhodja, P. Chenuet, A. Fries, T. Murray, P. M. Mondejar, O. Demaria, C. Conrad, B. Homey, S. Werner, D. E. Speiser, B. Ryffel and M. Gilliet (2020). "The commensal skin microbiota triggers type I IFN-dependent innate repair responses in injured skin." Nat Immunol **21**(9): 1034-1045.

Dudakov, J. A., A. M. Mertelsmann, M. H. O'Connor, R. R. Jenq, E. Velardi, L. F. Young, O. M. Smith, R. L. Boyd, M. R. M. van den Brink and A. M. Hanash (2017). "Loss of thymic innate lymphoid cells leads to impaired thymopoiesis in experimental graft-versus-host disease." Blood **130**(7): 933-942.

Elinav, E., T. Strowig, A. L. Kau, J. Henao-Mejia, C. A. Thaiss, C. J. Booth, D. R. Peaper, J. Bertin, S. C. Eisenbarth, J. I. Gordon and R. A. Flavell (2011). "NLRP6 inflammasome regulates colonic microbial ecology and risk for colitis." Cell **145**(5): 745-757.

Eming, S. A., T. A. Wynn and P. Martin (2017). "Inflammation and metabolism in tissue repair and regeneration." Science **356**(6342): 1026-1030.

Eriguchi, Y., K. Nakamura, Y. Yokoi, R. Sugimoto, S. Takahashi, D. Hashimoto, T. Teshima, T. Ayabe, M. E. Selsted and A. J. Ouellette (2018). "Essential role of IFN-gamma in T cell-associated intestinal inflammation." JCI Insight **3**(18).

Eriguchi, Y., S. Takashima, H. Oka, S. Shimoji, K. Nakamura, H. Uryu, S. Shimoda, H. Iwasaki, N. Shimono, T. Ayabe, K. Akashi and T. Teshima (2012). "Graft-versus-host disease disrupts intestinal microbial ecology by inhibiting Paneth cell production of alpha-defensins." Blood **120**(1): 223-231.

Farin, H. F., I. Jordens, M. H. Mosa, O. Basak, J. Korving, D. V. Tauriello, K. de Punder, S. Angers, P. J. Peters, M. M. Maurice and H. Clevers (2016). "Visualization of a short-range Wnt gradient in the intestinal stem-cell niche." Nature **530**(7590): 340-343.

Farin, H. F., J. H. Van Es and H. Clevers (2012). "Redundant sources of Wnt regulate intestinal stem cells and promote formation of Paneth cells." Gastroenterology **143**(6): 1518-1529 e1517.

Ferrara, J. L. M., J. E. Levine, P. Reddy and E. Holler (2009). "Graft-versus-host disease." The Lancet **373**(9674): 1550-1561.

Fischer, J. C., M. Bscheider, G. Eisenkolb, C. C. Lin, A. Wintges, V. Otten, C. A. Lindemans, S. Heidegger, M. Rudelius, S. Monette, K. A. Porosnicu Rodriguez, M. Calafiore, S. Liebermann, C. Liu, S. Lienenklaus, S. Weiss, U. Kalinke, J. Ruland, C. Peschel, Y. Shono, M. Docampo, E. Velardi, R. R. Jenq, A. M. Hanash, J. A. Dudakov, T. Haas, M. R. M. van den Brink and H. Poeck (2017). "RIG-I/MAVS and STING signaling promote gut integrity during irradiation- and immune-mediated tissue injury." Sci Transl Med **9**(386).

Flood, B. A., E. F. Higgs, S. Li, J. J. Luke and T. F. Gajewski (2019). "STING pathway agonism as a cancer therapeutic." Immunol Rev **290**(1): 24-38.

Fu, Y. Y., A. Egorova, C. Sobieski, J. Kuttiyara, M. Calafiore, S. Takashima, H. Clevers and A. M. Hanash (2019). "T Cell Recruitment to the Intestinal Stem Cell Compartment Drives Immune-Mediated Intestinal Damage after Allogeneic Transplantation." Immunity **51**(1): 90-103 e103.

Gehart, H. and H. Clevers (2019). "Tales from the crypt: new insights into intestinal stem cells." Nat Rev Gastroenterol Hepatol **16**(1): 19-34.

Ghosh, A., A. M. Holland, Y. Dogan, N. L. Yim, U. K. Rao, L. F. Young, M. L. West, N. V. Singer, H. Lee, I. K. Na, J. J. Tsai, R. R. Jenq, O. Penack, A. M. Hanash, C. Lezcano, G. F. Murphy, C. Liu, M. Sadelain, M. G. Sauer, D. Sant'angelo and M. R. van den Brink (2013). "PLZF confers effector functions to donor T cells that preserve graft-versus-tumor effects while attenuating GVHD." Cancer Res **73**(15): 4687-4696.

Gilbert, J. A., P. D. Schloss, D. Gevers and S. L. Westcott (2011). "Reducing the Effects of PCR Amplification and Sequencing Artifacts on 16S rRNA-Based Studies." PLoS ONE **6**(12).

Gregorio, J., S. Meller, C. Conrad, A. Di Nardo, B. Homey, A. Lauerma, N. Arai, R. L. Gallo, J. Digiovanni and M. Gilliet (2010). "Plasmacytoid dendritic cells sense skin injury and promote wound healing through type I interferons." J Exp Med **207**(13): 2921-2930.

Groschwitz, K. R. and S. P. Hogan (2009). "Intestinal barrier function: molecular regulation and disease pathogenesis." J Allergy Clin Immunol **124**(1): 3-20; quiz 21-22.

Gu, J., Y. Z. Chen, Z. X. Zhang, Z. X. Yang, G. X. Duan, L. Q. Qin, L. Zhao and J. Y. Xu (2020). "At What Dose Can Total Body and Whole Abdominal Irradiation Cause Lethal Intestinal Injury Among C57BL/6J Mice?" Dose Response **18**(3): 1559325820956783.

Hanash, A. M., J. A. Dudakov, G. Hua, M. H. O'Connor, L. F. Young, N. V. Singer, M. L. West, R. R. Jenq, A. M. Holland, L. W. Kappel, A. Ghosh, J. J. Tsai, U. K. Rao, N. L. Yim, O. M. Smith, E. Velardi, E. B. Hawryluk, G. F. Murphy, C. Liu, L. A. Fouser, R. Kolesnick, B. R. Blazar and M. R. van den Brink (2012). "Interleukin-22 protects intestinal stem cells from immune-mediated tissue damage and regulates sensitivity to graft versus host disease." Immunity **37**(2): 339-350.

Hansen, K., T. Prabakaran, A. Laustsen, S. E. Jorgensen, S. H. Rahbaek, S. B. Jensen, R. Nielsen, J. H. Leber, T. Decker, K. A. Horan, M. R. Jakobsen and S.

R. Paludan (2014). "Listeria monocytogenes induces IFNbeta expression through an IFI16-, cGAS- and STING-dependent pathway." EMBO J **33**(15): 1654-1666.

Harris, A. C., R. Young, S. Devine, W. J. Hogan, F. Ayuk, U. Bunworasate, C. Chanswangphuwana, Y. A. Efebera, E. Holler, M. Litzow, R. Ordemann, M. Qayed, A. S. Renteria, R. Reshef, M. Wolfl, Y. B. Chen, S. Goldstein, M. Jagasia, F. Locatelli, S. Mielke, D. Porter, T. Schechter, Z. Shekhovtsova, J. L. Ferrara and J. E. Levine (2016). "International, Multicenter Standardization of Acute Graft-versus-Host Disease Clinical Data Collection: A Report from the Mount Sinai Acute GVHD International Consortium." Biol Blood Marrow Transplant **22**(1): 4-10.

Heidegger, S., M. R. van den Brink, T. Haas and H. Poeck (2014). "The role of pattern-recognition receptors in graft-versus-host disease and graft-versus-leukemia after allogeneic stem cell transplantation." Front Immunol **5**: 337.

Henden, A. S. and G. R. Hill (2015). "Cytokines in Graft-versus-Host Disease." J Immunol **194**(10): 4604-4612.

Hill, G. R., J. M. Crawford, K. R. Cooke, Y. S. Brinson, L. Pan and J. L. M. Ferrara (1997). "Total Body Irradiation and Acute Graft-Versus-Host Disease: The Role of Gastrointestinal Damage and Inflammatory Cytokines." Blood **90**(8): 3204-3213.

Hill, G. R. and J. L. M. Ferrara (2000). "The primacy of the gastrointestinal tract as a target organ of acute graft-versus-host disease: rationale for the use of cytokine shields in allogeneic bone marrow transplantation." Blood **95**(9): 2754-2759.

Honda, K. and D. R. Littman (2016). "The microbiota in adaptive immune homeostasis and disease." Nature **535**(7610): 75-84.

Hornung, V., J. Ellegast, S. Kim, K. Brzozka, A. Jung, H. Kato, H. Poeck, S. Akira, K. K. Conzelmann, M. Schlee, S. Endres and G. Hartmann (2006). "5'-Triphosphate RNA is the ligand for RIG-I." Science **314**(5801): 994-997.

Hossain, M. S., D. L. Jaye, B. P. Pollack, A. B. Farris, M. L. Tselanyane, E. David, J. D. Roback, A. T. Gewirtz and E. K. Waller (2011). "Flagellin, a TLR5 agonist, reduces graft-versus-host disease in allogeneic hematopoietic stem cell transplantation recipients while enhancing antiviral immunity." J Immunol **187**(10): 5130-5140.

Hu, J., U. Protzer, A. Siddiqui and B. A. Glaunsinger (2019). "Revisiting Hepatitis B Virus: Challenges of Curative Therapies." Journal of Virology **93**(20).

Ishii, K. J., C. Coban, H. Kato, K. Takahashi, Y. Torii, F. Takeshita, H. Ludwig, G. Sutter, K. Suzuki, H. Hemmi, S. Sato, M. Yamamoto, S. Uematsu, T. Kawai, O. Takeuchi and S. Akira (2006). "A Toll-like receptor-independent antiviral response induced by double-stranded B-form DNA." Nat Immunol **7**(1): 40-48.

Ishikawa, H. and G. N. Barber (2008). "STING is an endoplasmic reticulum adaptor that facilitates innate immune signalling." Nature **455**(7213): 674-678.

Ishikawa, H., Z. Ma and G. N. Barber (2009). "STING regulates intracellular DNA-mediated, type I interferon-dependent innate immunity." Nature **461**(7265): 788-792.

Ivashkiv, L. B. and L. T. Donlin (2014). "Regulation of type I interferon responses." Nat Rev Immunol **14**(1): 36-49.

Jacobsohn, D. A. and G. B. Vogelsang (2007). "Acute graft versus host disease." Orphanet J Rare Dis **2**: 35.

Jagasia, M., M. Arora, M. E. Flowers, N. J. Chao, P. L. McCarthy, C. S. Cutler, A. Urbano-Ispizua, S. Z. Pavletic, M. D. Haagenson, M. J. Zhang, J. H. Antin, B. J. Bolwell, C. Bredeson, J. Y. Cahn, M. Cairo, R. P. Gale, V. Gupta, S. J. Lee, M. Litzow, D. J. Weisdorf, M. M. Horowitz and T. Hahn (2012). "Risk factors for acute GVHD and survival after hematopoietic cell transplantation." Blood **119**(1): 296-307.

Jalanka, J., J. Cheng, K. Hiippala, J. Ritari, J. Salojarvi, T. Ruuska, M. Kalliomaki and R. Satokari (2020). "Colonic Mucosal Microbiota and Association of Bacterial Taxa with the Expression of Host Antimicrobial Peptides in Pediatric Ulcerative Colitis." Int J Mol Sci **21**(17).

Jeanes, A., W. C. Haynes, C. A. Wilham, J. A. Rankin, E. H. Melvin, M. J. Austin, J. E. Cluskey, B. E. Fisher, H. M. Tsuchiya and C. E. Rist (1954). "Characterization and Classification of Dextrans from Ninety-six Strains of Bacteria." J. Am. Chem. Soc. **76**.

Johansson, J.-E. and T. Ekman (2007). "Gut Toxicity During Hemopoietic Stem Cell Transplantation May Predict Acute Graft-Versus-Host Disease Severity in Patients." Digestive Diseases and Sciences **52**(9): 2340-2345.

Johansson, M. E., M. Phillipson, J. Petersson, A. Velcich, L. Holm and G. C. Hansson (2008). "The inner of the two Muc2 mucin-dependent mucus layers in colon is devoid of bacteria." Proc Natl Acad Sci U S A **105**(39): 15064-15069.

Kappel, L. W., G. L. Goldberg, C. G. King, D. Y. Suh, O. M. Smith, C. Ligh, A. M. Holland, J. Grubin, N. M. Mark, C. Liu, Y. Iwakura, G. Heller and M. R. van den Brink (2009). "IL-17 contributes to CD4-mediated graft-versus-host disease." Blood **113**(4): 945-952.

Katakura, K., J. Lee, D. Rachmilewitz, G. Li, L. Eckmann and E. Raz (2005). "Toll-like receptor 9–induced type I IFN protects mice from experimental colitis." Journal of Clinical Investigation **115**(3): 695-702.

Keir, M., Y. Yi, T. Lu and N. Ghilardi (2020). "The role of IL-22 in intestinal health and disease." J Exp Med **217**(3): e20192195.

Kim, B. H., H. W. Jung, S. H. Seo, H. Shin, J. Kwon and J. M. Suh (2018). "Synergistic actions of FGF2 and bone marrow transplantation mitigate radiation-induced intestinal injury." Cell Death Dis **9**(3): 383.

Kim, H., M. Kim, S. K. Im and S. Fang (2018). "Mouse Cre-LoxP system: general principles to determine tissue-specific roles of target genes." Lab Anim Res **34**(4): 147-159.

Kim, T. D., T. H. Terwey, J. L. Zakrzewski, D. Suh, A. A. Kochman, M. E. Chen, C. G. King, C. Borsotti, J. Grubin, O. M. Smith, G. Heller, C. Liu, G. F. Murphy, O. Alpdogan and M. R. van den Brink (2008). "Organ-derived dendritic cells have differential effects on alloreactive T cells." Blood **111**(5): 2929-2940.

Lahaye, X., T. Satoh, M. Gentili, S. Cerboni, C. Conrad, I. Hurbain, A. El Marjou, C. Lacabaratz, J. D. Lelievre and N. Manel (2013). "The capsids of HIV-1 and HIV-2 determine immune detection of the viral cDNA by the innate sensor cGAS in dendritic cells." Immunity **39**(6): 1132-1142.

Lamas, B., M. L. Richard, V. Leducq, H. P. Pham, M. L. Michel, G. Da Costa, C. Bridonneau, S. Jegou, T. W. Hoffmann, J. M. Natividad, L. Brot, S. Taleb, A. Couturier-Maillard, I. Nion-Larmurier, F. Merabtene, P. Seksik, A. Bourrier, J. Cosnes, B. Ryffel, L. Beaugerie, J. M. Launay, P. Langella, R. J. Xavier and H. Sokol (2016). "CARD9 impacts colitis by altering gut microbiota metabolism of tryptophan into aryl hydrocarbon receptor ligands." Nat Med **22**(6): 598-605.

Lazear, H. M., J. W. Schoggins and M. S. Diamond (2019). "Shared and Distinct Functions of Type I and Type III Interferons." Immunity **50**(4): 907-923.

Le Naour, J., L. Zitvogel, L. Galluzzi, E. Vacchelli and G. Kroemer (2020). "Trial watch: STING agonists in cancer therapy." Oncoimmunology **9**(1): 1777624.

Lee, A. J. and A. A. Ashkar (2018). "The Dual Nature of Type I and Type II Interferons." Front Immunol **9**: 2061.

Li, T. and Z. J. Chen (2018). "The cGAS-cGAMP-STING pathway connects DNA damage to inflammation, senescence, and cancer." J Exp Med **215**(5): 1287-1299.

Li, T., H. Cheng, H. Yuan, Q. Xu, C. Shu, Y. Zhang, P. Xu, J. Tan, Y. Rui, P. Li and X. Tan (2016). "Antitumor Activity of cGAMP via Stimulation of cGAS-cGAMP-STING-IRF3 Mediated Innate Immune Response." Sci Rep **6**: 19049.

Lindemans, C. A., M. Calafiore, A. M. Mertelsmann, M. H. O'Connor, J. A. Dudakov, R. R. Jenq, E. Velardi, L. F. Young, O. M. Smith, G. Lawrence, J. A. Ivanov, Y. Y. Fu, S. Takashima, G. Hua, M. L. Martin, K. P. O'Rourke, Y. H. Lo, M. Mokry, M. Romera-Hernandez, T. Cupedo, L. Dow, E. E. Nieuwenhuis, N. F. Shroyer, C. Liu, R. Kolesnick, M. R. M. van den Brink and A. M. Hanash (2015). "Interleukin-22 promotes intestinal-stem-cell-mediated epithelial regeneration." Nature **528**(7583): 560-564.

Liu, Y., A. A. Jesus, B. Marrero, D. Yang, S. E. Ramsey, G. A. M. Sanchez, K. Tenbrock, H. Wittkowski, O. Y. Jones, H. S. Kuehn, C. R. Lee, M. A. DiMattia, E. W. Cowen, B. Gonzalez, I. Palmer, J. J. DiGiovanna, A. Biancotto, H. Kim, W. L. Tsai, A. M. Trier, Y. Huang, D. L. Stone, S. Hill, H. J. Kim, C. St Hilaire, S. Gurprasad, N. Plass, D. Chapelle, I. Horkayne-Szakaly, D. Foell, A. Barysenka, F. Candotti, S. M. Holland, J. D. Hughes, H. Mehmet, A. C. Issekutz, M. Raffeld, J. McElwee, J. R. Fontana, C. P. Minniti, S. Moir, D. L. Kastner, M. Gadina, A. C. Steven, P. T. Wingfield, S. R. Brooks, S. D. Rosenzweig, T. A. Fleisher, Z. Deng, M. Boehm, A. S. Paller and R. Goldbach-Mansky (2014). "Activated STING in a vascular and pulmonary syndrome." N Engl J Med **371**(6): 507-518.

Loonen, L. M., E. H. Stolte, M. T. Jaklofsky, M. Meijerink, J. Dekker, P. van Baarlen and J. M. Wells (2014). "REG3gamma-deficient mice have altered mucus distribution and increased mucosal inflammatory responses to the microbiota and enteric pathogens in the ileum." Mucosal Immunol **7**(4): 939-947.

MacMicking, J. D. (2012). "Interferon-inducible effector mechanisms in cell-autonomous immunity." Nat Rev Immunol **12**(5): 367-382.

Madison, B. B., L. Dunbar, X. T. Qiao, K. Braunstein, E. Braunstein and D. L. Gumucio (2002). "Cis elements of the villin gene control expression in restricted domains of the vertical (crypt) and horizontal (duodenum, cecum) axes of the intestine." J Biol Chem **277**(36): 33275-33283.

Markey, K. A., K. P. MacDonald and G. R. Hill (2014). "The biology of graft-versus-host disease: experimental systems instructing clinical practice." Blood **124**(3): 354-362.

Mathewson, N. D., R. Jenq, A. V. Mathew, M. Koenigsknecht, A. Hanash, T. Toubai, K. Oravecz-Wilson, S.-R. Wu, Y. Sun, C. Rossi, H. Fujiwara, J. Byun, Y. Shono, C. Lindemans, M. Calafiore, T. M. Schmidt, K. Honda, V. B. Young, S. Pennathur, M. van den Brink and P. Reddy (2016). "Gut microbiome–derived metabolites modulate intestinal epithelial cell damage and mitigate graft-versus-host disease." Nature Immunology **17**(5): 505-513.

Mayberry, J. and W. M. Lee (2019). "The Revolution in Treatment of Hepatitis C." Med Clin North Am **103**(1): 43-55.

McCoy, K. D., M. B. Geuking and F. Ronchi (2017). "Gut Microbiome Standardization in Control and Experimental Mice." Current Protocols in Immunology **117**(1).

McNab, F., K. Mayer-Barber, A. Sher, A. Wack and A. O'Garra (2015). "Type I interferons in infectious disease." Nat Rev Immunol **15**(2): 87-103.

Mosmann, T. (1983). "Rapid colorimetric assay for cellular growth and survival: application to proliferation and cytotoxicity assays." J Immunol Methods **65**(1-2): 55-63.

Motwani, M., S. Pesiridis and K. A. Fitzgerald (2019). "DNA sensing by the cGAS-STING pathway in health and disease." Nat Rev Genet **20**(11): 657-674.

Muller, L. P. and C. Muller-Tidow (2015). "The indications for allogeneic stem cell transplantation in myeloid malignancies." Dtsch Arztebl Int **112**(15): 262-270.

Muller, U., U. Steinhoff, L. F. Reis, S. Hemmi, J. Pavlovic, R. M. Zinkernagel and M. Aguet (1994). "Functional role of type I and type II interferons in antiviral defense." Science **264**(5167): 1918-1921.

Munoz, J., D. E. Stange, A. G. Schepers, M. van de Wetering, B. K. Koo, S. Itzkovitz, R. Volckmann, K. S. Kung, J. Koster, S. Radulescu, K. Myant, R. Versteeg, O. J. Sansom, J. H. van Es, N. Barker, A. van Oudenaarden, S. Mohammed, A. J. Heck and H. Clevers (2012). "The Lgr5 intestinal stem cell signature: robust expression of proposed quiescent '+4' cell markers." EMBO J **31**(14): 3079-3091.

Munroe, M. E., R. Lu, Y. D. Zhao, D. A. Fife, J. M. Robertson, J. M. Guthridge, T. B. Niewold, G. C. Tsokos, M. P. Keith, J. B. Harley and J. A. James (2016). "Altered type II interferon precedes autoantibody accrual and elevated type I interferon activity prior to systemic lupus erythematosus classification." Ann Rheum Dis **75**(11): 2014-2021.

Murphy, K. and C. Weaver (2016). Janeway's immunobiology. New York, NY, Garland Science/Taylor & Francis Group, LLC.

Muskardin, T. L. W. and T. B. Niewold (2018). "Type I interferon in rheumatic diseases." Nat Rev Rheumatol **14**(4): 214-228.

Passweg, J. R., H. Baldomero, C. Chabannon, G. W. Basak, R. de la Camara, S. Corbacioglu, H. Dolstra, R. Duarte, B. Glass, R. Greco, A. C. Lankester, M. Mohty, R. Peffault de Latour, J. A. Snowden, I. Yakoub-Agha, N. Kroger, B. European Society for and T. Marrow (2021). "Hematopoietic cell transplantation

and cellular therapy survey of the EBMT: monitoring of activities and trends over 30 years." Bone Marrow Transplant.

Peled, J. U., A. L. C. Gomes, S. M. Devlin, E. R. Littmann, Y. Taur, A. D. Sung, D. Weber, D. Hashimoto, A. E. Slingerland, J. B. Slingerland, M. Maloy, A. G. Clurman, C. K. Stein-Thoeringer, K. A. Markey, M. D. Docampo, M. Burgos da Silva, N. Khan, A. Gessner, J. A. Messina, K. Romero, M. V. Lew, A. Bush, L. Bohannon, D. G. Brereton, E. Fontana, L. A. Amoretti, R. J. Wright, G. K. Armijo, Y. Shono, M. Sanchez-Escamilla, N. Castillo Flores, A. Alarcon Tomas, R. J. Lin, L. Yanez San Segundo, G. L. Shah, C. Cho, M. Scordo, I. Politikos, K. Hayasaka, Y. Hasegawa, B. Gyurkocza, D. M. Ponce, J. N. Barker, M. A. Perales, S. A. Giralt, R. R. Jenq, T. Teshima, N. J. Chao, E. Holler, J. B. Xavier, E. G. Pamer and M. R. M. van den Brink (2020). "Microbiota as Predictor of Mortality in Allogeneic Hematopoietic-Cell Transplantation." N Engl J Med **382**(9): 822-834.

Peled, J. U., A. M. Hanash and R. R. Jenq (2016). "Role of the intestinal mucosa in acute gastrointestinal GVHD." Hematology Am Soc Hematol Educ Program **2016**(1): 119-127.

Penack, O., O. M. Smith, A. Cunningham-Bussel, X. Liu, U. Rao, N. Yim, I. K. Na, A. M. Holland, A. Ghosh, S. X. Lu, R. R. Jenq, C. Liu, G. F. Murphy, K. Brandl and M. R. van den Brink (2009). "NOD2 regulates hematopoietic cell function during graft-versus-host disease." J Exp Med **206**(10): 2101-2110.

Peterson, L. W. and D. Artis (2014). "Intestinal epithelial cells: regulators of barrier function and immune homeostasis." Nat Rev Immunol **14**(3): 141-153.

Prantner, D., D. J. Perkins, W. Lai, M. S. Williams, S. Sharma, K. A. Fitzgerald and S. N. Vogel (2012). "5,6-Dimethylxanthenone-4-acetic acid (DMXAA) activates stimulator of interferon gene (STING)-dependent innate immune pathways and is regulated by mitochondrial membrane potential." J Biol Chem **287**(47): 39776-39788.

Reich, D. S., C. F. Lucchinetti and P. A. Calabresi (2018). "Multiple Sclerosis." N Engl J Med **378**(2): 169-180.

Robb, R. J., E. Kreijveld, R. D. Kuns, Y. A. Wilson, S. D. Olver, A. L. Don, N. C. Raffelt, N. A. De Weerd, K. E. Lineburg, A. Varelias, K. A. Markey, M. Koyama, A. D. Clouston, P. J. Hertzog, K. P. Macdonald and G. R. Hill (2011). "Type I-IFNs control GVHD and GVL responses after transplantation." Blood **118**(12): 3399-3409.

Rusinova, I., S. Forster, S. Yu, A. Kannan, M. Masse, H. Cumming, R. Chapman and P. J. Hertzog (2013). "Interferome v2.0: an updated database of annotated interferon-regulated genes." Nucleic Acids Res **41**(Database issue): D1040-1046.

Sanchez Alvarado, A. and P. A. Tsonis (2006). "Bridging the regeneration gap: genetic insights from diverse animal models." Nat Rev Genet **7**(11): 873-884.

Sangiorgi, E. and M. R. Capecchi (2008). "Bmi1 is expressed in vivo in intestinal stem cells." Nat Genet **40**(7): 915-920.

Sato, T., J. H. van Es, H. J. Snippert, D. E. Stange, R. G. Vries, M. van den Born, N. Barker, N. F. Shroyer, M. van de Wetering and H. Clevers (2011). "Paneth cells constitute the niche for Lgr5 stem cells in intestinal crypts." Nature **469**(7330): 415-418.

Sato, T., R. G. Vries, H. J. Snippert, M. van de Wetering, N. Barker, D. E. Stange, J. H. van Es, A. Abo, P. Kujala, P. J. Peters and H. Clevers (2009). "Single Lgr5 stem cells build crypt-villus structures in vitro without a mesenchymal niche." Nature **459**(7244): 262-265.

Sauer, J. D., K. Sotelo-Troha, J. von Moltke, K. M. Monroe, C. S. Rae, S. W. Brubaker, M. Hyodo, Y. Hayakawa, J. J. Woodward, D. A. Portnoy and R. E. Vance (2011). "The N-ethyl-N-nitrosourea-induced Goldenticket mouse mutant reveals an essential function of Sting in the in vivo interferon response to Listeria monocytogenes and cyclic dinucleotides." Infect Immun **79**(2): 688-694.

Schloss, P. D., S. L. Westcott, T. Ryabin, J. R. Hall, M. Hartmann, E. B. Hollister, R. A. Lesniewski, B. B. Oakley, D. H. Parks, C. J. Robinson, J. W. Sahl, B. Stres, G. G. Thallinger, D. J. Van Horn and C. F. Weber (2009). "Introducing mothur: Open-Source, Platform-Independent, Community-Supported Software for Describing and Comparing Microbial Communities." Applied and Environmental Microbiology **75**(23): 7537-7541.

Schroeder, M. A. and J. F. DiPersio (2011). "Mouse models of graft-versus-host disease: advances and limitations." Dis Model Mech **4**(3): 318-333.

Shono, Y., M. D. Docampo, J. U. Peled, S. M. Perobelli, E. Velardi, J. J. Tsai, A. E. Slingerland, O. M. Smith, L. F. Young, J. Gupta, S. R. Lieberman, H. V. Jay, K. F. Ahr, K. A. Porosnicu Rodriguez, K. Xu, M. Calarfiore, H. Poeck, S. Caballero, S. M. Devlin, F. Rapaport, J. A. Dudakov, A. M. Hanash, B. Gyurkocza, G. F. Murphy, C. Gomes, C. Liu, E. L. Moss, S. B. Falconer, A. S. Bhatt, Y. Taur, E. G. Pamer, M. R. M. van den Brink and R. R. Jenq (2016). "Increased GVHD-related mortality with broad-spectrum antibiotic use after allogeneic hematopoietic stem cell transplantation in human patients and mice." Sci Transl Med **8**(339): 339ra371.

Shono, Y. and M. R. M. van den Brink (2018). "Gut microbiota injury in allogeneic haematopoietic stem cell transplantation." Nat Rev Cancer **18**(5): 283-295.

Shyer, A. E., T. R. Huycke, C. Lee, L. Mahadevan and C. J. Tabin (2015). "Bending gradients: how the intestinal stem cell gets its home." Cell **161**(3): 569-580.

Sisirak, V., J. Faget, M. Gobert, N. Goutagny, N. Vey, I. Treilleux, S. Renaudineau, G. Poyet, S. I. Labidi-Galy, S. Goddard-Leon, I. Durand, I. Le Mercier, A. Bajard, T. Bachelot, A. Puisieux, I. Puisieux, J. Y. Blay, C. Menetrier-Caux, C. Caux and N. Bendriss-Vermare (2012). "Impaired IFN-alpha production by plasmacytoid dendritic cells favors regulatory T-cell expansion that may contribute to breast cancer progression." Cancer Res **72**(20): 5188-5197.

Stetson, D. B., J. S. Ko, T. Heidmann and R. Medzhitov (2008). "Trex1 Prevents Cell-Intrinsic Initiation of Autoimmunity." Cell **134**(4): 587-598.

Sun, L., H. Miyoshi, S. Origanti, T. J. Nice, A. C. Barger, N. A. Manieri, L. A. Fogel, A. R. French, D. Piwnica-Worms, H. Piwnica-Worms, H. W. Virgin, D. J. Lenschow and T. S. Stappenbeck (2015). "Type I interferons link viral infection to enhanced epithelial turnover and repair." Cell Host Microbe **17**(1): 85-97.

Sun, L., J. Wu, F. Du, X. Chen and Z. J. Chen (2013). "Cyclic GMP-AMP synthase is a cytosolic DNA sensor that activates the type I interferon pathway." Science **339**(6121): 786-791.

Sun, Y., I. Tawara, T. Toubai and P. Reddy (2007). "Pathophysiology of acute graft-versus-host disease: recent advances." Transl Res **150**(4): 197-214.

Sung, N. S., W. F. Crowley, Jr., M. Genel, P. Salber, L. Sandy, L. M. Sherwood, S. B. Johnson, V. Catanese, H. Tilson, K. Getz, E. L. Larson, D. Scheinberg, E. A. Reece, H. Slavkin, A. Dobs, J. Grebb, R. A. Martinez, A. Korn and D. Rimoin (2003). "Central challenges facing the national clinical research enterprise." JAMA **289**(10): 1278-1287.

Takashima, S., M. L. Martin, S. A. Jansen, Y. Fu, J. Bos, D. Chandra, M. H. O'Connor, A. M. Mertelsmann, P. Vinci, J. Kuttiyara, S. M. Devlin, S. Middendorp, M. Calafiore, A. Egorova, M. Kleppe, Y. Lo, N. F. Shroyer, E. H. Cheng, R. L. Levine, C. Liu, R. Kolesnick, C. A. Lindemans and A. M. Hanash (2019). "T cell-derived interferon-gamma programs stem cell death in immune-mediated intestinal damage." Sci Immunol **4**(42).

Tang, K. Y., J. Lickliter, Z. H. Huang, Z. S. Xian, H. Y. Chen, C. Huang, C. Xiao, Y. P. Wang, Y. Tan, L. F. Xu, Y. L. Huang and X. Q. Yan (2019). "Safety, pharmacokinetics, and biomarkers of F-652, a recombinant human interleukin-22 dimer, in healthy subjects." Cell Mol Immunol **16**(5): 473-482.

Taur, Y., R. R. Jenq, M. A. Perales, E. R. Littmann, S. Morjaria, L. Ling, D. No, A. Gobourne, A. Viale, P. B. Dahi, D. M. Ponce, J. N. Barker, S. Giralt, M. van den Brink and E. G. Pamer (2014). "The effects of intestinal tract bacterial diversity on mortality following allogeneic hematopoietic stem cell transplantation." Blood **124**(7): 1174-1182.

Tian, H., B. Biehs, S. Warming, K. G. Leong, L. Rangell, O. D. Klein and F. J. de Sauvage (2011). "A reserve stem cell population in small intestine renders Lgr5-positive cells dispensable." Nature **478**(7368): 255-259.

Tschurtschenthaler, M., J. Wang, C. Fricke, T. M. Fritz, L. Niederreiter, T. E. Adolph, E. Sarcevic, S. Kunzel, F. A. Offner, U. Kalinke, J. F. Baines, H. Tilg and A. Kaser (2014). "Type I interferon signalling in the intestinal epithelium affects Paneth cells, microbial ecology and epithelial regeneration." Gut **63**(12): 1921-1931.

Turksen, K. and T. C. Troy (2004). "Barriers built on claudins." J Cell Sci **117**(Pt 12): 2435-2447.

Vaishnava, S., C. L. Behrendt, A. S. Ismail, L. Eckmann and L. V. Hooper (2008). "Paneth cells directly sense gut commensals and maintain homeostasis at the intestinal host-microbial interface." Proc Natl Acad Sci U S A **105**(52): 20858-20863.

Vaishnava, S., M. Yamamoto, K. M. Severson, K. A. Ruhn, X. Yu, O. Koren, R. Ley, E. K. Wakeland and L. V. Hooper (2011). "The Antibacterial Lectin RegIII Promotes the Spatial Segregation of Microbiota and Host in the Intestine." Science **334**(6053): 255-258.

Vaishnava, S., M. Yamamoto, K. M. Severson, K. A. Ruhn, X. Yu, O. Koren, R. Ley, E. K. Wakeland and L. V. Hooper (2011). "The antibacterial lectin RegIIIgamma promotes the spatial segregation of microbiota and host in the intestine." Science **334**(6053): 255-258.

van den Brink, M. R. and S. J. Burakoff (2002). "Cytolytic pathways in haematopoietic stem-cell transplantation." Nat Rev Immunol **2**(4): 273-281.

van der Flier, L. G. and H. Clevers (2009). "Stem cells, self-renewal, and differentiation in the intestinal epithelium." Annu Rev Physiol **71**: 241-260.

van der Flier, L. G., A. Haegebarth, D. E. Stange, M. van de Wetering and H. Clevers (2009). "OLFM4 is a robust marker for stem cells in human intestine and marks a subset of colorectal cancer cells." Gastroenterology **137**(1): 15-17.

Wang, F., D. Scoville, X. C. He, M. M. Mahe, A. Box, J. M. Perry, N. R. Smith, N. Y. Lei, P. S. Davies, M. K. Fuller, J. S. Haug, M. McClain, A. D. Gracz, S. Ding, M. Stelzner, J. C. Dunn, S. T. Magness, M. H. Wong, M. G. Martin, M. Helmrath and L. Li (2013). "Isolation and characterization of intestinal stem cells based on surface marker combinations and colony-formation assay." Gastroenterology **145**(2): 383-395 e381-321.

Wang, L., C. Llorente, P. Hartmann, A. M. Yang, P. Chen and B. Schnabl (2015). "Methods to determine intestinal permeability and bacterial translocation during liver disease." J Immunol Methods **421**: 44-53.

Wang, Q., G. M. Garrity, J. M. Tiedje and J. R. Cole (2007). "Naïve Bayesian Classifier for Rapid Assignment of rRNA Sequences into the New Bacterial Taxonomy." Applied and Environmental Microbiology **73**(16): 5261-5267.

Watson, R. O., S. L. Bell, D. A. MacDuff, J. M. Kimmey, E. J. Diner, J. Olivas, R. E. Vance, C. L. Stallings, H. W. Virgin and J. S. Cox (2015). "The Cytosolic Sensor cGAS Detects Mycobacterium tuberculosis DNA to Induce Type I Interferons and Activate Autophagy." Cell Host Microbe **17**(6): 811-819.

Wu, J., L. Sun, X. Chen, F. Du, H. Shi, C. Chen and Z. J. Chen (2013). "Cyclic GMP-AMP is an endogenous second messenger in innate immune signaling by cytosolic DNA." Science **339**(6121): 826-830.

Wysocki, C. A., A. Panoskaltsis-Mortari, B. R. Blazar and J. S. Serody (2005). "Leukocyte migration and graft-versus-host disease." Blood **105**(11): 4191-4199.

Xia, T., H. Konno, J. Ahn and G. N. Barber (2016). "Deregulation of STING Signaling in Colorectal Carcinoma Constrains DNA Damage Responses and Correlates With Tumorigenesis." Cell Rep **14**(2): 282-297.

Yan, K. S., L. A. Chia, X. Li, A. Ootani, J. Su, J. Y. Lee, N. Su, Y. Luo, S. C. Heilshorn, M. R. Amieva, E. Sangiorgi, M. R. Capecchi and C. J. Kuo (2012). "The intestinal stem cell markers Bmi1 and Lgr5 identify two functionally distinct populations." Proc Natl Acad Sci U S A **109**(2): 466-471.

Yang, D., O. Chertov, S. N. Bykovskaia, Q. Chen, M. J. Buffo, J. Shogan, M. Anderson, J. M. Schroder, J. M. Wang, O. M. Howard and J. J. Oppenheim (1999). "Beta-defensins: linking innate and adaptive immunity through dendritic and T cell CCR6." Science **286**(5439): 525-528.

Yang, J. Y., M. S. Kim, E. Kim, J. H. Cheon, Y. S. Lee, Y. Kim, S. H. Lee, S. U. Seo, S. H. Shin, S. S. Choi, B. Kim, S. Y. Chang, H. J. Ko, J. W. Bae and M. N. Kweon (2016). "Enteric Viruses Ameliorate Gut Inflammation via Toll-like Receptor 3 and Toll-like Receptor 7-Mediated Interferon-beta Production." Immunity **44**(4): 889-900.

Yi, T., Y. Chen, L. Wang, G. Du, D. Huang, D. Zhao, H. Johnston, J. Young, I. Todorov, D. T. Umetsu, L. Chen, Y. Iwakura, F. Kandeel, S. Forman and D. Zeng (2009). "Reciprocal differentiation and tissue-specific pathogenesis of Th1, Th2, and Th17 cells in graft-versus-host disease." Blood **114**(14): 3101-3112.

Yin, X., H. F. Farin, J. H. van Es, H. Clevers, R. Langer and J. M. Karp (2014). "Niche-independent high-purity cultures of Lgr5+ intestinal stem cells and their progeny." Nat Methods **11**(1): 106-112.

Zhang, X. X., R. C. Li, G. H. Liu, W. Cong, H. Q. Song, X. L. Yu and X. Q. Zhu (2014). "High seroprevalence of Chlamydia infection in sows in Hunan province, subtropical China." Trop Anim Health Prod **46**(4): 701-704.

Zitvogel, L., L. Galluzzi, O. Kepp, M. J. Smyth and G. Kroemer (2015). "Type I interferons in anticancer immunity." Nat Rev Immunol **15**(7): 405-414.

8 Abbreviations

3pRNA	5'-triphosphate RNA
AGS	Aicardi Goutières Syndrome
aGVHD	Acute graft-versus-host disease
allo-BMT	allogeneic bone marrow transplantation
allo-HSCT	allogeneic hematopoietic stem cell transplantation
AMP	Adenosine monophosphate
AMP	Antimicrobial peptide
APC	Antigen presenting cell
ATP	Adenosine triphosphate
BM	Bone marrow
BMP	Bone morphogenetic protein
BMT	Bone marrow transplantation
BRCA1	BRCA1 DNA repair associated
CBC	crypt-base columnar cell
CD	Cluster of differentiation
cDNA	complementary DNA
cGAMP	cyclic GMP-AMP
cGAS	Cyclic GMP-AMP synthase
cGVHD	Chronic graft-versus-host disease
CLR	C-type lectin receptor
CTL	cytotoxic T cell
DAMP	Damage associated molecular pattern
DC	Dendritic cell
Dll4	Delta-like 4
DMXAA	5,6-dimethylxanthenone-4-acetic acid
DNA	Deoxyribonucleic acid
dsDNA	double-stranded DNA
DSS	Dextran sodium sulfate
EBMT	European Society for Blood and Marrow Transplantation
EGF	Epidermal growth factor
ELISA	enzyme-linked immunosorbent assay
ER	Endoplasmatic reticulum
FACS	Fluorescence-activated cell sorting

FITC	Fluorescein isothiocyanate
GAS	Gamma activated sequences
GFP	Green fluorescent protein
GI	Gastrointestinal
GMP	Guanosine monophosphate
GTP	Guanosine triphosphate
GVHD	Graft-versus-host disease
GVL	Graft-versus-leukemia
GVT	Graft-versus-tumor
Gy	Gray
HIV	Human immunodeficiency virus
HLA	Human leukocyte antigen
HSCT	Hematopoietic stem cell transplantation
HSV-1	Herpes simplex virus 1
IBD	Inflammatory bowel disease
IEC	Intestinal epithelial cell
IFN	Interferon
IFN-I	Type I Interferon
IFNAR	Interferon alpha receptor
IKK	Inhibitor of nuclear factor kappa B kinase
IL-1β	Interleukin-1beta
IL-6	Interleukin-6
IRF	Interferon regulatory factor
ISC	Intestinal stem cell
ISD	Interferon stimulatory DNA
ISG	Interferon stimulated genes
JAK1	Janus kinase 1
Lgr5	Leucine-rich repeat-containing G-protein coupled receptor 5
LPS	Lipopolysaccharide
MAVS	Mitochondrial antiviral signaling protein
MHC	Major histocompatibility complex
mRNA	Messenger RNA
MTT	3-(4,5-dimethylthiazol-2-yl)-2,5-diphenyltetrazolium bromide
MyD88	Myeloid differentiation primary response 88

NADPH	Nicotinamide adenine dinucleotide phosphate
NFκB	Nuclear factor kappa-light-chain-enhancer of activated B cells
NK cell	Natural killer cell
NOD	Nucleotide binding oligomerization domain
Olfm4	Olfactomedin 4
PAMP	Pathogen associated molecular pattern
PCR	Polymerase chain reaction
pDC	Plasmacytoid dendritic cell
qPCR	quantitative real-time PCR
RegIIIγ	Regenerating islet-derived protein 3 gamma
RIG-I	Retinoic acid-inducible gene I
RNA	Ribonucleic acid
rRNA	ribosomal RNA
SAVI	STING associated vasculopathy with onset in infancy
STAT	signal transducer and activator of transcription
STING	STimulator of INterferon Genes
TBI	Total boldy irradiation
TBK1	TANK-binding kinase 1
TCD	T cell depleted
TGF	Transforming growth factor
Th cell	T-helper cell
TJ	Tight junction
TLR	Toll-like receptor
TNF	Tumor necrosis factor
Trex1	Three prime repair exonuclease 1
TRIF	TIR-domain-containing adapter-inducing interferon-β
TYK2	tyrosine kinase 2
WT	Wild-type

9 Acknowledgements

First, I would like to thank Prof. Dr. Hendrik Poeck for the many opportunities he opened up for me: conducting this fascinating research and completing my doctoral thesis in his group, joining him at MSKCC in New York City and for the great enthusiasm, ideas and support he provided over the many years.

My thanks also go to PD Dr. Tobias Haas for giving me the chance to start this research project and for his supervision in our lab in Munich.

I am very grateful to Marcel van den Brink, MD, PhD who gave me the chance to work in the truly inspiring environment of his lab at MSKCC. His scientific input and the way of leading and supporting his lab members is exceptional.

Many thanks to Dr. Julius Fischer, who has accompanied me as a colleague and friend since my first day in the laboratory. Without his never-ending fascination for science, his many ideas and his thoroughness our common projects would not have been as successful.

I would like to thank Prof. Dr. Dirk Busch and Prof. Dr. Olaf Groß for being on my thesis committee and the opportunity to take part in the doctoral program in translational medicine.

I thank the members of the Poeck lab: Simon Heidegger, Chia-Ching Lin, Sascha Göttert, Sarah Bek, Alexander Wintges and Martina Schmickl for introducing me into lab techniques and methods, for patiently answering all my questions and providing scientific input. You have been great companions.

At MSKCC, I would like to thank Melissa Docampo and Robert Jenq for the assistance and analysis of 16S-rRNA sequencing experiments, Marsinay Smith and Sophie Lieberman for helping with mouse and allo-BMT experiments. I thank Chen Liu, MD, PhD at Rutgers University for histopathologic analyses of tissue samples from murine GVHD experiments.

Above all, I would like to express my gratitude to my parents Rose-Marie and Gerhard and my brother Viktor. Your endless support helped me reach so many of my goals.